SOFIA Observer's Handbook
for Cycle 3: v3.3.5

SOFIA User Support Group*

Contents

Updates

- April 2, 2015 – v3.3.5

  1. Figure 16 – FORCAST – Corrected a problem with alignment between the plotted atmospheric transmission curve and grism sensitivity

- January 22, 2015 – v3.3.4

  1. Section 4.1.4 – FLITECAM – Clarified discussion of problems observing with FLITECAM L & M band filters

- October 23, 2014 – v3.3.3

  1. Section 9.1 – FIFI-LS – Specified offset between red and blue channels
  2. Section 9.2.2 – FIFI-LS – Added discussion about calculation of on-source integration time
  3. Section 9.3.2 – FIFI-LS – Clarified discussion of the calculation of the total observing time for Asymmetric and Fast Asymmetric Chop Modes
  4. Section 9.3.3 – FIFI-LS – Additional discussion added about observing efficiencies for Asymmetric and Fast Asymmetric Chop Modes
  5. Section 9.3.4 – FIFI-LS – Clarified discussion of grating scans in Symmetric or Asymmetric Chop Modes

- October 16, 2014 – v3.3.2

  1. Section 3.7 – Cycle 3: Calibration – Clarified discussion of calibration plans
  2. Section 8.2.2 – EXES – Added a section describing flux calibration and atmospheric line correction of EXES data
  3. Section 8.2.3 – EXES – Added a section discussing EXES overheads

- October 9, 2014 – v3.3.1

  1. Table 2 – FLITECAM – Updated grism characteristics to reflect empirical measurements of the spectral resolution and noted issues related to grism C
  2. Figure 10 – FLITECAM – Updated the figure to include both FLITECAM and FLIPO spectroscopic sensitivities

- September 26, 2014 – v3.3.0

  1. Section 9 – FIFI-LS – Updated throughout to reflect new results from instrument commissioning
  2. Section 9.1.2 – FIFI-LS – Updated dichroic cut-off wavelengths to reflect commissioning results
  3. Section 9.2.2 – FIFI-LS – Updated text to allow greater accuracy in estimating on-source time and overheads

4. Figure 32 – FIFI-LS – Corrected caption to indicate that sensitivity values are per pixel

5. Section 9.3.1 – FIFI-LS – Updated discussion of overhead estimates

6. Section 9.3.2 – FIFI-LS – Updated discussion of overhead estimates

7. Section 9.3.3 – FIFI-LS – Added a section discussing the observing efficiencies for each observation mode

8. Section 9.3.4 – FIFI-LS – Added details to the discussion of spectral dithering

9. Section 9.3.5 – FIFI-LS – Added details to the discussion of spatial mapping

- July 10, 2014 – v3.2.3

  1. Section 1.3 – Introduction – Corrected a stale link to the Guide to Observation Planning with GREAT (GOPG)

  2. Section 4.1.4 – FLITECAM – Updated Table 1 & Figure 8 to include empirical MDCF values for FLITECAM when mounted in the FLIPO configuration.

  3. Section 6.2 – GREAT – Corrected a stale link to the Guide to Observation Planning with GREAT (GOPG)

- June 20, 2014 – v3.2.2

  1. Section 9.2.1 & Figure 31 – FIFI-LS – Updated with measured and calculated values of the spectral resolution.

- June 20, 2014 – v3.2.1

  1. Section 9 – FIFI-LS – Updated with corrected information on observing modes and Cycle 3 Phase I/II requirements.

  2. Section 4.2.3 – FLITECAM – Updated web address for the new FLITECAM grism exposure time calculator.

- June 1, 2014 – v3.2.0

  1. Section 4 – FLITECAM – Updated for Cycle 3

- May 30, 2014 – v3.1.0

  1. Section 6.1 – GREAT – Updated channel configuration for Cycle 3

- May 23, 2014 – v3.0.0

  1. Updated from Cycle 2 (v2.1.2) to Cycle 3

1 Introduction

The Stratospheric Observatory for Infrared Astronomy (SOFIA) is a telescope with an effective diameter of 2.5 meters, carried aboard a Boeing 747-SP aircraft. It is the successor to the smaller Kuiper Airborne Observatory, which was operated by NASA from 1974 to 1996. The observing altitudes for SOFIA are between 37,000 and 45,000 feet, above 99% of the water vapor in the Earth's atmosphere. Once the observatory has achieved Full Operational Capability, the telescope and scientific instruments will provide imaging and spectroscopic capabilities across the 0.3 – 1600 μm wavelength range, making it one of the premier facilities for astronomical observations at infrared and sub-millimeter wavelengths. The first generation instrument suite provides coverage from 0.3 – 240 μm and will be fully operational within the next few years.

SOFIA is a joint project of NASA and the Deutsches Zentrum für Luft und Raumfahrt (DLR). The SOFIA Science Center (SSC), responsible for overseeing the scientific aspects of the mission, is located at the NASA Ames Research Center in Moffett Field, CA. Flight operations are conducted out of the NASA Dryden Flight Research Center's Aircraft Operations Facility (DAOF) in Palmdale, CA. The Science Mission Operations are jointly managed by the Universities Space Research Association (USRA) for NASA and by the Deutsches SOFIA Institut (DSI), in Stuttgart, for DLR. Aircraft operations are managed by NASA Dryden.

Most of the observing time on SOFIA is open to the international astronomical community via General Investigator (GI) proposal calls, which are issued on a yearly basis. The first of these proposal calls was for "Early Science," for which observations were obtained in a series of flights from May – July, September, and November 2011. The first open call for proposals, Cycle 1, covered the period from late 2012 to the end of 2013. The current proposal call is for Cycle 3 observations, which will take place between 1 March, 2015 and 31 January, 2016.

1.1 Intended Readership

This document, "SOFIA Observer's Handbook for Cycle 3" (hereafter the Observer's Handbook), provides information about SOFIA operations and the instruments that will be available for observations during Cycle 2, nominally scheduled for 1 March, 2015 - 31 January, 2016. The Observer's Handbook is the primary technical reference for astronomers who wish to submit a proposal for SOFIA Cycle 3. The information contained herein, and in documents and websites explicitly referred to, should be sufficient to allow proposers to plan viable SOFIA observations.

1.2 Updates to the Observer's Handbook

This version of the handbook is applicable to for Cycle 3. Between the time of writing and the start of Cycle 3 observations, the analysis of data obtained as part of the Instrument Commissioning process are likely to provide more empirical information regarding telescope and instrument performance. The Observer's Handbook will be updated as necessary and the list of changes will be included at the beginning of the document. Critical updates will also be published on the Cycle 3 web page[1]. Any information that supersedes what is given in this document will be explicitly indicated.

---

[1]http://www.sofia.usra.edu/Science/proposals/Cycle3/

1.3 Other Documents and Resources

The following additional documents are available on the SOFIA Information for Researchers web pages[2].

- The "**SOFIA Cycle 3 Call for Proposals**" describes how to prepare and submit proposals. It includes details on how proposals will be evaluated. It formally establishes the policies for all matters concerned with the rules governing SOFIA Cycle 3 for guest investigators.

- The "**FORCAST Observation Modes**"[3] document provides an explanation of the basic FORCAST observing modes for imaging observations. It is referred to explicitly in §5 below.

- The "**HIPO Throughput/Sensitivity Spreadsheet**" provides tools to estimate the signal-to-noise for HIPO observations.

- The "**Guide to Observation Planning with GREAT**"[4] is a tutorial for estimating exposure times for observations using GREAT. It is referred to explicitly in §6 below.

- The **1st Generation Instruments web pages**[5] provide a brief overview of the suite of first generation instruments that will be available on SOFIA once it reaches full operational capability.

- "**The Science Vision for the Stratospheric Observatory for Infrared Astronomy**"[6] presents many compelling science questions that SOFIA is uniquely positioned to address. The complementarity among several astronomical facilities (current and future, particularly in the IR/mm wavelength regime) are discussed where relevant. *Please note, that any information regarding the performance of the telescope and instruments contained within the "Science Vision" is superseded by this document and the SOFIA web sites.*

---

[2]http://www.sofia.usra.edu/Science/index.html

[3]http://www.sofia.usra.edu/Science/instruments/FORCAST_observations_modes.pdf

[4]http://www.sofia.usra.edu/Science/proposals/cycle3/Guide_To_GREAT_v7.pdf

[5]http://www.sofia.usra.edu/Science/instruments/index.html

[6]http://www.sofia.usra.edu/Science/docs/SofiaScienceVision051809-1.pdf

2 Overview

2.1 The Observatory

The telescope for SOFIA was supplied by the DLR as the major part of the German contribution to the observatory. It is a bent Cassegrain with 2.7-m parabolic primary mirror (2.5-m effective aperture) and a 0.35-m diameter hyperbolic secondary mirror. The telescope is mounted in an open cavity in the aft section of the aircraft and views the sky through a port-side door. The telescope is articulated by magnetic torque motors around a spherical bearing through which the Nasmyth beam passes. The unvignetted elevation range of the telescope is $20° - 60°$. The cross-elevation travel is only $\pm3°$, and therefore most of the azimuthal telescope movement required for tracking is provided by steering the airplane. The flight plan is thus determined by the list of targets to be observed during the flight.

The telescope feeds two f/19.6 Nasmyth foci, an IR focus for the science instruments and a visible light focus for guiding, using a dichroic and an aluminum flat. The secondary mirror provides chop amplitudes of up to $\pm5'$ (at chopping rates ≤ 10 Hz) and up to $\pm10'$ (at a rate ≤ 2 Hz). The visible beam is fed into the Focal Plane Imager (FPI), which is an optical focal plane guiding camera. Independent of the FPI are two other optical imaging and guiding cameras, the Wide Field Imager (WFI) and the Fine Field Imager (FFI), both of which are installed on the front ring of the telescope.

Seven first generation instruments, covering a wide range of wavelengths and resolving powers, will be used on SOFIA. Three of the instruments are Facility-class Science Instruments (FSIs), which will be maintained and operated by the Science Mission Operations (SMO) staff.

- Faint Object InfraRed Camera for the SOFIA Telescope (FORCAST)

- First Light Infrared Test Experiment Camera (FLITECAM)

- High-resolution Airborne Wideband Camera + Polarimeter (HAWC+)

The other four instruments are Principal Investigator-class Science Instruments (PSIs), which will be maintained and operated by the Instrument Principal Investigator (PI) teams. Two are German,

- German Receiver for Astronomy at Terahertz Frequencies (GREAT)

- Field Imaging Far Infrared Line Spectrometer (FIFI LS)

and two are from the US,

- Echelon-Cross-Echelle Spectrograph (EXES)

- High-speed Imaging Photometer for Occultation (HIPO)

3 Cycle 3

Cycle 3 observations will take place between 1 March, 2015 and 31 January 2016. **The observing time available to the astronomical community and the possibility of Southern Hemisphere deployments during Cycle 3 are contingent on the FY2015 budget appropriation for the SOFIA project. Information will be provided here when available.**

SOFIA cycle 3 observations will take place in a number of Science Flight Campaigns over the duration of the cycle. The campaigns will be interspersed with aircraft maintenance and instrument commissioning. Instruments that will be commissioned in 2015 are the multi-beam heterodyne receiver upGREAT and the far infrared camera and polarimeter HAWC+. These new capabilities will be offered in Cycle 4. Up to two Southern Hemisphere observing series are under consideration for the Cycle 3 time period, nominally in the summer of 2015.

Six instruments, FORCAST, GREAT, FLITECAM, EXES, FIFI-LS, and HIPO will be available during Cycle 3. The instrument capabilities, the available modes, and the resulting performance specifications of the telescope are described in later sections. **Some of the modes offered for FLITECAM will be available as "Shared Risk".**

Proposals are being solicited for the Cycle 3 SOFIA flights by USRA on behalf of NASA.

3.1 Observing with SOFIA during Cycle 3

The duration of each SOFIA Cycle 3 flight is expected to be between $9-10$ hours, $8-9$ hours of which will be available for observing at altitudes of $37,000-45,000$ feet. There will be only one instrument on board the aircraft for any given flight, with the exception of the FLIPO configuration (FLITECAM + HIPO). The SMO director will determine the total number of flights dedicated to each instrument, after consideration of the number of TAC-approved proposals for each.

Proposals should request observing time in units of hours. Once a proposal has been approved, the first stage is complete and the GI is then expected to carry out the detailed planning of their observations in consultation with a support scientist. This second stage of observation planning is known as Phase II. The GIs will be informed who their SMO support scientists are and how to contact them.

On each SOFIA Cycle 3 flight, there will be one or more seats available for GIs or designated CoIs of the proposals scheduled for that flight. Since there are a limited number of seats available on each flight, the choice of GIs given the opportunity to fly on SOFIA will be made by the SMO director according to a number of considerations, including the duration of science observations for each program on the flight and the proposal rank.

The observations will be carried out either by members of the instrument team along with SOFIA personnel, or solely by SOFIA personnel. The GIs on board SOFIA will participate in the observing, and monitor the data as it is received, but will have limited decision making abilities. For example, the GI will be allowed to make real-time changes to exposure times for different filters or channels. However, changing targets or any modifications that alter the durations of flight-legs will not be allowed.

Those GIs or CoIs chosen to fly aboard SOFIA will be required to complete a flight participation form, a medical release form, and documentation related to badging. In addition, they will be required to participate in an Egress Training course prior to being allowed on board the aircraft. Full details will be provided to GIs of approved proposals during the Phase II process.

3.2 Scheduling and Flight Planning

Scheduling and flight planning will be handled by the SMO staff and is not the responsibility of the GI. However, an understanding of the flight planning process and the restrictions inherent to airborne astronomy may be useful in preparing a successful proposal.

The most distinctive aspect of SOFIA flight planning is the interdependency of the targets observed in a flight. Because the azimuthal pointing is controlled primarily by the aircraft heading and because, in normal operations, the take-off and landing air fields are the same, efficient flight plans must generally balance East-bound with West-bound flight legs and South-bound with North-bound legs. This also means that for any flight only a limited fraction of the observing can be performed in a given region of the sky. An example of a flight plan flown during Basic Science in May 2011 is shown in Figure 1 below. Several more examples of flight plans flown during Basic Science can be found on the Information for Researchers Flight Plans[7] web page.

For the proposer this leads to several considerations:

- A strong scientific case must be made for observations with rigid time constraints or strict cadences in order to justify the restrictions they will impose on flight planning.

- Because the sky distribution of targets typically proposed for SOFIA observations (centered on the Galactic plane and certain regions of star formation, including Orion) is highly inhomogeneous, targets in areas that complement these high-target-density regions will allow more efficient flight planning and will likely have a higher chance - for a given scientific rating - to be scheduled. Consequently, it may be advantageous for those who can choose between targets from a large source pool for their SOFIA proposals and for those who plan to submit survey proposals to emphasize sources from complementary regions.

  For example, objects that complement the potentially popular Orion molecular clouds include circumpolar targets or targets north of about $40°$ with a right ascension in a roughly 6 to 8 hour wide window centered about 6 hours before or after the right ascension of Orion.

- The maximum length of flight legs will be determined by the need for efficient flight plans as well as the typical requirement that SOFIA take-off and land in Palmdale, California. In most cases, the longest possible observing leg on a given target is ~ 4 hours. Therefore, observations of targets requiring long integrations may have to be done over multiple flights and flight legs.

- GIs may propose for observations for which the flight does not originate or end in Palmdale, CA, for example, in order to conduct observations under time constraints that require a specific flight path or that require a single flight leg in excess of ~ 4 hours. Such proposals would be equivalent to a deployment and due to resource requirements and the impact that this would have on flight planning, the scientific justification must be strong. The final decision on whether to allow programs with such a high impact on scheduling and flight planning will be made at the Director's discretion.

GIs are encouraged to review the Flight Planning presentation delivered by Dr. Randolf Klein at the SOFIA User's Workshop in November, 2011. The full list of presentations can be found on

---

[7]http://www.sofia.usra.edu/Science/proposals/basic_science/FlightPlans_current.html
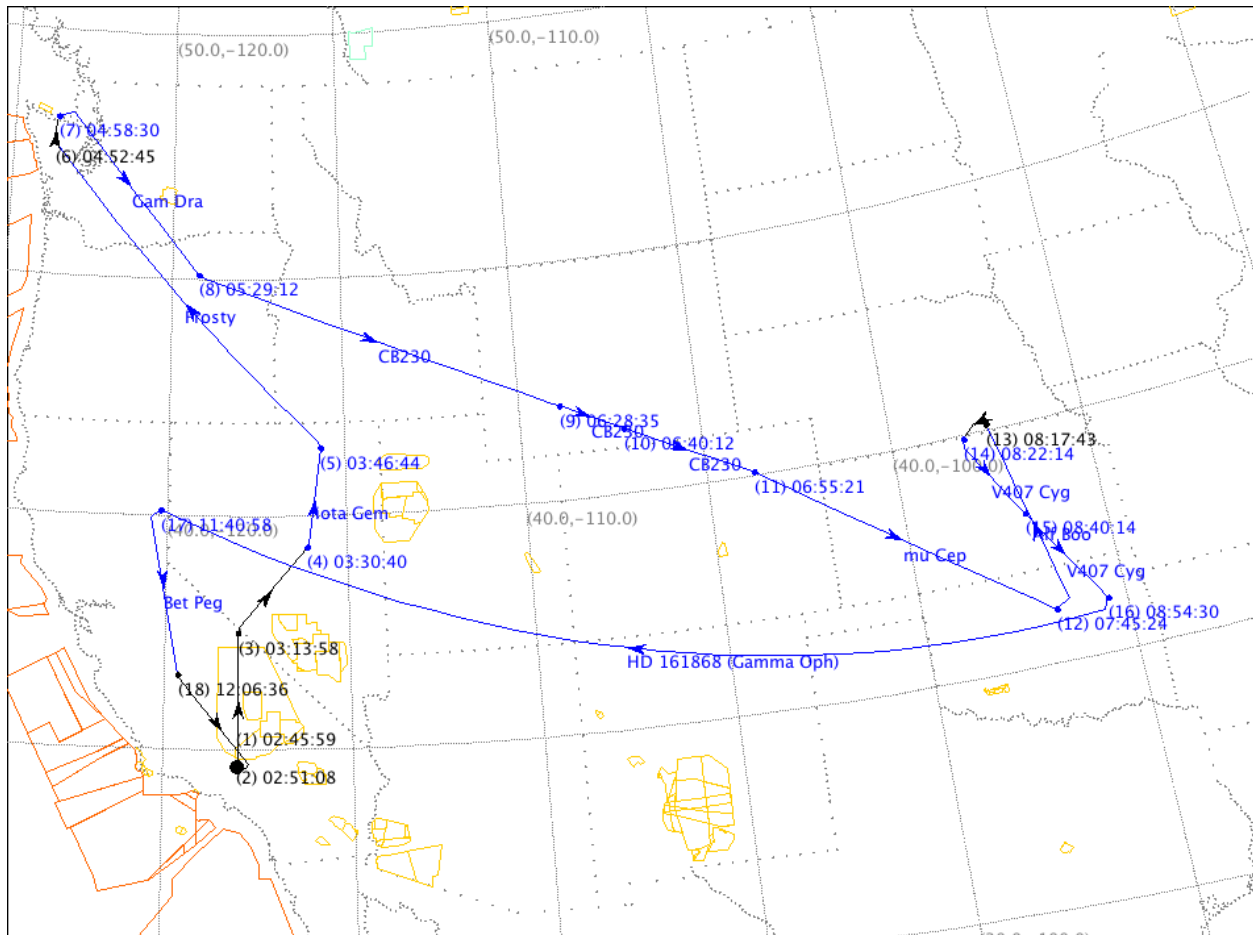
Figure 1: This is a sample flight plan flown in May 2011 during Basic Science. The take-off and landing were both from Palmdale, CA. Each leg is labeled with a time stamp and observing target when appropriate. Flight legs shown in black were "dead legs" during which no target was observed. The orange and yellow outlines indicate airspace with varying degree of restrictions which add to the complexity of designing efficient flight plans.

the SOFIA web site[8]. In addition, a much more detailed discussion of target scheduling and flight planning can be found in the Observation Scheduling and Flight Planning White Paper[9]

---

[8]http://www.sofia.usra.edu/Science/workshops/SOFIA_Workshop_2011/index.html

[9]http://www.sofia.usra.edu/Science/observing/flightPlanning_whitePaper.pdf

3.3 Acquisition and Guiding

SOFIA has three optical cameras for acquisition, guiding and tracking. The Wide Field Imager (WFI) and Fine Field Imager (FFI) are mounted on the telescope head ring. The upgraded Focal Plane Imager (FPI+) images the focal plane of the telescope via a dichroic and a tertiary mirror. All three imagers use "High Speed Slow Scan" CCD cameras.

The WFI has a $6° \times 6°$ field of view, and is expected to achieve a centroid precision of $\sim 8''$ for stars brighter than R=9. The field of view of the FFI is $1° \times 1°$. It is expected to achieve a centroid precision of $\sim 1''$ for R=11 or brighter stars. **The FPI+ has an $8'$ diameter and is expected to provide a centroid precision of $0.''05$ for R=16 or brighter stars.**

Most observers do not need to select guide stars as they will be chosen by the SMO staff. However proposers should be aware that the guiding cannot be done on IR sources unless they are optically bright.

3.4 Observing Moving Targets during Cycle 3

Once SOFIA achieves its nominal operating capabilities, it will be able to observe solar system targets by (i) guiding on the object itself, (ii) offset guiding from field stars, or (iii) predictive tracking based on accurate ephemerides. However, by the time of Cycle 3 observations, **only the first of these techniques will have been tested and implemented.**

The SOFIA project will make every attempt to observe Solar System targets in highly ranked proposals. However, proposers should bear in mind that Cycle 3 observations of moving targets are "Shared Risk". The observatory is still in development so many of its performance characteristics will not be fully known at the time of the Cycle 3 proposal deadline.

Successful guiding on a moving target requires it to be bright at visible wavelengths, where the guider cameras operate. Our current estimate is that we will be able to guide on solar system targets with R $\leq$ 10 and that have a non-sidereal angular speed of $1''$/s or less. The minimum acceptable solar elongation for a target is limited by the lower elevation limit of the telescope and the rule that no observations can be acquired before sunset or after sunrise. For Cycle 3, the minimum solar elongation is 25 degrees.

Identification of solar system targets will be done manually by the Telescope Operator by inspecting images obtained with the FPI. The ephemerides of the proposed target must be accurate enough to allow for unambiguous identification. While the required accuracy could vary somewhat based on the complexity of the background star field, it should in general be better than about $30''$.

For moving objects with visible magnitude fainter than 10th, it will be possible (on a Shared Risk basis) to utilize the fast diagnostic camera (FDC) as a guider camera. This mode has not yet been tested and requires a custom installation, so only a limited number of such observations will be performed. With this camera sources brighter than 15th magnitude should be usable for guiding. Proposals requesting this configuration should note the Shared Risk involved and make the case for why such observations should be performed during Cycle 3.

3.5 Line-of-Sight (LOS) Rewinds

In many respects, the design of the SOFIA telescope is similar to that of a typical altitude-azimuth telescope. One such similarity is that as the telescope tracks a target it must rotate in

order for the sky to remain at the same orientation on the detectors. The range of free rotation by the telescope is limited, however, to $\pm \sim 3°$. Hence, the telescope must periodically undergo a "Line-of-Sight (LOS) rewind", or de-rotation. The required frequency of LOS rewinds depends on rate of field rotation experienced by the target, which is a complex function of the position of the target in the sky relative to that of the aircraft heading. Since the relative target position is not known *a priori*, but is only determined during flight planning, it is not possible to determine precisely the field rotation rate until after the observations have been scheduled. However, one can estimate either the rate of field rotation using Figure 2 or the time it takes for a field of view to rotate by six degrees using Figure 3.
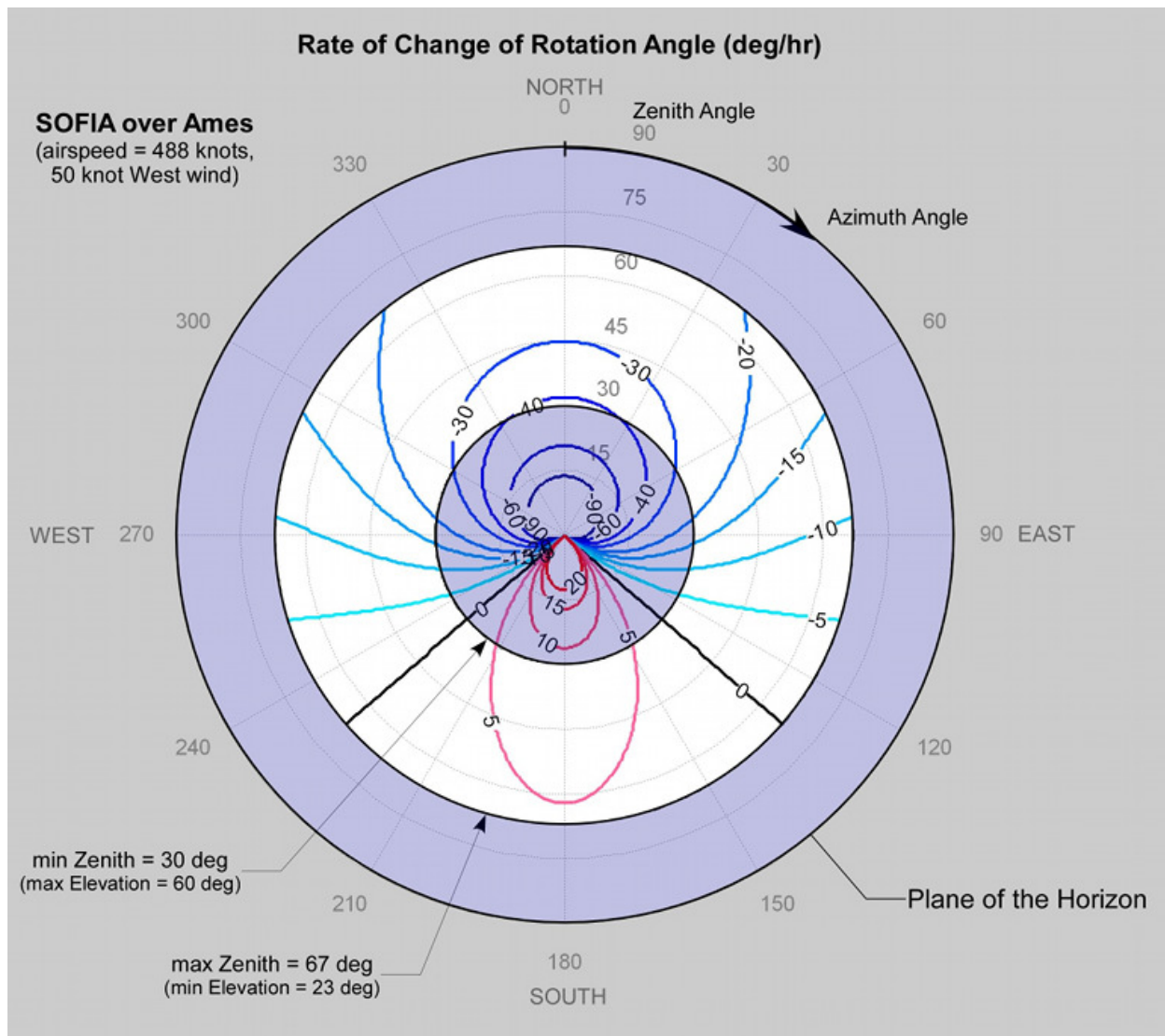
Figure 2: This plot shows the rate of change in the rotation angle (degrees/hour) as a function of target zenith angle and azimuth angle. The rates are calculated assuming an aircraft latitude of 37.415° N. The unvignetted range of zenith angles is shown in white.

In order to use the plots effectively, one must first use the SOFIA Target Visibility Tool[10] or similar visibility planning tool to determine the airplane heading (AH) and the target elevation (El) at the desired date of observation. Since the telescope is situated in the port side (i.e. the left side as seen by a person on board, facing the front of the aircraft), the target azimuth angle (Az) is calculated according to, $Az = AH - 90°$. The zenith angle (ZA) is calculated according to, $ZA = 90° - El$. Once the ZA and Az of the target have been determined for a sample observation date, then the LOS plots provide an estimate of the rotation of field for the target.

---

[10]https://dcs.sofia.usra.edu/observationPlanning/visibilityTool.jsp
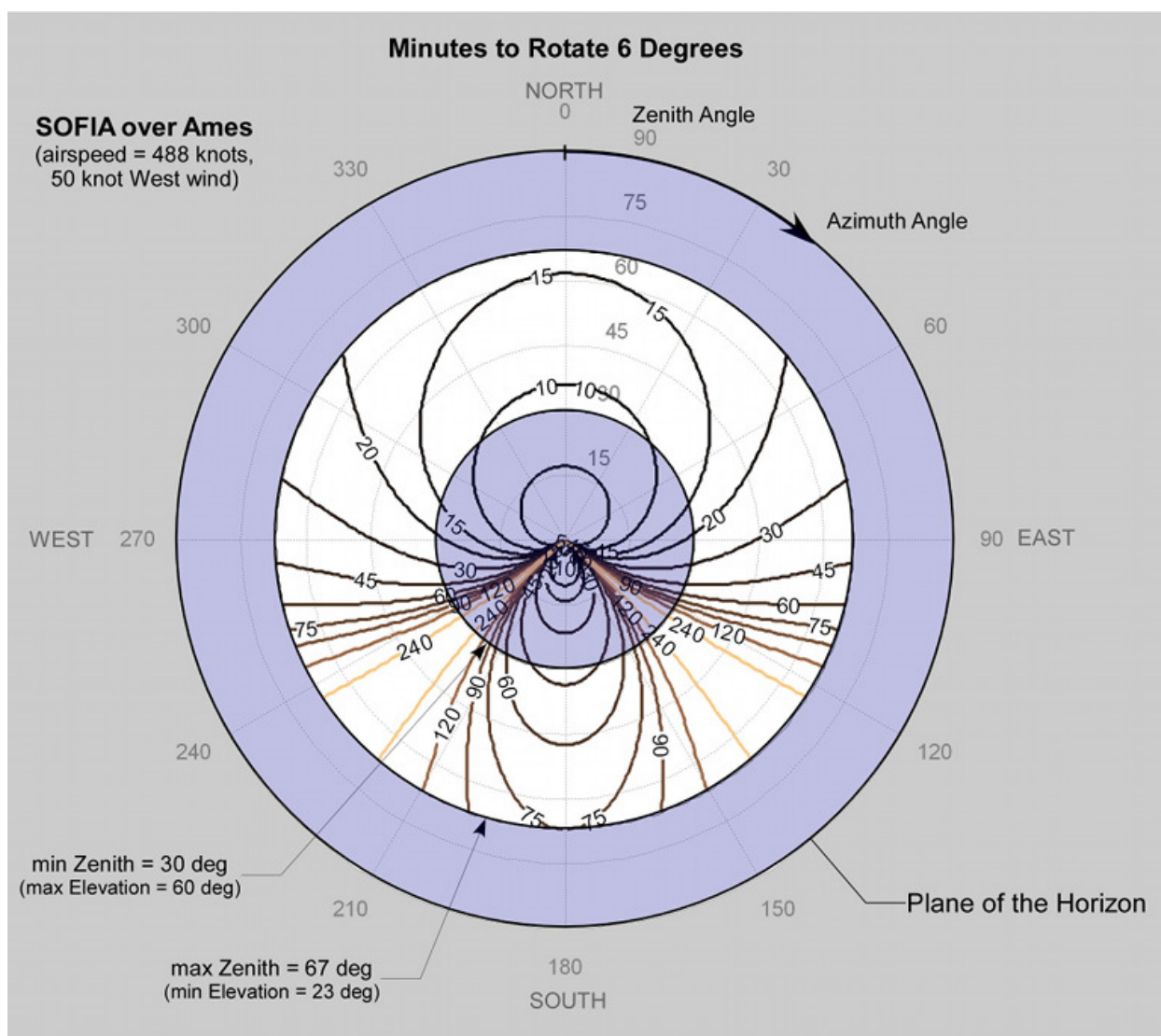

Figure 3: This plot shows the time it takes for the field of view to rotate by 6 degrees as a function of target zenith angle and azimuth angle. The times are calculated assuming an aircraft latitude of 37.415° N. The unvignetted range of zenith angles is shown in white.

For example, according to the SOFIA Target Visibility Tool, during the month of August, the W3 star forming region, is at an elevation that ranges from between about $20°$ and $60°$ throughout the evening. The aircraft heading would be $\sim 130°$. Hence, $ZA = 70° - 30°$ for an average of $\sim 50°$ and $Az \simeq 40°$. On Figure 2, these coordinates correspond to a field rotation rate of approximately -25° per hour, or roughly 6 degrees every 15 minutes as indicated on Figure 3.

When using Figures 2 and 3 to estimate the rotation of field, it is important to bear in mind the associated caveats. First, the plots were calculated assuming that the aircraft position was at $37.415°$, the latitude of NASA Ames. In practice, the latitude of the aircraft may deviate significantly from this. In addition, in the example, we made the estimates using the average ZA of the target, but in practice, neither the ZA at the time of observation nor the actual observation date will be known until flight planning is complete. This means that one should consider the estimates of the rotation of field as being only approximate. Finally, in flight, the LOS rewinds are performed after a field rotation of $\sim 3°$ rather than the maximum possible range of $6°$, in order to account for slight deviations in the airplane heading.

Special care must be taken when designing spectroscopic observations. GIs should bear in mind that the orientation of the slit on their targets will change with each LOS rewind. For point sources, this should not cause problems, but for extended sources, this means that after each rewind the slit will be sampling a slightly different region of the source. In addition, there is no way to choose the orientation of the slit on the target.

3.6 Atmospheric Transmission

SOFIA operates at altitudes above 99% of the water vapor in the atmosphere. The average atmospheric transmission across the SOFIA bandpasses is about 80% at these altitudes. There are however a number of strong absorption features which, even at these altitudes, make the atmosphere nearly opaque. Broad band filters, such as those on FORCAST, account for the presence of such features. However, when using high-resolution tunable instruments such as GREAT and EXES, it is necessary to examine the atmospheric transmission at the wavelengths of interest in detail. This may be done using the web interface to the ATRAN program[11] that was developed and kindly provided to the SOFIA program by Steve Lord. A plot of the atmospheric transmission seen by SOFIA in comparison to that achieved at Mauna Kea is shown in Figure 4 below.

In addition to its dependence on wavelength due to the presence of absorption features, the atmospheric transmission varies with latitude and with time of year, primarily due to differences in the amount of water vapor. It also exhibits variations on smaller time scales due to changes in the location of the tropopause. Full discussions of these issues may be found in Haas & Phister 1998 (PASP, 110, 339) and Horn & Becklin 2001 (PASP, 113, 997).

The variations in atmospheric water vapor could have a significant impact on some observations, particularly when using GREAT and EXES or grism modes with FLITECAM and FORCAST. For example, GREAT observations of a line situated on the shoulder of an atmospheric water feature could be strongly affected by water vapor variability. SITE allows the user to specify the water vapor overburden and adjusts the time estimates appropriately. A water vapor monitor will be functioning during full operations, but may not be fully functional during Cycle 3.

---

[11]http://atran.sofia.usra.edu/cgi-bin/atran/atran.cgi

3.7 Calibration

Calibration observations will be planned by the SMO staff and instrument scientists using standard stars, asteroids, and planets. Calibration plans will be specific to each instrument. In all cases, **except EXES**, the time used for calibration observations are considered part of the general overhead and will not be charged against the GI program time. GIs should look at the calibration details provided in each instrument chapter below for specific calibration plans.

The calibration accuracy will depend on the instrument and observation mode, but an accuracy of $\leq 20\%$ is expected to be obtained, even in "Shared Risk" modes. Unless the proposer requires more accurate calibration, there is no need to request time for calibration or to choose calibration targets. If the GI has such requirements for more accurate calibration, they must be justified in the proposal, and the time required for the calibration observations should be included in the total time request. The only exception to this is EXES, for which all calibration observations must be specified in the proposal and will be charged to the science program time.

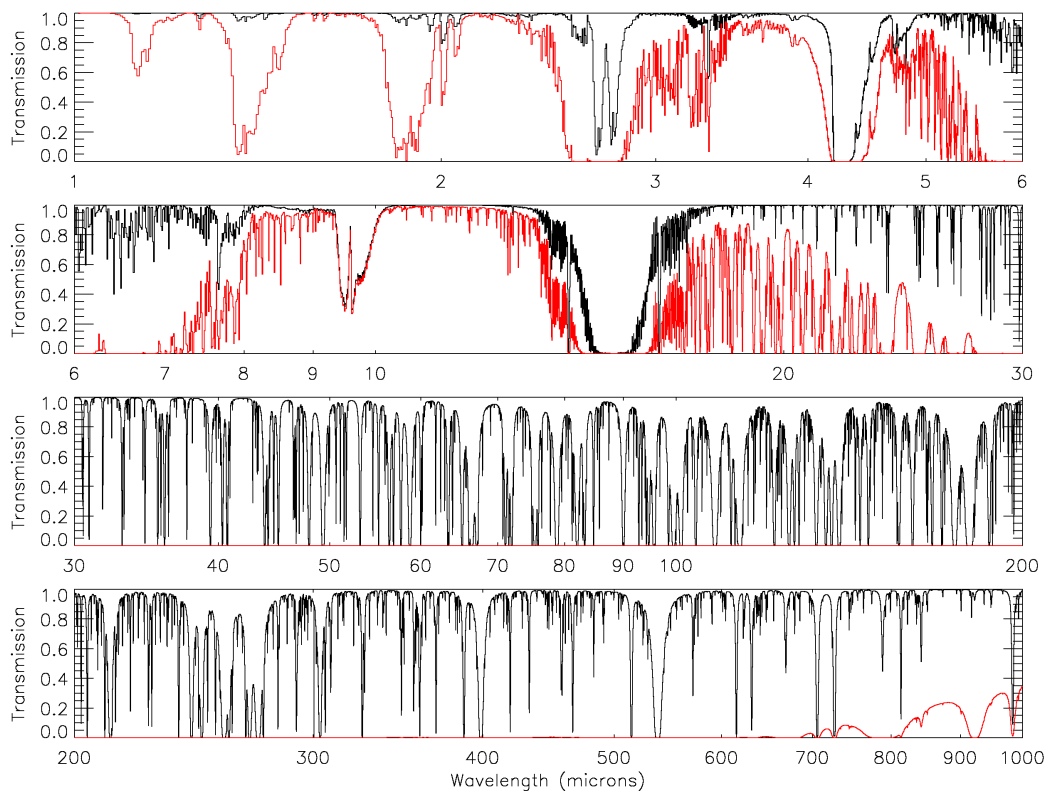Figure 4: This is a plot showing the atmospheric transmission for SOFIA (black) at an altitude of 41K feet and 7.3 μm of precipitable water vapor compared to Mauna Kea (red) at an altitude of 13.8K feet and 3.4 mm water vapor over the range of $1 - 1000$ μm. The transmission was calculated using the ATRAN code with a telescope zenith angle of $45°$. and the data were smoothed to a resolution of R=2000.

4 Instruments I: FLITECAM

4.1 Instrument Overview

The **F**irst **L**ight **I**nfrared **TE**st **CAM**era (FLITECAM) is an infrared camera operating in the 1.0 – 5.5 μm waveband. It consists of a 1024×1024 InSb detector with $0\rlap{.}''475 \times 0\rlap{.}''475$ pixels and uses refractive optics to provide a $\sim 8'$ diameter field of view. The instrument has a set of broadband filters for imaging, as well as grisms for moderate resolution spectroscopy.

Additionally, FLITECAM was designed to be co-mounted on the telescope with the **H**igh-speed **I**maging **P**hotometer for **O**ccultations (HIPO), providing simultaneous optical through near-IR (NIR) imaging capabilities. This mode, called FLIPO, is described in detail under Section 7, below.

4.1.1 Design

FLITECAM consists of a cryogenically cooled near-IR (NIR) camera that can be used for both imaging and grism spectroscopy. A schematic of the optical bench is shown in Figure 5 with a full ray trace diagram in Figure 6. The incoming beam first passes through the entrance aperture and into the collimator assembly, a stack of custom designed lenses that allow imaging of nearly the entire $8' \times 8'$ SOFIA field of view (FOV). The beam is then repositioned using three flat fold-mirrors so that it passes through the image pupil and through a pair of 12-position filter wheels. A fourth flat fold-mirror redirects the beam through the f/4.7 refractive imaging assembly, which then focusses the beam on the array.

When observing in spectroscopy mode, only minimal changes to the optical path are required. First, the slit mask is inserted into the beam immediately behind the aperture window at the telescope focus. The slit is a single 16.5 mm long slit ($2'$ on the detector) divided in half with two different widths, one $2''$ and the other $1''$. Second, the chosen grism and order sorting filter, located in filter wheel #2 and #1, respectively, are set in place. Details are presented in Section 4.1.5 below.

4.1.2 Camera Performance

The FLITECAM detector is a 1024×1024 pixel indium antimonide (InSb) Raytheon ALADDIN III array cryogenically cooled to 30 K. The detector has 27 μm pixels which translate to a plate scale of $0\rlap{.}''475$ per pixel, resulting in a nearly $8'$ square FOV. The detector is optimized for use between $1 - 5.5$ μm with a relatively high quantum efficiency (QE) of $\sim$80%. The system has a read noise of ~ 40 e$^-$ and dark current of ≤ 1 e$^-$ sec^{-1}.

The on-axis image quality (IQ) of the camera is excellent and images obtained with FLITECAM are expected to be diffraction limited from 3-5.5 μm. From 1-3 μm, the IQ will be limited by contributions from the telescope optics, telescope jitter, shear layer seeing, and the diffraction limit. Ground based tests under the best conditions at the Lick Observatory indicated that the IQ is stable within $1\rlap{.}'5$ of the optical axis, but that beyond this distance, coma begins to appear. The extent of the coma has not yet been parameterized.

The detector well depth is relatively shallow, $\sim$80,000 e$^-$, which, when combined with the high detector QE, may necessitate relatively short exposure times, particularly on bright sources or in
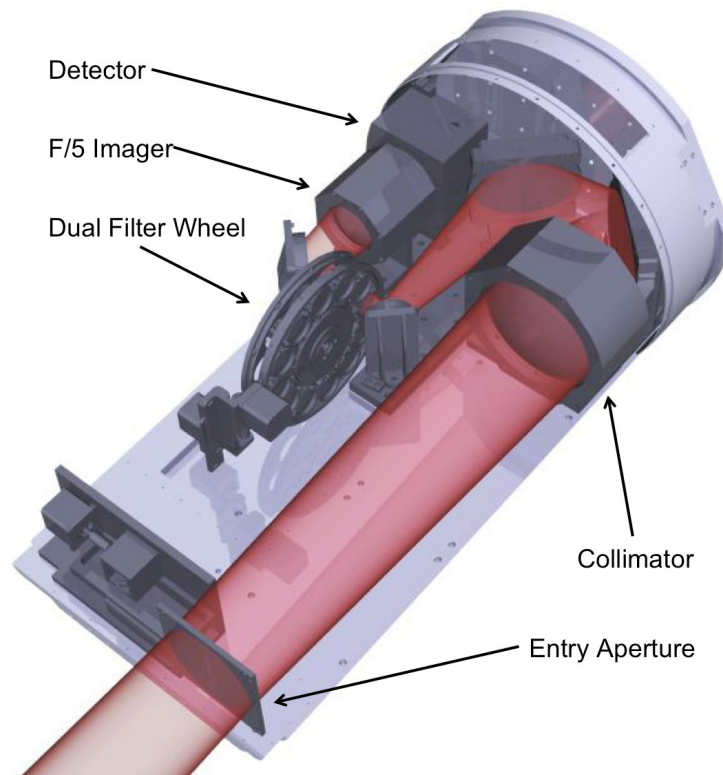
Figure 5: This is a block diagram of the front end of the FLITECAM instrument with labels of important components.

regions of high sky background. The shortest exposure time available for a full 1024×1024 detector readout is 0.3 seconds. However, faster readout times can be achieved using sub-arrays – 0.1 sec for a 512×512 sub-frame and 0.02 sec (50 Hz) for a 64×64 pixel sub-frame. An additional "movie" mode sampling a 32×32 sub-frame at $\sim$1.6 msec is available for use with HIPO, allowing rapid image acquisition for occultation studies.

Care must be taken not to over-expose the detector since charge persistence can be a significant problem for InSb arrays. If the detector is over-exposed, it is necessary to take several long exposures ($\sim$5 minutes each) of blanks mounted in the filter wheel to allow the detector to recover. To help mitigate the problem of accidental saturation of the detector, filter changes are carefully orchestrated to ensure that the sky is never viewed through the two open filter wheel positions.

4.1.3 Filter Suite

The core of the FLITECAM filter suite is a set of standard Barr bandpass filters used for imaging at J, H, K, L, & M, which are all located in filter wheel #1. In addition, filter wheel #2 holds a selection of specialty, narrow-band imaging filters, including Paschen α and Paschen α continuum filters, an ice filter centered on the 3.07 μm H_2O ice feature, a polycyclic aromatic hydrocarbon (PAH) filter centered on the prominent 3.3 μm feature, and L_{narrow} and M_{narrow} filters. Finally,
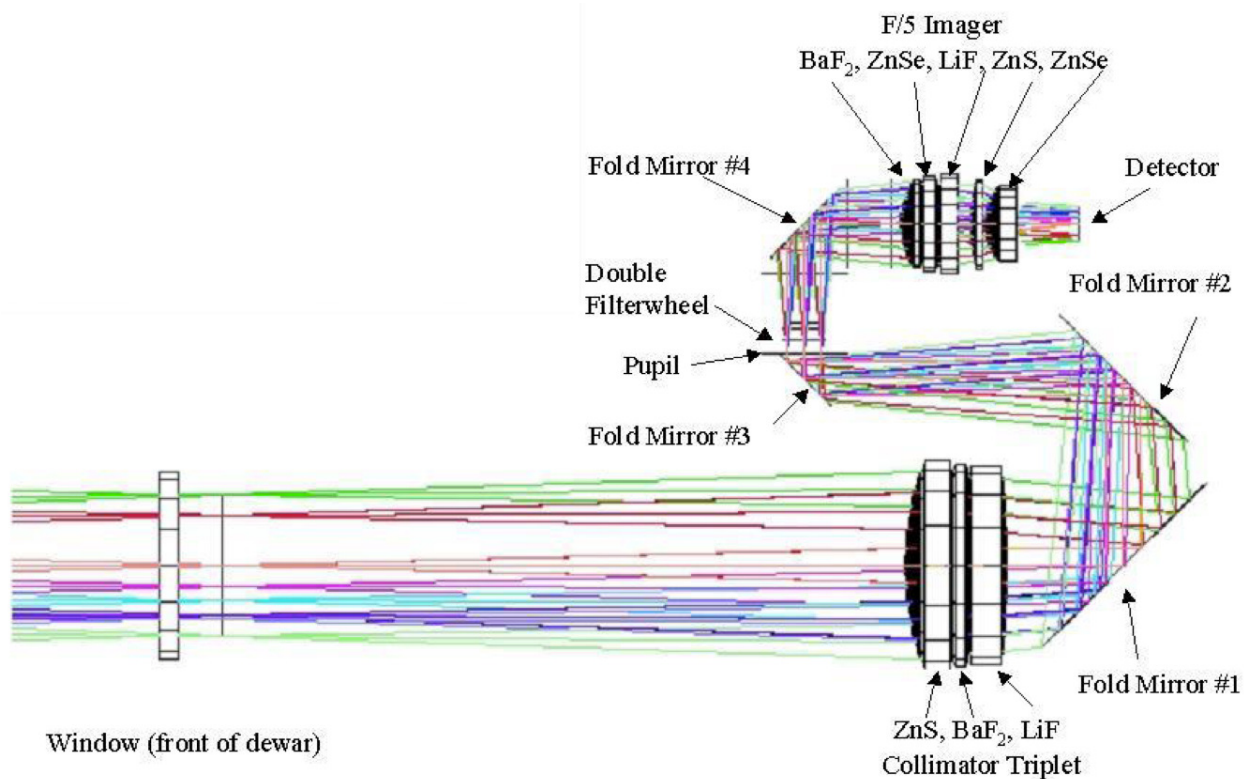
Figure 6: This is the ray diagram for the FLITECAM instrument. The inset at the upper left displays the additional lenses inserted into the light path for the pupil-viewing mode .

there are a number of order sorting filters (OSFs) for use with the grisms, including J and H (both dual purpose), K_{wide}, K_{long}, and "L&M". Additional details of the OSFs are given in Section 4.1.5.

As the instrument commissioning was performed in the combined FLITECAM/HIPO mode, with its associated elevated long-wavelength background, the performance in L and M band (regular and narrow filters), and the LMA grism mode (grism A with the L+M order sorting filter) have not been verified. Hence these modes, as well as the PAH (3.29 μm) and Water Ice (3.08 μm) filters, and the "LMB" grism mode, are *Shared Risk* observations. If the elevated backgrounds are not (fully) rectified, accepted proposals requesting these filters will be executed only after a case-by-case analysis of their actual feasibility.

The central wavelengths and band widths of the available imaging filters are provided in Table 1. This table also includes the sensitivity values (Minimum Detectable Continuum Flux; MDCF) discussed in Section 4.1.4. Filters that will only be available on a shared risk basis during Cycle 3 are indicated. Figure 7 displays the transmission profiles (normalized to their peak transmission) for the imaging filters over-plotted on an ATRAN model of the atmospheric transmission. The filter transmission curves are available on the SOFIA "Science Instrument Suite" website in the section for FLITECAM[12].

Table 1: FLITECAM Filter Characteristics

Passband	λ_{eff} (μm)	$\Delta\lambda$ (μm)	Filter Wheel	MDCF[a] (μJy)	MDCF[b] (μJy)
Standard Filters					
J	1.25	0.26	1	25.7	27.4
H	1.64	0.27	1	33.5	35.7
K	2.12	0.35	1	38.7	57.5
L [c]	3.55	0.55	1	440	–
M [c]	4.87	0.51	1	2720	–
Specialty Filters					
Pa α	1.88	0.02	2	179	195
Pa α Cont.	1.90	0.02	2	178	195
Ice [c]	3.05	0.16	2	504	1130
PAH [c]	3.30	0.09	2	1070	2260
L_{narrow}^{c}	3.61	0.18	2	1010	2110
M_{narrow}^{c}	4.81	0.15	2	5430	–
Order Sorting Filters[d]					
H_{wide}	1.80	0.80	1	–	–
K_{wide}	2.34	0.81	1	–	–
K_{long}	2.54	0.48	1	–	–
L+M	4.11	2.63	1	–	–

[a]See Section 4.1.4
[b]Empirically measured MDCF values when FLITECAM is co-mounted with HIPO in the FLIPO configuration.
[c]Will be offered as *Shared Risk* during Cycle 3
[d]Will not be available for imaging

4.1.4 Imaging Sensitivities

At the time of writing, the commissioning of FLITECAM has yet to be completed, and therefore the results of the analysis of in-flight data are not available. Instead, the Minimum Detectable Continuum Flux (MDCF; 80% enclosed energy) in μJy needed to get S/N = 4 in 900 seconds has been estimated for each filter for an altitude of 41,000 feet (7.3 μm of precipitable water vapor) from a model of the instrument and the atmosphere. The values are presented in Table 1 above and are plotted in Figure 8. The horizontal bars on the data in the figure indicate the effective bandpass at each wavelength. At the shorter wavelengths the bandpass is sometimes narrower than the symbol size. In addition to the theoretical sensitivity values for FLITECAM we have included the as-measured imaging sensitivities in the FLIPO (combined HIPO+FLITECAM) mode.
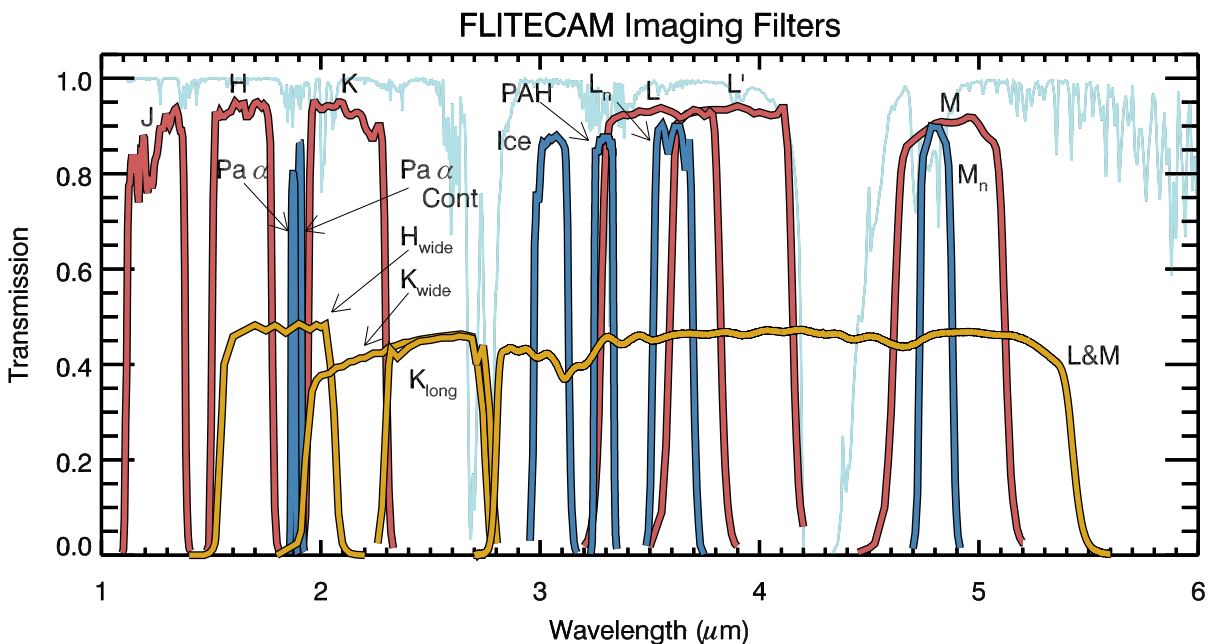
Figure 7: Plotted here are the FLITECAM filter transmission curves overlayed on an ATRAN model of the atmospheric transmission across the FLITECAM bandpass assuming a zenith angle of 45 degrees and 7 μm of precipitable water vapor. The transmission profiles of the standard filters are shown in red, specialty filters are shown in blue, and OSFs in gold. The OSF transmission profiles have been scaled by 50% for clarity.

Atmospheric transmission will affect sensitivity, particularly at wavelengths > 4 μm, depending on water vapor overburden. Until the instrument has been more accurately characterized at these longer wavelengths, the L and M band filters will be offered on a *shared risk* basis.

4.1.5 Grisms

A selection of three grisms is available in FLITECAM to provide medium resolution spectroscopic capabilities across the entire $1 - 5.5$ μm range. The grisms are mounted in filter wheel #2 and are used along with Order Sorting Filters (OSFs) mounted in filter wheel #1 (see Table 1) to prevent order contamination. A summary of the grism properties is provided in Table 2.

Grisms were chosen for use in FLITECAM since they minimize the changes necessary to the optical path while still allowing moderate spectral resolution. The grisms are made of direct-ruled (i.e. etched) KRS-5 (thallium bromoiodide) material that provides a relatively high index of refraction (n $\sim$ 2.4) without the significant absorption features that plague grisms with adhered transmission gratings. The three grisms were fabricated by Carl-Zeiss (Jena, Germany) each with an apex angle of 34.4°, but with different groove spacings to allow coverage of the entire $1 - 5.5$ μm band (see Table 2).

The FLITECAM slit mask is mounted in a slide mechanism at the telescope focus, immediately inside the entrance window to the dewar. The mask is an aluminum plate with a 16.5-mm long
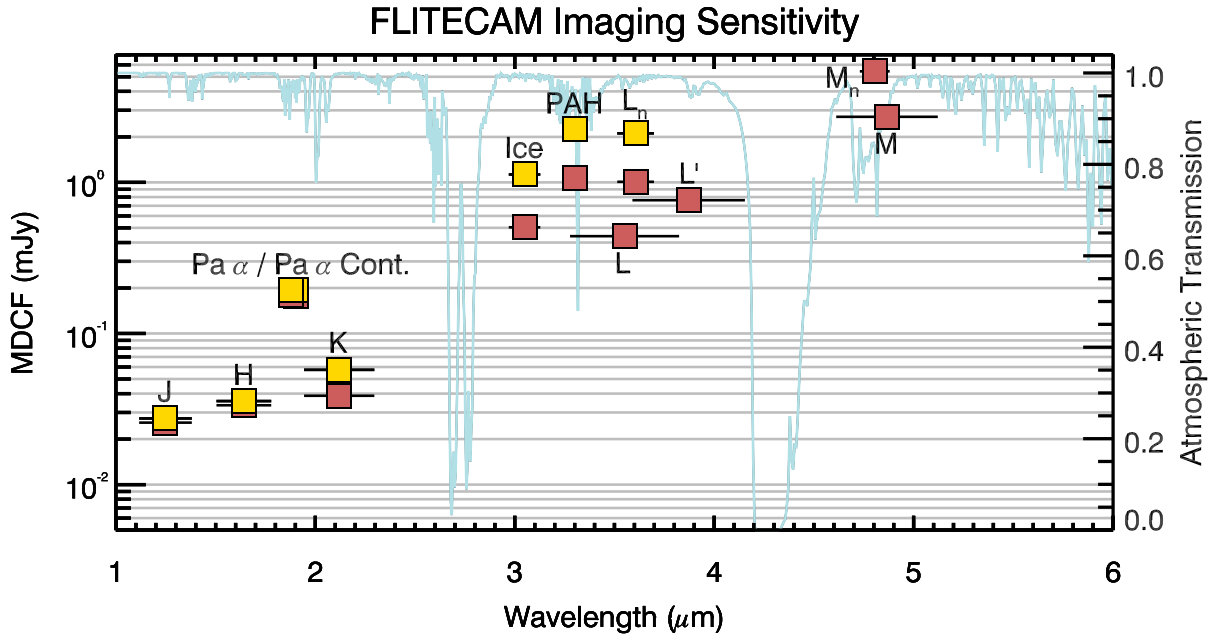
Figure 8: Theoretical FLITECAM imaging sensitivities for a continuum point source at the effective wavelengths of the FLITECAM filters listed above (red boxes). Yellow boxes indicate the imaging sensitivities for the FLIPO configuration (i.e. FLITECAM co-mounted with HIPO). The values reported are for a S/N of 4 in 900 seconds at water vapor overburdens of 7 μm. The horizontal bars correspond to the photometric band pass.

(2$'$ as seen from the detector) slit, half of which is 675 μm wide ($\sim$1$''$5 on the detector) and the other half of which is 450 μm wide (1$''$), allowing both low and high-resolution spectra at R = $\lambda/\Delta\lambda \sim 850$ and ~ 1700 respectively.

No calibration lamps are installed in FLITECAM. Consequently, wavelength calibration will be performed using atmospheric absorption lines.

4.1.6 Spectroscopic Sensitivities

At the time of writing, the commissioning of FLITECAM has yet to be completed and the results of the analysis of in-flight data are not available. Instead, Figure 10 presents the *expected* continuum point source sensitivities for the FLITECAM grisms combined with an ATRAN model of the atmospheric transmission. The Minimum Detectable Continuum Flux (MDCF; 80% enclosed energy) in Jy needed for a S/N of 4 in 900 seconds at a water vapor overburden of 7.3 μm, an altitude of 41K feet, and an elevation angle of 45° (an airmass of 1.4) is shown.

Table 2: FLITECAM Grism Characteristics

Grism	Groove Sep. (l/mm)	Order	OSF[a]	SPT Ident.[b]	Coverage (μm)	High-Res (R= $\lambda/\Delta\lambda$)	Low-Res (R= $\lambda/\Delta\lambda$)
A	162.75	1	L+M[c]	A1_LM	$4.395 - 5.533$	N/A	N/A
		2	K$_{long}$	A2_KL	$2.211 - 2.722$	1690	1140
		3	H$_{wide}$	A3_Hw	$1.493 - 1.828$	1710	1290
B	217	1	L+M[c]	B1_LM	$3.303 - 4.074$	1780	1200
		2	H$_{wide}$	B2_Hw	$1.675 - 2.053$	1750	1320
		3	J	B3_J	$1.141 - 1.385$	1720	1425
C[d]	130.2	2	L+M	C2_LM	$2.758 - 3.399$	1670	1300
		3	K$_{wide}$	C3_Kw	$1.854 - 2.276$	1650	1390
		4	H	C4_Hw	$1.408 - 1.718$	1640	1400

[a]Order Sorting Filter

[b]Identifier used in the SOFIA Proposal Tool (SPT)

[c]This combination of Grism and OSF will be available on a shared risk basis during Cycle 3.

[d]Grism C suffers from excess light at the blue end of each order. This issue is under investigation at the time of this writing.

4.2 Planning FLITECAM Observations

Two basic observing modes will be available during Cycle 3, imaging and grism spectroscopy. At present, however, commissioning of FLITECAM has not been completed, so the imaging and spectroscopic capabilities have not been fully characterized for use. For this reason, it is important for GIs to verify that they are using the most recent version of this document as it will be updated regularly as new information becomes available.

4.2.1 Planning Imaging Observations

FLITECAM Imaging observations can be obtained in two different modes, Stare (with 5 or 9 point dither) or Nod mode, depending on the target and astronomical background. Chopping will generally not be used.

Stare mode observations involve a single telescope pointing centered on the source. It is recommended that the observation be dithered to facilitate background subtraction. Dithering can be performed by selecting from two pre-programmed dither patterns. The user can choose either a 5-point diamond or a 9-box dither pattern. Both patterns are scalable, i.e., though the relative separation between the points in these patterns are fixed, the absolute separation can be specified by the user.

If the science target is extended or if it is located in a crowded region or region of extended emission, dithering alone may not be able to produce a suitable sky background frame. In this case the GI may elect to observe using Nod mode. Selection of the nod direction and amplitude
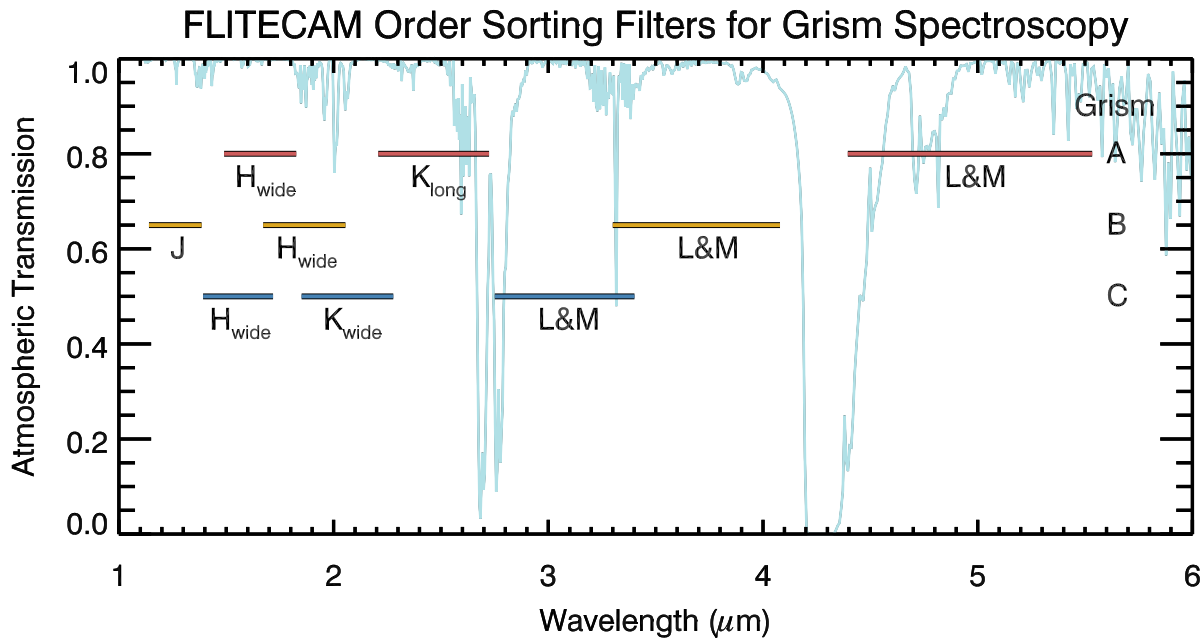
Figure 9: Plotted here are band passes for each of the grism + order sorting filter (OSF) combinations available for FLITECAM grism spectroscopy. The grism used for each OSF set is labeled on the right. In light blue is a plot of the ATRAN model of the atmospheric transmission across the FLITECAM bandpass (assuming a zenith angle of 45 degrees and 7 μm of precipitable water vapor).

depends on the field of view around the target and will need to be chosen carefully to allow proper background subtraction. In Nod mode, it is recommended that the observation include dithering.

The observing efficiency for FLITECAM Stare mode observations with dithering is expected to be on the order of 70%. Observations in Nod mode are expected to result in a decrease in observing efficiency to around 35%. However, these efficiencies are built-in to the SOFIA Proposal Tool (SPT; further details in §11.1) and do not need to be specified by the GI.

4.2.2 Planning Spectroscopic Observations

Grism spectroscopy with FLITECAM will also be available during Cycle 3.

Observations may be obtained with either an "ABBA" or an "AB" nod pattern that is either on-slit or off-slit.

Guiding during spectroscopic observations will be conducted with either the telescope guide cameras or with HIPO, if FLITECAM and HIPO are co-mounted in the FLIPO configuration (see Section 7).

It is important to note that due to the fixed position of the grisms/slits in the filter/aperture wheels, the orientation of the slit on the sky will be dependent on the flight plan and will not be able to be predetermined. Further, the slit orientation rotates on the sky with each telescope Line-of-Sight (LOS) rewind. These limitations may be especially important to consider when proposing
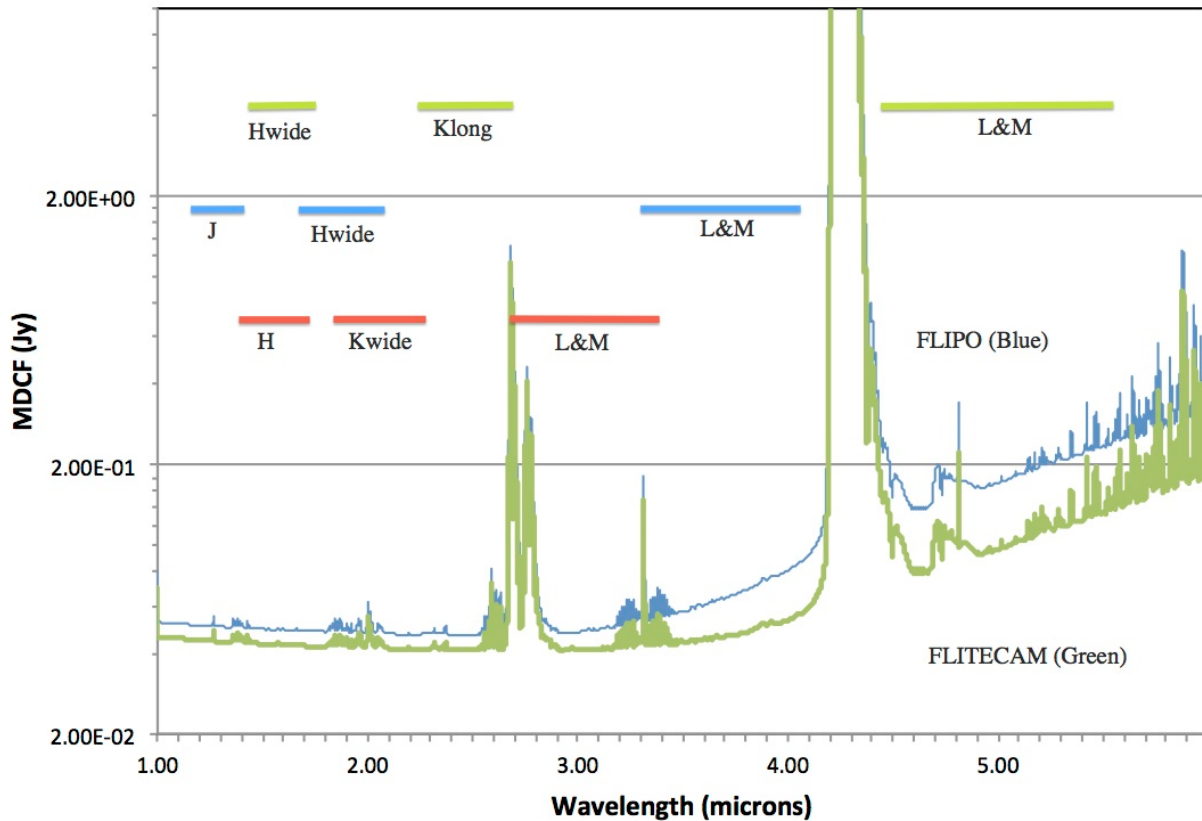
Figure 10: Plotted here are the FLITECAM (green line) and FLIPO (blue line) grism sensitivities for a continuum point source across the entire FLITECAM bandpass. The values reported are for a S/N of 4 in 900 seconds at a water vapor overburdens of 7.3 μm at an altitude of 41K feet and a 45° elevation angle.

observations of extended objects.

The observing efficiency for FLITECAM spectroscopic observations is currently unknown, but is expected to be of order 25%. However, these efficiencies are built-in to the SPT and do not need to be specified.

4.2.3 Estimation of Exposure Time

The exposure times for FLITECAM imaging observations should be estimated using the on-line exposure time calculator, SITE[13]. SITE can be used to calculate the signal-to-noise ratio (S/N) for a given "total integration time", or to calculate the total integration time required to achieve a specified S/N. The format of the S/N values output by SITE depends on the source type. For Point Sources, the reported S/N is per resolution element, but for Extended Sources, it is the S/N

---

[13]http://dcs.sofia.usra.edu/proposalDevelopment/SITE/index.jsp

per pixel. The total integration time used by SITE corresponds to the time for a single chop/nod pair, without overheads.

The exposure times for FLITECAM grism mode spectroscopic observations should be estimated using the on-line exposure time calculator[14]. This calculator can be used to calculate the signal-to-noise ratio (S/N) for a given "total integration time", to calculate the total integration time required to achieve a specified S/N, or to estimate the limiting flux for a desired S/N.

For both imaging and spectroscopy modes, the estimated total integration time from the respective calculators should be used as the time for an observation in the SOFIA Proposal Tool (SPT; further details in §11.1). **Overheads should not be included**, as SPT calculates them independently.

---

[14]http://flitecam.sofia.usra.edu/cgi-bin/flitecam/flitecam_calc3.cgi

5   Instruments II: FORCAST

5.1   Instrument Overview

The **F**aint **O**bject infra**R**ed **CA**mera for the **S**OFIA **T**elescope (FORCAST) is a dual-channel mid-infrared camera and spectrograph sensitive from $5 - 40 \ \mu$m. Each channel consists of a 256×256 pixel array that yields a $3\rlap{.}'4 \times 3\rlap{.}'2$ instantaneous field-of-view with $0\rlap{.}''768$ pixels, after distortion correction. The Short Wave Camera (SWC) uses a Si:As blocked-impurity band (BIB) array optimized for $\lambda < 25 \ \mu$m, while the Long Wave Camera's (LWC) Si:Sb BIB array is optimized for $\lambda > 25 \ \mu$m. Observations can be made through either of the two channels individually or, by use of a dichroic mirror, with both channels simultaneously across the entire range. Spectroscopy is also possible using a suite of six grisms, which provide coverage from $5 - 40 \ \mu$m with a low spectral resolution of R $= \lambda/\Delta\lambda \sim 200$ and with high resolution at R $\sim 800 - 1200$ in the $5 - 14 \ \mu$m range.

5.1.1   Design

The FORCAST instrument is composed of two cryogenically cooled cameras of functionally identical design. A schematic of the instrument layout is provided in Figure 11 below. Light enters the dewar through a 7.6 cm (3.0 in) CsI window and cold stop and is focused at the field stop, where a six position aperture wheel is located. The wheel holds the imaging aperture, the slits used for spectroscopy, and a collection of field masks for instrument characterization. The light then passes to the collimator mirror (an off-axis hyperboloid) before striking the first fold mirror, which redirects the light into the LHe-cooled portion of the cryostat.

The incoming beam then reaches a four-position slide, which includes an open position, a mirror, and two dichroics, one for normal use and the other as a spare. The open position passes the beam to a second fold mirror, which sends the beam to the LWC, while the mirror redirects the light to the SWC. The magnesium oxide (MgO) dichroic reflects light below 26 μm to the SWC and passes light from $26 - 40 \ \mu$m to the LWC. The light then passes through a Lyot stop at which are located two filter wheels of six positions each, allowing combinations of up to 10 separate filters and grisms per channel. Well characterized, off-the-shelf filters can be used, since the filter wheel apertures have a standard 25 mm diameter (see §5.1.3).

Finally, the incoming beam enters the camera block and passes through the camera optics. These two-element catoptric systems are composed of an off-axis hyperboloid mirror and an off-axis ellipsoid mirror that focuses the light on the focal plane array. Also included is an insertable pupil viewer that images the Lyot stop on the arrays to facilitate alignment of the collimator mirror with the telescope optical axis and to allow characterization of the emissivity of both the sky and telescope.

5.1.2   Camera Performance

The SWC and LWC arrays were selected to optimize performance across the $5 - 40 \ \mu$m bandpass. Both arrays have a quantum efficiency (QE) greater than 25% over most of their spectral range. The cameras can be operated with variable frame rates and in either high or low capacitance modes (with well depths of 1.8×10^7 and 1.9×10^6 e$^-$ respectively) depending upon the sky background and source brightness.
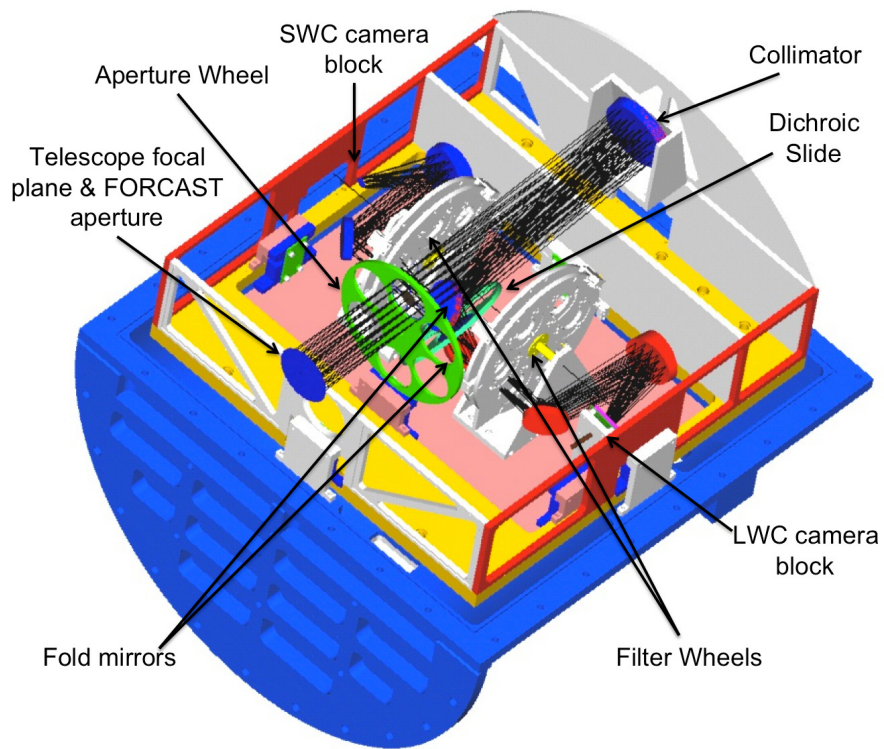
Figure 11: Color block diagram of the optical bench of the FORCAST instrument with labels to important components.

The best measured image quality (IQ) obtained by FORCAST on SOFIA is in the $7 - 11$ μm range with a FWHM PSF of $\sim 2{''}7$. This measured image quality in-flight is limited by telescope jitter arising from vibrations of the telescope itself (e.g., due to wind loading in the cavity), turbulence, and tracking accuracy. Figure 12 shows a sample of FWHM IQ measurements made during a single observatory characterization flight during the winter of 2010 in comparison to the theoretical diffraction limit calculated for a 2.5-m primary with a 14% central obstruction combined with the FWHM telescope jitter, here assumed to be $2{''}08$ ($1{''}25$ rms). The values shown are comparable to those achieved during Cycle 2.

5.1.3   Filter Suite

Imaging with FORCAST can be performed in a single channel or in the SWC and LWC channels simultaneously (dual channel mode). In single channel mode any one of the available filters may be used. In dual channel mode, a dichroic is used to split the incoming beam into both the SWC and LWC.

The dichroic reduces the overall throughput. Table 3 shows the throughput with the dichroic in (Dual Channel mode) relative to that for the Single Channel mode. The degradation of the system throughput by the dichroic can have a significant effect on the instrument sensitivities as discussed in more detail in §5.1.4. In addition, since there are more short wavelength filters available
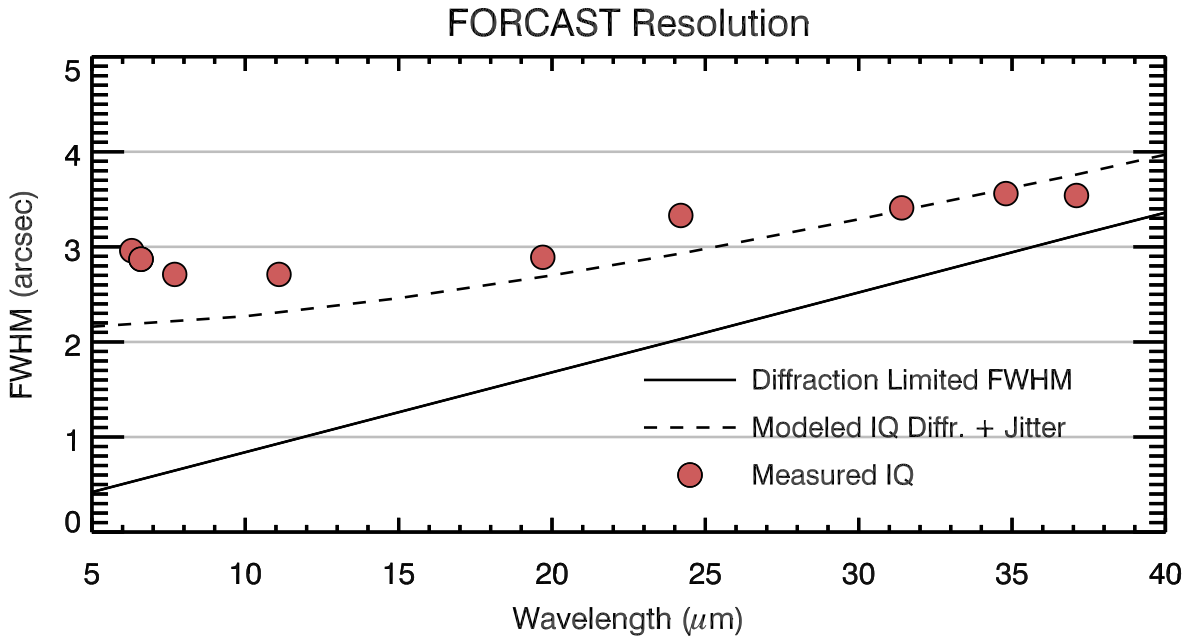
Figure 12: Measured FWHM Image Quality of the FORCAST camera in select filters relative to the diffraction limited FWHM (solid line; calculated for a 2.5-m primary with a 14% central obstruction) and the modeled IQ (dashed line), which includes shear layer seeing and $1''25$ rms telescope jitter.

than slots in the SWC filter wheels, some short wave filters will be housed in the LWC. The final distribution will be determined once demand has been established by the Cycle 3 response to the Call-for-Proposals. Depending on the final filter configuration, it is possible that not all LWC filters will be able to be used in dual channel mode due to the cutoff in the dichroic transmission at short wavelengths. Additional details are provided below and will be updated once the results of the Cycle 3 Call-for-Proposals are known.

Table 3: FORCAST Dichroic Throughput[a]

Bandpass	Throughput[a]
$5 - 10$ μm	60%
$11 - 25$ μm	85%
$25 - 40$ μm	40%

[a]Relative to the Single Channel mode throughputs

The filters in the SWC are standard Optical Coating Laboratory, Inc. (OCLI) thin-film interference filters. These filters are stacked with blocking filters to prevent light leaks. The only exception is the 25.4 μm University of Reading filter, which is a custom double half-wave (three mesh) scattering filter stacked with a diamond scattering blocking filter to provide blue-light rejection. The 33.6, 34.7, and 37.1 μm filters in the LWC are LakeShore custom double half-wave (three mesh) scattering filters. The 31.5 μm filter is Fabry-Perot Interferometer filter.

The central wavelengths, bandwidths, and the expected FWHM IQ in each of the filters are given in Table 4 below. The first column under "Imaging FWHM" presents the best measured FWHM IQ with a telescope jitter of $\sim 1''25$ rms. These values are representative of the IQ observed in Cycle 2. The second column is the average measured FWHM IQ from Basic Science with a $\sim 2''1$ rms jitter and indicates the "worst case" IQ. Not all of the filters have measured IQ values, but we expect that they will be comparable to those with measured values that are of similar $\lambda_{\rm eff}$. Figure 13 shows the filter transmission profiles (normalized to their peak transmission) over-plotted on an ATRAN model of the atmospheric transmission. The filter transmission curves are available on the SOFIA Science Instrument Suite website in the section for FORCAST[15].
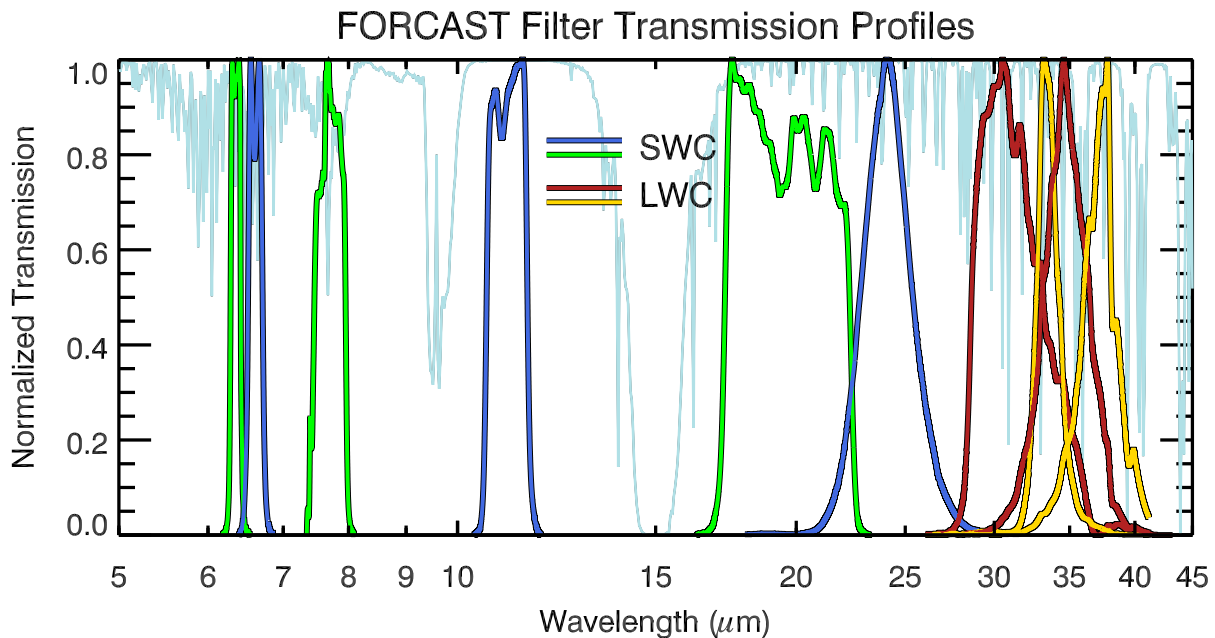
Figure 13: FORCAST filter transmission profiles along with an ATRAN model of the atmospheric transmission across the FORCAST band (assuming a zenith angle of 45 degrees and 7 μm of precipitable water vapor). For clarity the filter profiles have been normalized to their peak transmission. SWC filters alternate between green and blue, while LWC filters alternate between red and yellow.

Due to the limited number of slots available in the filter wheels, not all of the filters listed in Table 4 are available at any one time. For Cycle 3, there will be a "default" filter set (indicated by

---

[15]http://www.sofia.usra.edu/Science/instruments/instruments_forcast.html

bold type in Table 4). GIs may request that other filters be used for their observations, but they must make a convincing scientific argument to justify swapping out the existing filters for those they desire. We anticipate that a single filter swap may be permitted during Cycle 3 provided there is adequate scientific justification. More details are available in the Cycle 3 Call for Proposals.

Table 4: FORCAST Filter Characteristics

Channel	λ_{eff} (μm)	$\Delta\lambda$ (μm)	Imaging FWHM ($''$)	
SWC	5.4	0.16	$-^b$	$-$
	5.6	0.08	$-$	$-$
	6.4^a	**0.14**	**3.0**	**3.5**
	6.6^a	**0.24**	**2.9**	**3.5**
	7.7^a	**0.47**	**2.7**	**3.5**
	8.6	0.21	$-$	$-$
	11.1^a	**0.95**	**2.7**	**3.6**
	11.3	0.24	$-$	$-$
	11.8	0.74	$-$	$-$
	19.7^a	**5.5**	**2.9**	**3.8**
	25.4^a	**1.86**	$-$	$-$
LWC	24.2	2.9	3.3	4.0
	25.3	1.86	$-$	$-$
	31.5^a	**5.7**	**3.4**	**4.3**
	33.6^a	**1.9**	$-$	**4.5**
	34.8^a	**3.8**	**3.6**	**4.5**
	37.1^a	**3.3**	**3.5**	**4.7**

^{a}Entries in **bold** font are expected to be part of the "default" filter set for Cycle 3.

^{b}IQ values for some filters have not been measured at this time, but it is expected that they will be similar to those of similar λ_{eff} with measured values.

5.1.4 Imaging Sensitivities

Figure 14 presents the FORCAST imaging sensitivities for a continuum point source at the effective wavelengths of the ten "default" filters listed above. The Minimum Detectable Continuum Flux (MDCF; 80% enclosed energy) in mJy needed to obtain a S/N = 4 in 900 seconds of on-source integration time is plotted versus wavelength. The red squares and blue dots correspond to sensitivities for the single and dual channel modes respectively. The MDCF scales roughly as $(S/N)/\sqrt{t}$ where t = net integration time. The horizontal bars indicate the effective bandpass at each wavelength. At the shorter wavelengths the bandpass is sometimes narrower than the symbol size.

Atmospheric transmission will affect sensitivity, depending on water vapor overburden. The sensitivity is also affected by telescope emissivity, estimated to be 15% for Figure 14.

Observations with FORCAST will be performed using standard IR chop-nod techniques. The GIs can choose chop/nod amplitudes small enough to leave the source on the array in each position or large enough that the source is positioned off the chip for one of the chop positions. For background-limited observations, as will be the case with FORCAST on SOFIA, chopping and nodding off-chip in nod-match-chop (NMC; see §5.3.1) will generally result in the same signal to noise (S/N) as chopping and nodding on-chip in nod-perp-chop (NPC; see §5.3.1). Calculations of S/N for various chop-nod scenarios are provided here[16].
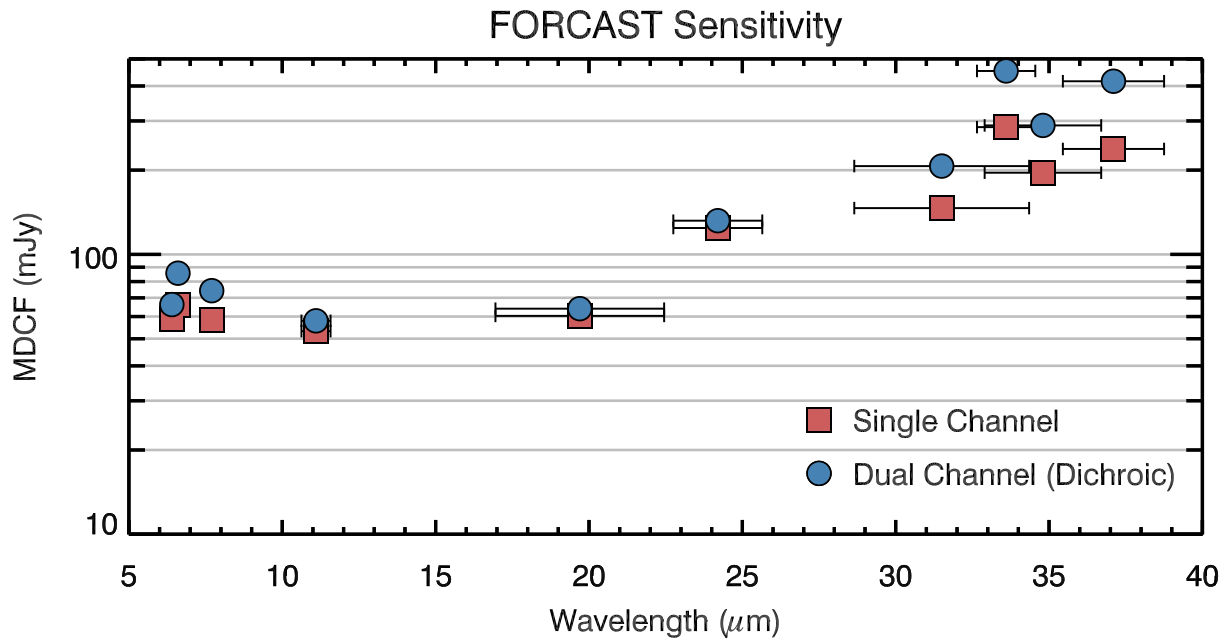
Figure 14: FORCAST imaging sensitivities for a continuum point source at the effective wavelengths of a selection of the FORCAST filters listed above. The values reported are for a S/N of 4 in 900 seconds at an altitude of 41,000 feet and a water vapor overburden of 7 μm. The red squares indicate the MDCF values in Single Channel mode while the blue circles are for Dual Channel mode using the Dichroic.

5.1.5   Grisms

The suite of 6 grisms available for FORCAST provide low to medium resolution coverage throughout most of the range from 5 – 40 μm. The grisms are situated in the four filter wheels, two in each SWC wheel and one in each LWC wheel. The arrangement is chosen to minimize the impact on the imaging capabilities of the instrument. The grisms are blazed, diffraction gratings used in transmission and stacked with blocking filters to prevent order contamination. A summary of the grism properties is provided in Table 5.

Grisms FOR_G063, FOR_G227, FOR_G329, and the FOR_XG063 dispersing grism, provided by the University of Texas at Austin, are made of silicon to take advantage of its high index of

---

[16]http://www.sofia.usra.edu/Science/instruments/Chopnod_SN_20130503.pdf

refraction, which allows optimum spectral resolution. However, these grisms suffer from various absorption artifacts precluding their use in the $8 - 17$ μm window. Coverage in this region is provided by the FOR_G111 grism and the FOR_XG111 disperser, constructed of KRS-5 (thallium bromoiodide) by Carl-Zeiss (Jena, Germany). These latter two grisms have a lower spectral resolution due to the lower index of refraction of the KRS-5 material.

Three slits are available, two long slits ($2''.4 \times 191''$, $4''.7 \times 191''$) and a short slit ($2''.4 \times 11''.2$). The narrow slits yield higher resolution data. All of the slits are located in the aperture wheel of the instrument. The cross-dispersed spectra are obtained by using the short slit and passing the beam first through the low-resolution grism (either FOR_G063 or FOR_G111), followed by a disperser. Although grisms are available in both cameras, during Cycle 3 grism spectroscopy will be available only in single channel mode.

It is important to note that due to the fixed position of the slits in the aperture wheels, the lack of a field de-rotator, and the fact that SOFIA behaves in many respects as an Alt-Az telescope, the orientation of the slit on the sky will be dependent on the flight plan and will not be able to be predetermined. Furthermore, the slit orientation rotates on the sky with each telescope Line-of-Sight (LOS) rewind. These limitations may be especially important to consider when proposing observations of extended objects.

Table 5: FORCAST Grism Characteristics

Channel	Grism	Material	Groove Sep. (μm)	Prism Angle (°)	Order	Coverage (μm)	R ($\lambda/\Delta\lambda$)
SWC	FOR_G063	Si	25	6.16	1	$4.9 - 8.0$	$90/180^a$
	FOR_XG063	Si	87	32.6	$15 - 23$	$4.9 - 8.0$	1200^b
	FOR_G111	KRS-5	32	15.2	1	$8.4 - 13.7$	$150/300^a$
	FOR_XG111	KRS-5	130	36.8	$8 - 13$	$8.4 - 13.7$	800^b
LWC	FOR_G227	Si	87	6.16	1	$17.6 - 27.7$	$70/140^a$
	FOR_G329	Si	142	11.07	2	$28.7 - 37.1$	$110/220^a$

[a]For the $4''.7 \times 191''$ and the $2''.4 \times 191''$ slits, respectively
[b]Only available with the $2''.4 \times 11''.2$ slit

5.1.6 Spectroscopic Sensitivities

At the time of this writing, the FORCAST spectroscopic sensitivities have not been measured empirically. Instead the sensitivities have been derived from the FORCAST imaging sensitivities, the SOFIA observatory specifications, and laboratory tests of the grism spectroscopy modes. The model is based on the most recent measurements of the image quality, FORCAST camera responsivity, and filter and grism transmission curves.

Tables 6 and 7 provide samples of the MDCF and Minimum Detectable Line Flux (MDLF) calculated at three different wavelengths across each grism bandpass for each of the available spectroscopic modes – long slit and cross-dispersed. The data are provided for point sources only. The

MDCF and MDLF estimates are for the raw integration time of 900 seconds and do not include observing overheads, but do account for a a two-position chop (perpendicular to the slit).

Figures 15 and 16 below present the continuum point source sensitivities for the FORCAST grisms. The plots are the MDCF in Jy needed for a S/N of 4 in 900 seconds at a water vapor overburden of 7 μm, an altitude of 41K feet, and a zenith angle of 60°. The rapid variations with λ are due to discrete atmospheric absorption features (as computed by ATRAN).

To determine the required integration times necessary to achieve a desired S/N ratio for a given source flux, GIs are encouraged to use the FORCAST on-line grism exposure time calculator[17]. Alternatively, the FORCAST grism sensitivity values in Tables 6 and 7 and Figures 15 and 16 can be used to estimate the required integration time necessary to achieve a desired S/N ratio for a given source flux. Since FORCAST observations are background limited, this can be done by using the relation,

$$\frac{[S/N]_{req}}{4} = \frac{F_{src} \cdot \sqrt{t_{exp}}}{MDCF \cdot \sqrt{900}},$$

where $[S/N]_{req}$ is the desired signal-to-noise ratio, F_{src} is the continuum flux of the target, t_{exp} is the exposure time on source (without taking into consideration observational overheads), and the MDCF is taken from the tables for the point-source sensitivities or estimated from the figures. For emission lines, simply use the line flux for F_{src} and use the MDLF value instead of the MDCF.

For extended sources, GIs are required to use the FORCAST on-line grism exposure time calculator. Since the on-line calculator does not calculate extended source sensitivities directly, it is necessary for GIs to follow the following procedure to estimate extended source sensitivities:

1. Select the appropriate instrument set-up for the extended source observations and enter these values into the on-line calculator.

2. Run the calculator using the desired setup. This will yield results for a point source, but it will also provide details necessary for the extended source sensitivity calculation, such as:

   - Instrument FWHM resolution at three representative wavelengths across the bandpass
   - Point source fractional slit transmission at each of those three wavelengths

3. Estimate the extended source flux per resolution element as follows:

$$\frac{F_{src}[Jy('')^{-2}] \cdot w_{slit} \cdot 1.2 \cdot FWHM}{f_{trans}},$$

   where F_{src} is the source flux density in units per square arcsecond, w_{slit} is the selected slit width in arcseconds, the FWHM is in arcseconds as reported in Step 2 above, and f_{frac} is the fractional slit width (also from Step 2). The factor of 1.2 is required since the on-line calculator uses an optimal extraction.

4. Entering this scaled flux value into the on-line point source sensitivity calculator will yield the appropriate sensitivity estimate for the extended source.

---

[17]http://forcast.sofia.usra.edu/cgi-bin/forcast/forcast_grisms_calc.cgi

Table 6: FORCAST Long Slit Point Source Sensitivities

		4″7 Slit			2″4 Slit		
Grism	λ (μm)	R = ($\lambda/\Delta\lambda$)	MDCF (mJy)	MDLF (W m^{-2})	R = ($\lambda/\Delta\lambda$)	MDCF (mJy)	MDLF (W m^{-2})
FOR_G063	5.0	90	101	7.1E-16	180	169	6.0E-16
FOR_G063	6.4	90	179	9.9E-15	180	296	8.2E-16
FOR_G063	7.7	90	397	1.8E-15	180	625	1.4E-16
FOR_G111	8.5	150	386	9.6E-16	300	610	7.6E-16
FOR_G111	11.1	150	386	7.4E-16	300	606	5.8E-16
FOR_G111	13.6	150	843	1.3E-15	300	1336	1.0E-15
FOR_G227	17.7	70	967	2.5E-15	140	1579	2.0E-15
FOR_G227	22.7	70	799	1.6E-15	140	1399	1.4E-16
FOR_G227	27.6	70	892	1.5E-15	140	1476	1.2E-15
FOR_G329	28.8	110	1166	1.2E-15	220	1879	9.4E-16
FOR_G329	32.9	110	2218	1.9E-15	220	3577	1.6E-15
FOR_G329	37.0	110	2050	1.6E-15	220	3817	1.5E-15

Table 7: FORCAST Cross-Dispersed Point Source Sensitivities

		2″4 × 11″2 Slit		
Grisms	λ (μm)	R = ($\lambda/\Delta\lambda$)	MDCF (mJy)	MDLF (W m^{-2})
FOR_XG063	5.0	1200	820	4.3E-16
FOR_XG063	6.4	1200	893	3.7E-16
FOR_XG063	7.7	1200	1450	5.0E-16
FOR_XG111	8.5	800	1036	4.8E-16
FOR_XG111	11.1	800	1003	3.6E-16
FOR_XG111	13.6	800	1979	5.8E-16

5.2   Planning FORCAST Imaging Observations

As is the case with ground based observations at mid-IR wavelengths, individual FORCAST exposures will be dominated by the sky and telescope background. Therefore chopping and nodding are essential for each observation. Selection of the observing mode, including the distance and
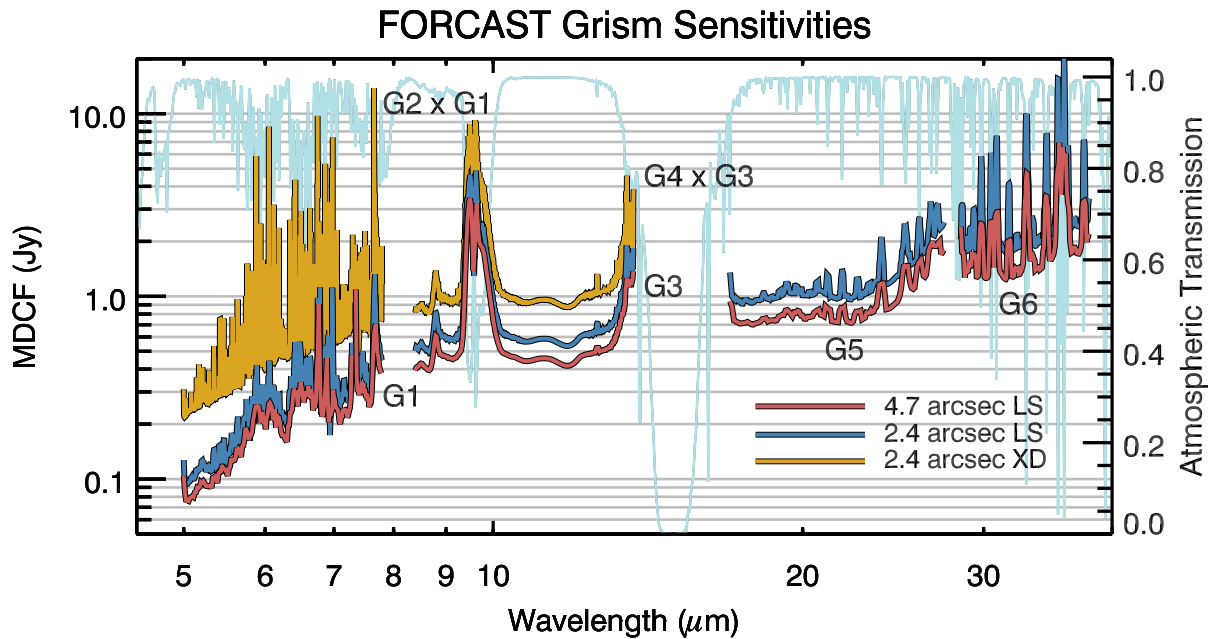
Figure 15: FORCAST grism sensitivities for a continuum point source in each of the grisms listed above in Table 5 overlaid on an ATRAN model in light blue. The values reported are for a S/N of 4 in 900 seconds at a water vapor overburdens of 7 μm at an altitude of 41K feet and a 60° zenith angle. Sensitivities are plotted for each of the three available slits.

direction of chop and nod throws, depends on the details of the field of view around the target. The source(s) of interest may be surrounded by other IR-bright sources or may lie in a region of extended emission, which needs to be avoided to ensure proper background subtraction.

5.2.1 Chopping and Nodding in Imaging Mode

During Cycle 3, three FORCAST imaging observation modes will be available including: (1) symmetric nod-match-chop (NMC), (2) symmetric nod-perp-chop (NPC), and (3) asymmetric chop-offset-nod (C2NC2). NMC and NPC are both variations of the standard two-position chop with nod (C2N) IR observing mode. A brief description of each observing mode is provided below, but users are strongly encouraged to read the more complete description provided in the **FORCAST Observing Modes** document[18].

- **NMC:** In NMC mode, the chop is symmetric about the optical axis of the telescope with one of the two chop positions centered on the target. The nod throw is oriented 180° from the chop, i.e. anti-parallel, such that when the telescope nods, the source is located in the opposite chop position. The chop/nod subtraction results in two negative beams on either side of the positive beam, which is the sum of the source intensity in both nod positions and therefore has twice the intensity of either negative beam. This mode uses the standard ABBA

---

[18]http://www.sofia.usra.edu/Science/instruments/FORCAST_observations_modes.pdf
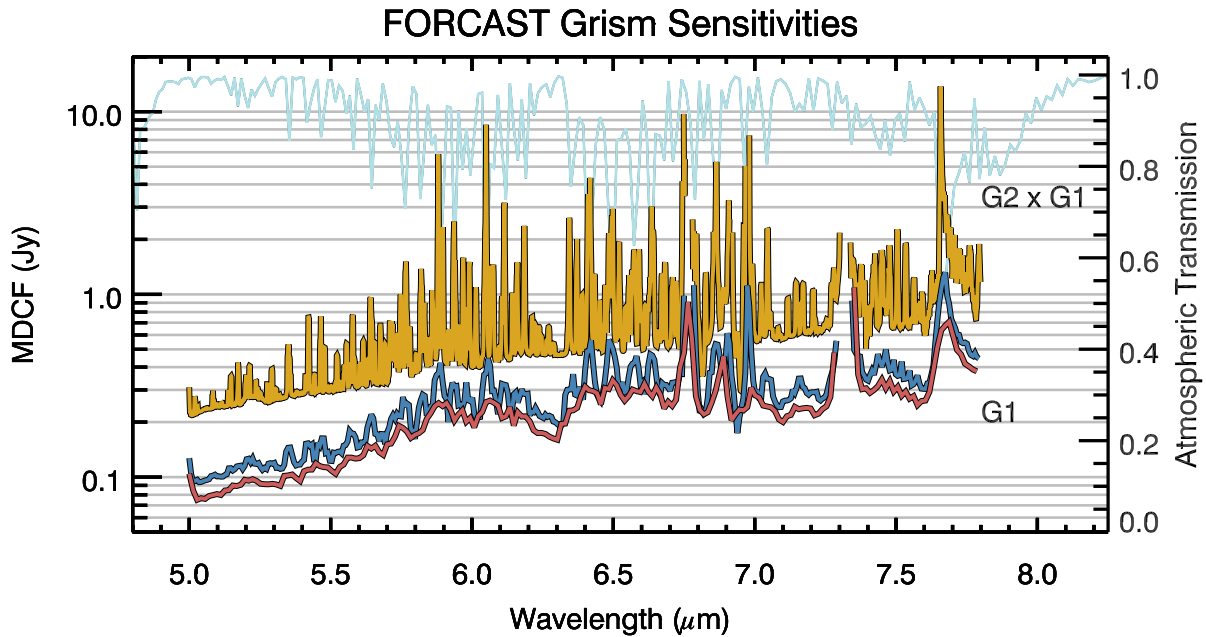
Figure 16: FORCAST grism sensitivities for a continuum point source using the grisms 1 and 2 listed above in Table 5. Otherwise as above.

nod cadence. An example of an observation taken in this mode is presented in the left panel of Figure 17.

- **NPC:** NPC mode also uses a chop that is symmetric about the optical axis, but in this case the nod is perpendicular to the chop. The final images produced using NPC show four sources arranged in a parallelogram with alternating positive and negative beams. Unlike NMC, each beam in NPC has the same relative intensity. This mode also uses the standard ABBA nod cadence. The right side of Figure 17 shows data obtained using NPC.

- **C2NC2:** The third supported observing mode is asymmetric chop with offset nod (C2NC2). This mode is particularly useful for large extended objects, smaller objects that are situated within crowded fields, or regions of diffuse emission with only limited sky positions suitable for background removal. In this mode, the chop throw is asymmetric, such that one chop position is centered on the optical axis (and the target) while the second (sky) position is off-axis. Rather than nodding, the telescope then slews to an offset position free of sources or significant background and the same chop pattern is repeated. Observations in C2NC2 mode follow a nod cadence of ABA and, by default, are dithered to remove correlated noise.

  Figure 18 is a cartoon demonstrating how a C2NC2 observation might be designed for a large, extended object. Each source position (solid line) with its associated asymmetric chop position (dashed line) have matching colors. After a full chop cycle at each position, the telescope is slewed to a location off of the source, shown in black and labeled with the coordinates (600, 600). The chop throw and angle at that position is the same as it is for the source position to which it is referenced (not shown in the figure). It is immediately apparent

from the figure, that C2NC2 has an efficiency of only $\sim 20\%$. This is a much lower efficiency than either NMC or NPC since only a single chop position out of a full chop/nod cycle is on source. This should be taken into consideration when designing science proposals.
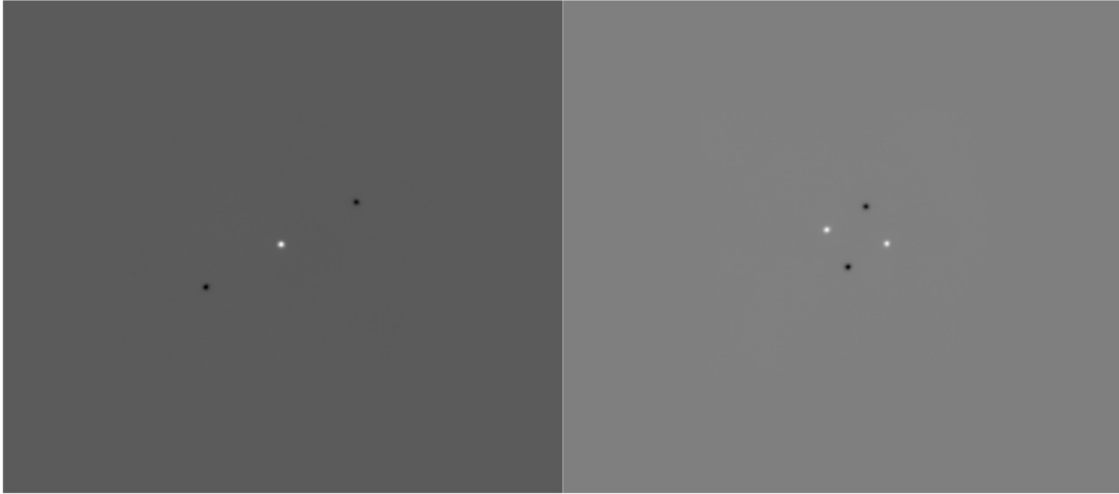

Figure 17: *Left:* FORCAST image of β And taken in Nod-Match-Chop (NMC) mode. *Right:* FORCAST image of α Boo taken in Nod-Perp-Chop (NPC) mode.

Once a proposal has been accepted, the GI, in collaboration with the SMO instrument scientist, will specify the details of chopping and nodding for each observation using the SOFIA observation preparation tool https://dcs.sofia.usra.edu/observationPlanning/installSSPOT/sspotDownload.jspSSPOT[19]; scheduled for release in July, 2014). Experienced GIs are encouraged to design their observations using SSPOT *before* writing their proposals to prevent the loss of observing time that might occur if, during Phase II, the observations are discovered to be more challenging than expected.

Following are a few of the most important issues that GIs should consider when preparing a proposal.

- It is recommended that a near-IR or mid-IR database (e.g., 2MASS, *Spitzer*, *WISE*, MSX or IRAS) be checked to see if the target of interest is near other IR sources of emission. In the case of extended sources, where on-chip chop and nod is not possible, it is necessary to pick areas free of IR emission for the chop and nod positions to get proper background subtracted images.

- If the IR emission from the region surrounding the source is restricted to a region smaller than half the FORCAST field of view (i.e. $\sim 1.6'$) then the chop and nod can be done "on-chip". Observations performed in NMC mode either "on-chip" or "off-chip" yield a S/N equal to or slightly better than that obtained in NPC mode. For additional discussion of this point, see the calculations of S/N for various FORCAST chop-nod scenarios provided here[20].

---

[19]https://dcs.sofia.usra.edu/observationPlanning/installSSPOT/sspotDownload.jsp
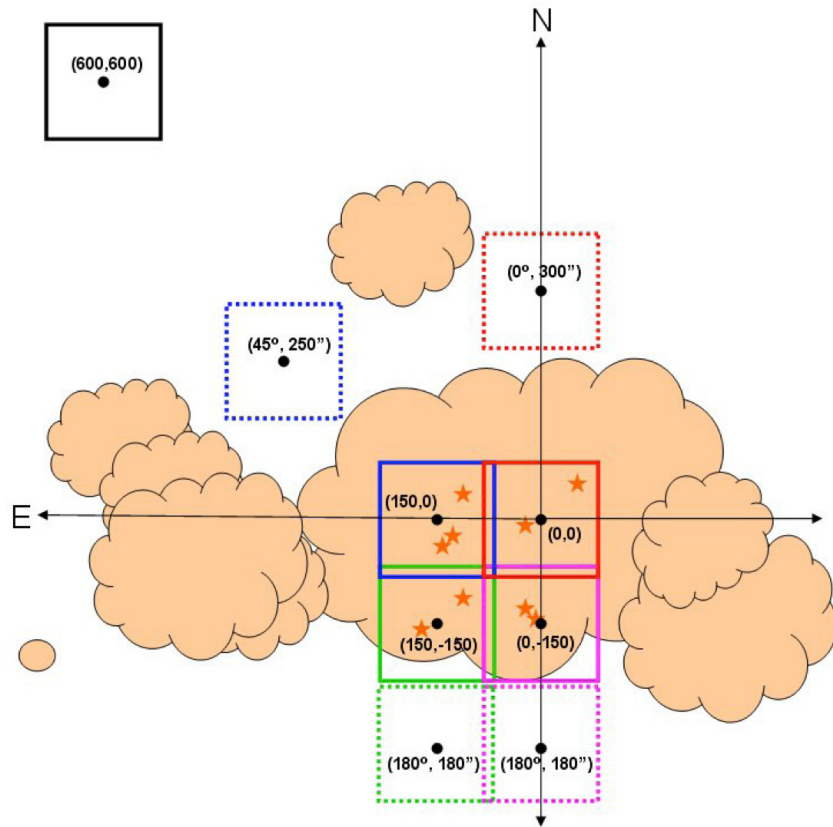[20]http://www.sofia.usra.edu/Science/instruments/Chopnod_SN_20130503.pdf

Figure 18: Cartoon of a C2NC2 mode FORCAST observation with mosaic.

- The chop throw is defined as the distance between the two chop positions in either symmetric or asymmetric chopping modes. When using a symmetric chop, e.g., in the either NMC or NPC modes, chopping and nodding can be performed in any direction for chop throws less than $584''$.

- When observing in one of the symmetric chop modes, large chop amplitudes may degrade the image quality due to the introduction of coma. This effect causes asymmetric smearing of the PSF parallel to the direction of the chop at a level of $2''$ per $1'$ of chop amplitude.

- When using an asymmetric chop, the maximum possible chop throw is $420''$. However, some chop angles (as measured in the instrument reference frame) are not allowed for asymmetric chop throws between $292''$ and $420''$. Since the orientation of the instrument relative to the sky will not be known until the flight plan is generated, GIs requesting chop throws between $292 - 420''$ are required to specify a range of possible chop angles from which the instrument scientists can choose when the flight plan is finalized.

- For large, extended objects, it may not be possible to obtain clean background positions due to these limitations on the chop throw.

There are some additional considerations for observations of faint targets.

- Currently, the longest nod dwell time (that is, the time spent in either the nod A or nod B position) for FORCAST is 30 sec in the SWC-only and dual channel modes and up to 120 sec in the LWC-only modes (depending on the filter). Proposers should run the exposure time estimator to determine if the object will be visible in a single A-B chop-subtracted, nod-subtracted pair, with an exposure time of 30 sec in each nod position. If the object is bright enough to be detectable with S/N greater than a few, it is recommended that dithering be used when observing in NMC or NPC mode. The dithering will mitigate the effects of bad pixels when the individual exposures are co-added.

- If the object is not visible in a single A-B chop/nod-subtracted pair, with a nod dwell time of 30 sec in each nod position (60 sec integration), then dithering should NOT be used. Images of objects this faint cannot be shifted prior to co-adding because the object cannot be used in the registration process. By taking the observations without dithering all of the images can be stacked and co-added directly, and the object can be detected in the final image. Note however that bad pixels may be present in the final image.

- GIs are strongly encouraged to use NMC mode when possible, since this mode yields a S/N equal to or slightly better than NPC. Nevertheless, there may be cases for which NMC may not be the optimal observing strategy and NPC should be used instead. If this is the case, GIs should contact their support scientist to discuss the optimal solution.

5.2.2 Mosaicking

If the source has an angular extent large enough that multiple pointings are required, the central position of each FORCAST field must be specified, with due consideration of the desired overlap of the individual frames. Mosaicking can be performed in each of the three available observing modes, NMC, NPC, and C2NC2. A sample mosaic using C2NC2 mode is demonstrated in Figure 18. One should keep in mind that for fields requiring large chop amplitudes, the effects of coma may compromise the image severely when in symmetric chopping mode (NMC and NPC).

5.3 Planning FORCAST Spectroscopic Observations

Spectroscopic observations with FORCAST are subject to many of the same considerations as imaging observations. Both low-resolution, long-slit and high-resolution, short-slit observations require chopping and nodding with careful consideration of chop/nod angles and throws necessary to prevent extended source or background contamination. During Cycle 2, grism spectroscopy with FORCAST will only be available in single channel mode.

5.3.1 Chopping and Nodding in Grism Mode

By default, observations will be set up using NMC aligned along the slit in long-slit mode and perpendicular to the slit in XD mode. Due to the size of the PSF, neither chopping or nodding along the slit nor dithering are possible for high-resolution XD observations. For long-slit observations, it is possible to use NPC, either chopping or nodding along the slit, but GIs are discouraged from doing so unless they provide adequate justification for doing so. Those wishing to use NPC should discuss the possibility with their SMO Support Scientist. GIs should also bear in mind that for

sources smaller than the slit length, NMC yields slightly improved efficiency over NPC. For larger sources and for targets embedded in crowded fields, GIs are advised to use C2NC2 mode.

The observing efficiency for FORCAST spectroscopic observations is currently unknown, but is expected to be of order 25 – 50%, depending on the chosen observing mode. These efficiency estimates are built-in to the SPT and do not need to be specified.

It is important to note that due to the fixed position of the grisms/slits in the filter/aperture wheels, the orientation of the slit on the sky will be dependent on the flight plan and will not be able to be predetermined. Further, the slit orientation rotates on the sky with each telescope Line-of-Sight (LOS) rewind. These limitations may be especially important to consider when proposing observations of extended objects.

5.4   Estimation of Exposure Times

5.4.1   Estimation of Exposure Times for Imaging Observations

The exposure times for FORCAST imaging observations should be estimated using the on-line exposure time calculator, SITE[21]. SITE can be used to calculate the signal-to-noise ratio (S/N) for a given "total integration time", or to calculate the total integration time required to achieve a specified S/N. The total integration time used by SITE corresponds to the time for a single chop/nod pair, without overheads. The format of the S/N values output by SITE depends on the source type. For Point Sources, the reported S/N is per resolution element, but for Extended Sources, it is the S/N per pixel.

For mosaic observations the total integration time required for a single field should be multiplied by the number of fields in the mosaic to obtain the total time, which is to be entered in SPT.

An important consideration in planning observations is whether FORCAST should be used in single channel mode, or in dual channel mode, since one gains the extra filter observation at the cost of lower system throughput in the individual bands. On the SITE form, the single channel mode is specified by selecting the filter of interest for one channel and "Ignore" on the other channel in the "Instrument properties" section.

5.4.2   Estimation of Exposure Times for Spectroscopic Observations

The exposure times for FORCAST grism mode spectroscopic observations should be estimated using the FORCAST on-line grism exposure time calculator[22]. This calculator can be used to calculate the signal-to-noise ratio (S/N) for a given "total integration time", to calculate the total integration time required to achieve a specified S/N, or to estimate the limiting flux for a desired S/N.

Alternatively, the exposure times for the FORCAST grism mode spectroscopic observations could be estimated with methods described in Section 5.4.2 using the MDCF or MDLF values provided in Tables 6 – 7 and Figures 15 & 16. In this case, the GI should estimate the "total integration time" and enter it into the SOFIA Proposal Tool (SPT; further details in §11.1).

In either case, **overheads should not be included**, as SPT calculates them independently.

---

[21]http://dcs.sofia.usra.edu/proposalDevelopment/SITE/index.jsp

[22]http://forcast.sofia.usra.edu/cgi-bin/forcast/forcast_grisms_calc.cgi

6 Instruments III: GREAT

6.1 Instrument Overview

GREAT is a dual channel heterodyne instrument that will provide high resolution spectra (up to R=10^8) in several frequency windows in the 1.2 – 5 THz range. The front-end unit consists of two independent dewars, each containing a set of mixers, labeled L1, L2, M_a, M_b, and H, sensitive to "**L**ow", "**M**edium" and "**H**igh" frequencies.

L1 operates in the range 1.262 – 1.396 THz (237.7 – 214.9 μm) and 1.432 – 1.523 THz (209.5 – 197.0 μm). The gap matches frequencies blocked by the atmosphere. L2 operates in the range 1.800 – 1.910 THz (166.7 – 157.1 μm). The M channel requires two local oscillators. M_a operates in the range 2.495 – 2.519 THz (120.2 – 119.1 μm) and M_b in the range 2.67 – 2.68 THz (112.28 – 111.86 μm). The H channel operates at 4.745 THz (63.18 μm).

During Cycle 3, L1, L2, and H will be offered in the configurations L1-L2 and L2-H only. The H channel range is currently limited by the tuning range of the quantum cascade laser local oscillator and, therefore, only the velocity range -25 – +90 km/s around the 4744.77749 GHz [O I] line will be available for Cycle 3. With the negative velocity setup, the useable velocity range is -140 – -30 km/s.

The GREAT instrument provides two backends for each mixer. The backends are Fast Fourier Transform (FFT) spectrometers. Each XFFTS spectrometer has a bandwidth of 2.5 GHz and 64,000 channels, providing a resolution of 44 kHz. Each AFFTS spectrometer has a bandwidth of 1.5 GHz and provides a resolution of 212 kHz.

The beam size is close to the diffraction limit - about 16″ at 160 μm.

6.1.1 Observing Modes

Four observing modes are supported by GREAT.

- **Position switching (PSW):** In this mode the telescope nods between a target and nearby emission-free reference position. This mode should be used for observing one or more positions on an extended source. The reference position should ideally be less than 30′ away from the source positions.

- **Beam switching (BMSW):** In this mode, the secondary mirror chops between the source and a reference position less than 10′ away at a rate of about 1 – 2 Hz. The telescope nods between these positions at a slower rate. This mode results in better sky cancellation than position switching, but can be used only for compact targets, where the chop/nod throw would move the beam off-source.

- **Raster mapping:** In this mode, the telescope points to an off position, followed by several on-position observations. The user must specify the map positions, the off-position for a PSW observation or the chopper set-up for a BMSW observation, and the totl integration time per map position. This mode is ideally used for small maps or strips, where relatively long exposure times (> 30 s) per map point are required.

- **On-the-fly mapping (OTF):** In this mode the telescope scans along a line of constant latitude (a row) with the backends continuously integrating the incoming signal and recording

an average after the telescope has moved a fraction (typically 1/3) the beam size. Once the end of the row is reached, the telescope moves off-source to a reference position. Then, the telescope steps half a beam width in longitude and scans the next row. This process continues until a map of the desired size has been observed. The whole map is repeated until the required sensitivity is reached.

6.2   Planning GREAT Observations

The Guide to Observation Planning with GREAT (GOPG)[23] describes the GREAT instrument and the available observing modes. The information required to estimate observing times in each mode, along with examples on how to do so, are also contained in the GOPG.

Note that the sensitivity calculations for PSW and BMSW modes are the same. In the case of OTF mapping, the sensitivity reached depends on the scan rate and the overlap between successive rows.

If the frequency of interest has not already been used by GREAT, please contact the GREAT team to ensure that the line is feasible. There may be gaps where the broadband Local Oscillators do not provide enough power to pump the mixers.

6.2.1   Estimating exposure time

The exposure times for GREAT observations may be estimated using the Online Calculator[24].

---

[23]http://www.sofia.usra.edu/Science/proposals/cycle3/Guide_To_GREAT_v7.pdf
[24]http://great.sofia.usra.edu/cgi-bin/great/great.cgi

7 Instruments IV: HIPO

The **H**igh **S**peed **I**maging **P**hotometer for **O**ccultation (HIPO) is a special-purpose science instrument for SOFIA that is designed to provide simultaneous high-speed time resolved imaging photometry at two optical wavelengths. It is possible to mount HIPO and FLITECAM on the SOFIA telescope simultaneously, called the FLIPO configuration, to allow data acquisition at two optical wavelengths and one near-IR wavelength. HIPO has a flexible optical system and numerous readout modes, allowing many specialized observations to be made. The instrument characteristics required for our proposed scientific pursuits are closely aligned to those needed for critical tests of the completed SOFIA Observatory, and HIPO has been used heavily for these tests. The general design and performance goals of the instrument are described in Dunham et al. (2004, SPIE, 5492, 592)[25]. Additional references are available on the HIPO website[26].

The primary scientific use of HIPO is for observing stellar occultations. In a stellar occultation, a star serves as a small probe of the atmospheric structure of a solar system object or the surface density structure of a planetary ring or comet. Such observations provide information at high spatial resolution that would otherwise require a space mission to obtain. This work makes use of SOFIA's mobility, freedom from clouds, and near-absence of scintillation noise to provide the best possible occultation data.

The low atmospheric scintillation in airborne photometry gives HIPO the potential to detect P-mode stellar oscillations in sunlike stars and will provide excellent photometry of stellar transits by extrasolar planets. HIPO will be available for Guest Investigator use on a collaborative basis, and potential Guest Investigators should contact the PI prior to proposing to ensure that the proposed observations are feasible, that they make the best use of HIPO's capabilities, and that the proposal is as strong as possible.

7.1 Instrument Overview

The instrument sensitivity and resolution summaries are provided to permit estimating feasibility of scientific investigations. The HIPO performance summaries show the expected system performance for Full Operational Capability, which may differ from that during commissioning.

7.1.1 Instrument Design

The HIPO optical system is reconfigurable to meet its varied requirements. It incorporates two dichroic beamsplitters, one to divert the infrared beam to FLITECAM (if mounted) and one to split the red and blue sides of the HIPO optical paths. Either or both of these may be removed if desired. It is also possible to move either CCD so it is placed directly at the optimal SOFIA focal plane for highest spatial resolution and throughput. The optical design is described in detail in Dunham (2003, SPIE, 4857 62)[27].

The 8-position filter wheels are located near the pupil image formed by the collimator optics. Two positions in the red CCD's filter wheel are normally used for Shack-Hartmann lenslet arrays, but these may be replaced if necessary for a particular observation. We have contemplated adding grism capability to HIPO but have not yet carried this out.

---

[25]http://dx.doi.org/10.1117/12.552152
[26]http://www.sofia.usra.edu/Science/instruments/instruments_hipo.html
[27]http://dx.doi.org/10.1117/12.458819

The region between the mounting flange and the gate valve on the telescope can be evacuated to reduce image degradation due to density fluctuations in this region of the optical path. When this is done a window is installed at the location of the gate valve.

HIPO provides a number of CCD readout modes as described in Dunham et al. (2008, SPIE, 7014, 70144Z)[28]. The most commonly used are the single frame mode and a frame transfer time series (basic occultation) mode with readout frequency up to 50 Hz. A variety of readout rates are available allowing the observer to optimize the subframe size, speed, noise, full well, and linearity tradeoff for a particular event. This is also discussed together with HIPO data format details in the "HIPO Data Cycle System Software Interface" document.

7.1.2 Angular Resolution

The primary HIPO detectors are e2v CCD47-20 1024 × 1024 pixel frame transfer CCDs with plate scales of $0\rlap{.}''33 \times 0\rlap{.}''33$ pixels at low resolution and $0\rlap{.}''05 \times 0\rlap{.}''05$ pixels at high resolution. The HIPO field of view (FOV) is a $5\rlap{.}'6$ square, the $8'$ diagonal of which corresponds to the $8'$ diameter SOFIA FOV. Pixels will normally be binned to best match the seeing blur size and to reduce the effect of read noise. The high resolution mode includes no re-imaging optics. It is possible to replace one or both of the CCD47's with CCD67's having half the field of view, twice the pixel size, and much faster imaging operation.

The HIPO image quality is dominated by seeing and image motion effects. The red curve in Figure 19 is the nominal image quality expected at first light for SOFIA, based on the expected shear layer seeing, the as-built optical performance, and $2''$ rms image motion. The blue curve represents the ultimate combined optical quality and image motion requirement (80% encircled energy in a $1\rlap{.}''6$ diameter circle) convolved with the expected shear layer seeing. Also plotted are representative photometry aperture diameters likely to be used for processing occultation frames under both conditions described above. The image motion assumed is larger than will be experienced when observing at high frame rates. Occultation photometry will be extracted from data frames using effective aperture sizes comparable to the 80% enclosed light diameter plotted here.

7.1.3 Filter Suite

Wavelength range: 0.3 - 1.1 μm. HIPO currently includes standard Johnson UBVRI filters and Sloan Digital Sky Survey u' g' r' i' z' filters. Occultation observations will normally be unfiltered for events involving faint stars or will use specialized filters such as the narrow-band methane filter ($\lambda_c \sim 0.89$ μm) for events with bright stars. Additional custom filters will be added for specific events.

HIPO uses a dichroic reflector to separate its blue and red channels. Two dichroics are currently available with transition wavelengths of 0.575 and 0.675 μm respectively. Other dichroics will be added as necessary for specific events. The 0.575 μm dichroic transition wavelength is close to the boundary between the Sloan g' and r' filters and the 0.675 μm transition is close to the boundary between the Sloan r' and i' filters.

HIPO has been upgraded recently with the addition of deep depletion CCDs having a multi-layer antireflection coating. This provides higher quantum efficiency across the board with much higher

---

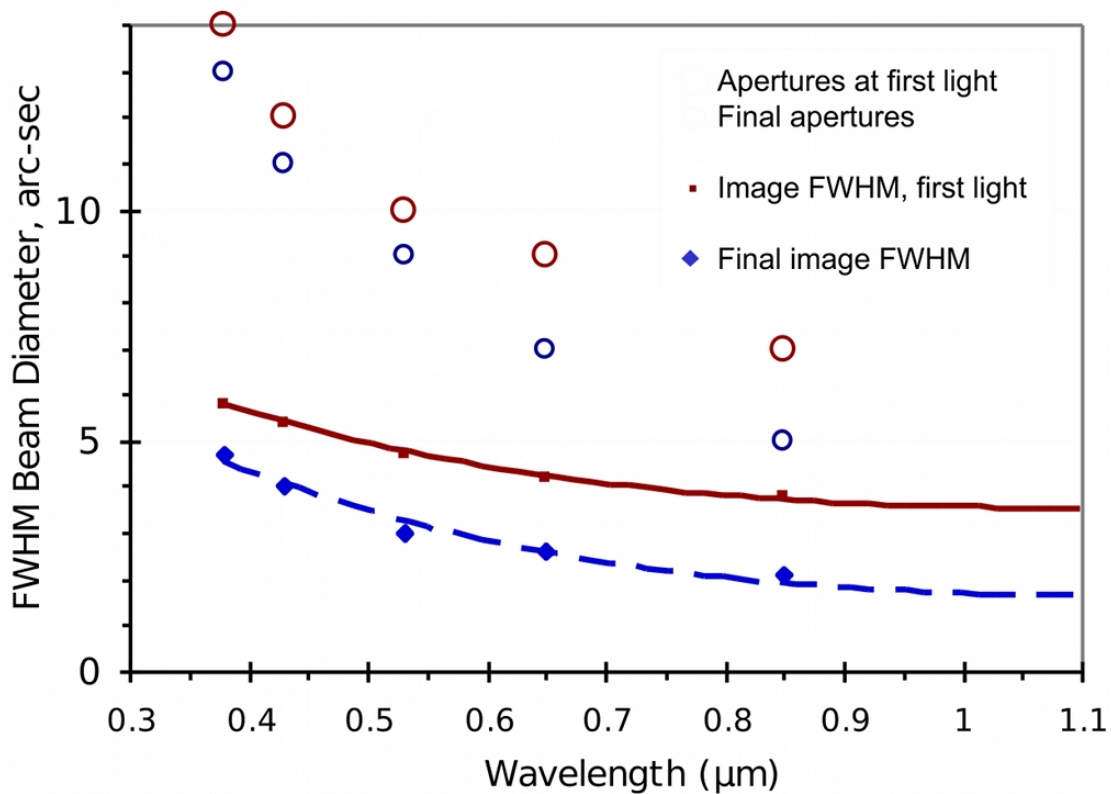[28]http://dx.doi.org/10.1117/12.788040

Figure 19: Plotted here is the expected instrument FWHM beam diameter as a function of wavelength.

quantum efficiency at longer wavelengths. It also nearly eliminates fringing at longer wavelengths. The figures below reflect this improvement.

Below are two plots of the HIPO total system throughput including atmospheric extinction, SOFIA telescope throughput, and instrument throughput for each of the available bandpasses (Figure 20). The first figure shows the total system throughput for the Johnson and methane filters with the 0.575 μm dichroic. The second figure shows the Sloan filters with the 0.675 μm dichroic. These figures assume that the FLITECAM dichroic beamsplitter is not installed. The very low total system throughput for HIPO is due to the dichroic tertiary mirror in the telescope. The long-planned aluminized tertiary will increase our throughput by a factor of nearly 3, on average, when it becomes available. The corresponding throughputs are presented in Figure 21.

7.1.4 Imaging Sensitivities

Plotted in Figure 22 below are HIPO first-light sensitivities for several representative cases. These figures assume that the FLITECAM dichroic beamsplitter is not installed. The upper figures correspond to occultations by Pluto or Triton while the lower two are for the case of a very faint occulting object. The left and right figures are for 0.5 sec and 50 ms integrations, respectively. Each figure shows S/N for no filter (dichroic only) and for the 0.675 μm dichroic plus standard

HIPO Total System Throughput
0.575 um Dichroic

HIPO Total System Throughput
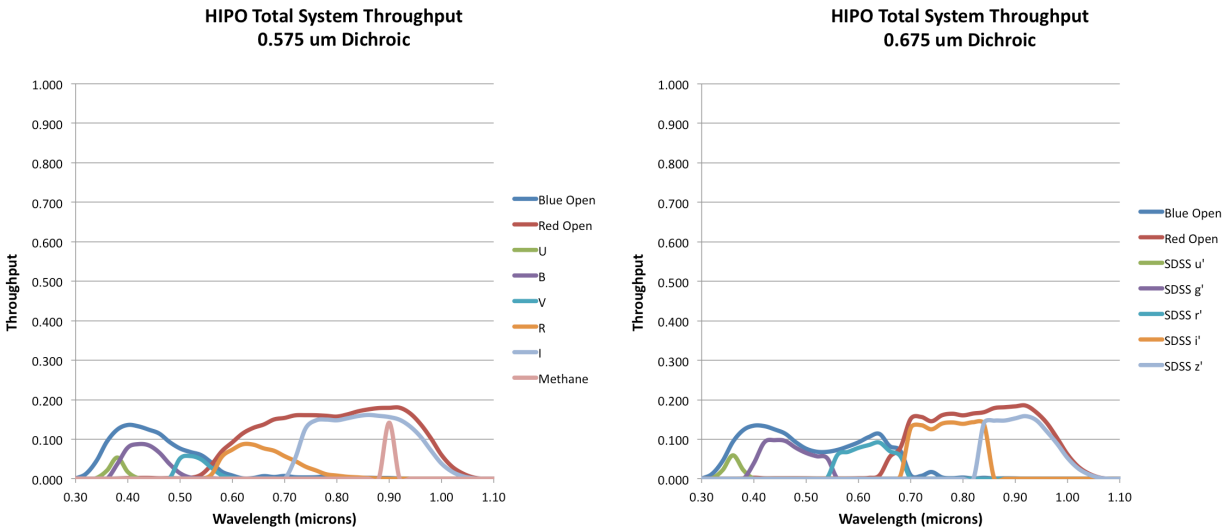**0.675 um Dichroic**

Figure 20: *Left:* Plotted here are the total system throughputs for the Johnson + Methane filter set with the 0.575 μm dichroic. *Right:* Plotted here are the total system throughputs for Sloan filters with the 0.675 μm dichroic.

HIPO Throughput
0.575 um Dichroic

HIPO Throughput
0.675 um Dichroic

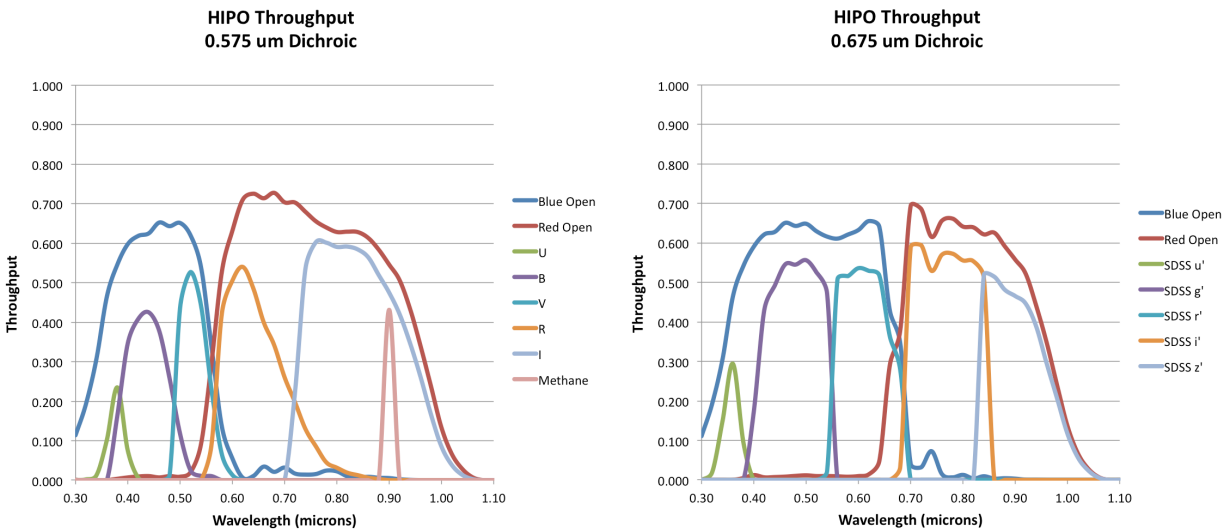Figure 21: HIPO only throughputs, i.e. without the telescope contribution. Otherwise, as in Figure 20, above.

Sloan filters.

The deviation of S/N from a square root dependence is mostly due to shot noise on the occulting object in the upper left figure, about equally shot noise on the occulting object and read noise in the upper right figure, about equally shot noise on the sky and read noise in the lower left figure,

and read noise in the lower right figure. Once the aluminized tertiary mirror is available read noise will only be significant in the lower right figure. The improved final SOFIA pointing stability will increase sensitivity for sky-limited events and improve discrimination from nearby bright objects (e.g. Neptune for a Triton occultation).

7.1.5 Imaging Sensitivities

A spreadsheet exposure time and SNR estimator for HIPO is available on the Information for Researchers web page. This spreadsheet accounts for transmission of all optical components from the atmosphere through the telescope, and inside HIPO, ending with the quantum efficiency of the detectors. It accounts for shot noise on the target, a possible background object (important for occultation work), and sky brightness as well as read noise. The wavelength dependence of the stellar flux is simply modeled as blackbody radiation, with the effect that there are systematic errors in the predictions that vary with wavelength and spectral type. The spreadsheet has been checked against a number of spectrophotometric standard stars with calibrations traceable through Vega to blackbody sources. Observed signals of these standards with the deep depletion CCDs is typically 10% higher than predicted but in the Johnson I and Sloan i' bands the observed signals are 30% higher than predicted.

THE SPREADSHEET SNR ESTIMATION DOES NOT ACCOUNT FOR SYSTEMATICS THAT DOMINATE AT HIGH SNR VALUES (∼500 OR HIGHER) ON TIMESCALES OF ∼10 MINUTES OR LONGER. THIS REMAINS A RESEARCH AREA! PLEASE CONTACT THE PI IF YOU HAVE QUESTIONS ALONG THESE LINES!

The spreadsheet is operated from its first tab, the Control Sheet. The next four tabs deal with optics that are common to both sides of HIPO (e.g. the atmosphere and telescope optics), optics peculiar to the blue or red sides, and the special case of the bare CCD. The last two tabs deal with blackbody and sky fluxes and the final combination of all the previous calculations that eventually appear back on the Control Sheet.

The spreadsheet is operated by filling in the yellow (most commonly used) and orange (less commonly used) cells to account for the star brightness and effective temperature, observing circumstances, CCD operations (integration time, binning, photometric aperture diameter), optics selections, and CCD choices. Results are returned in the light green cells. The main results are the signal levels from target, sky, and background object and the various noise contributions modeled by the spreadsheet. Scintillation noise is very difficult to measure and its value is not well determined yet. Finally the overall S/N ratio and fractional error are given. An estimate of the peak pixel signal in a star image is given in cells G34-H36. This is highly dependent on focus state and image jitter, and somewhat dependent on altitude so should be only used as a guide. The peak signal for the target star is also given in units of full well (assumed to be 100,000 electrons) in cells G35-H35. Note that full well is not affected by binning in a CCD47-20 since this CCD has no summing well. It is sometimes convenient to know the flux-weighted effective wavelength of a given filter/star combination. These are returned near the top center of the Control Sheet for the blue and red sides. For convenience the names of the beamsplitters, filters, and windows, or an indication if they have been removed, is given in the green cell above the selection cell for each optical element. The same applies to the CCD selection cells.

The optical elements modeled, in order, follow:

- Atmosphere: Atmospheric extinction is a combination of ozone (assumed to be 300 Dobson

units) and Rayleigh scattering appropriate for 41,000 foot altitude. This matches observations quite closely. The usual sec(Z) airmass correction is applied.

- Telescope: The condition of the aluminum coatings on the telescope optics can be changed using cells J43-L43. At present the only tertiary mirror available is the dichroic tertiary and cell L43 has no effect. Cell B26 allows selection of either the dichroic tertiary or the not-yet-available aluminized one. If the aluminized tertiary is selected the aluminum coating condition in L43 does have an effect. The SOFIA coatings are maintained in excellent condition so cases 0 and 1 are the only reasonable ones to use.

- Fore optics: If the tub is to be evacuated the gate valve window must be installed. Whether this window is installed or not is modeled by selecting 1 or 0 in cell C26. The dichroic reflector used in the FLIPO configuration is controlled by cell D26. It can be left out (0), be the new Reynard dichroic (1), or the old Lick dichroic (2). The Reynard dichroic has about half the emissivity of the Lick one and similar optical performance so is likely to be preferred in most cases.

- The dichroic beamsplitter internal to HIPO is controlled by cell E26 and can be left out (0) or be one of the two presently available ones (1 or 2). If it is left out no light reaches the blue side CCD.

- Filters for the blue, red, and bare CCD cases are controlled by cells F26-H26. There is a short explanation of what the various codes mean to the right of the cells used to select the various optics. New filters are certain to be added from time to time.

- CCD selection is made using cells F30-H30 with 0 being the original standard silicon CCDs and 1 being the newer deep depletion CCDs. The deep depletion CCDs have substantially higher QE and will be preferred in most cases in spite of their greater cosmic ray sensitivity. For UV work the thin blue CCD has better sensitivity than the deep depletion CCD.

A helpful figure showing the total signal per micron of bandwidth as a function of wavelength is shown in the upper right of the Control Sheet. It gives a graphical representation of the total signal accounting for everything from the star and sky through the CCD. The vertical axis on this graph autoscales.

An informational box related to the systematic error introduced by the blackbody approximation for stellar fluxes is given in the lower right of the control sheet. Errors at the ends of the wavelength range for very red stars can be 50% but are 30% or less for most cases.

Another informational box at bottom center provides a crude estimate of effective temperature given either spectral class or B-V for a target object.

Finally the revision list is given at bottom left. This spreadsheet will be updated from time to time as optics or detector selections change, or as additional information becomes available. The sky brightness estimate is currently a weak area and may be changed relatively soon.

7.2 Planning HIPO Observations

HIPO is a special purpose instrument, and the material included here is suitable for getting an initial idea of its capabilities. In order to propose to use HIPO, or the combination of HIPO

and FLITECAM it is *necessary* to consult with the Instrument Principal Investigator, Dr. E. W. Dunham. It is expected that the details of observation planning will be a central part of the discussions. HIPO (and HIPO+FLITECAM) proposals require the endorsement of the instrument PI.

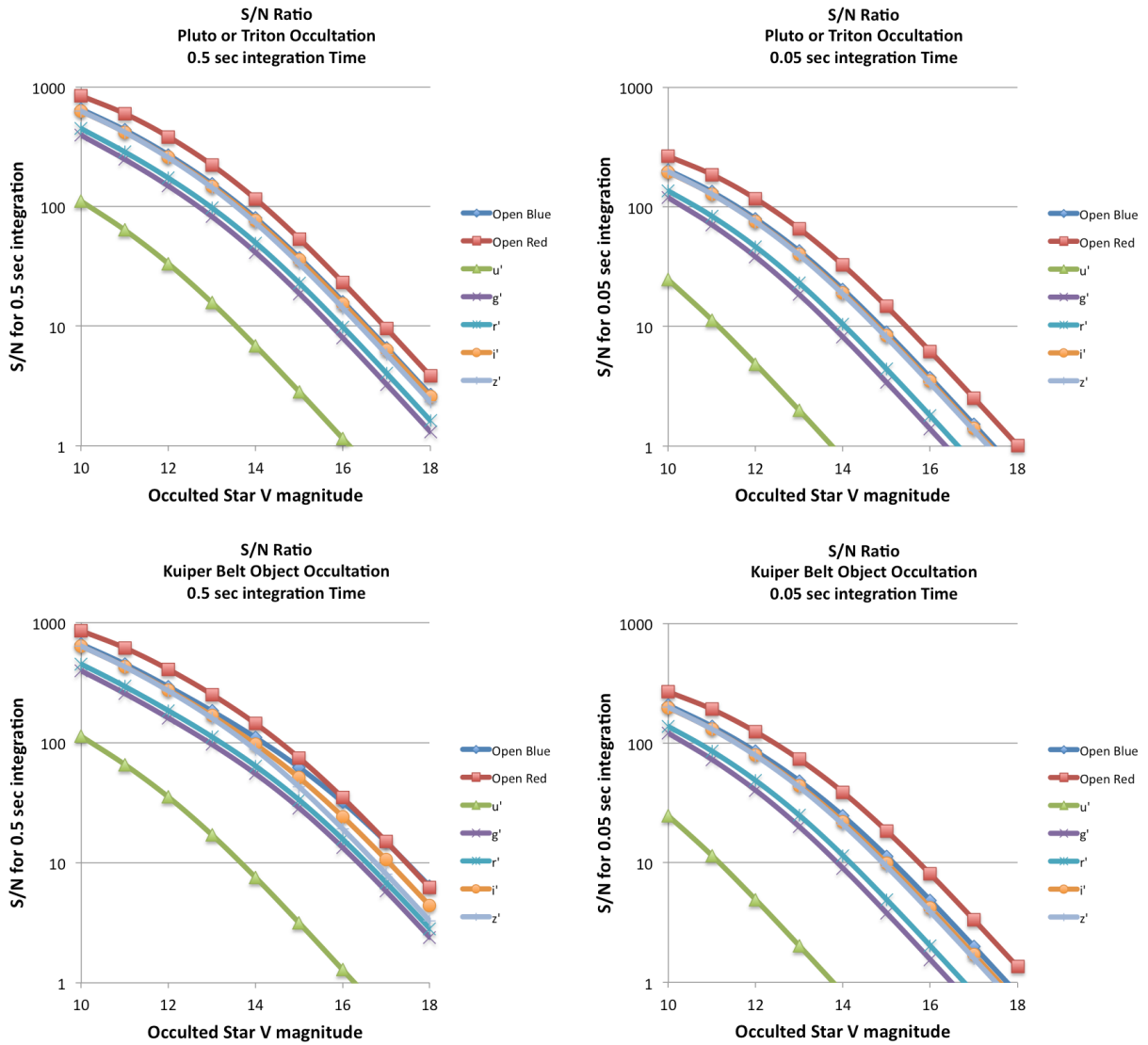Email: dunham@lowell.edu
Phone: 928-233-3221

Figure 22: Plotted here are the anticipated sensitivities for HIPO for several representative occultation scenarios.

8 Instruments V: EXES

8.1 Instrument Overview

The **E**chelon-**cross**-**E**chelle **S**pectrograph (EXES) operates in the $4.5 - 28.3\,\mu$m wavelength region, at high (R $\approx$ 50,000–100,000), medium (R $\approx$ 5000–20,000) and low (R $\approx$ 1000–3000) spectral resolution. The instrument uses a 1024×1024 Si:As detector array. High resolution is provided by an echelon — a coarsely-ruled, steeply-blazed aluminum reflection grating — along with an echelle grating to cross-disperse the spectrum. The echelon can be bypassed so that the echelle acts as the sole dispersive element. This results in single order spectra at medium- or low-resolution depending on the incident angle.

8.1.1 Design

EXES is a liquid helium cooled instrument. The cryostat is approximately 24 inches in diameter and 72 inches long. There are two cryogen reservoirs, one for liquid nitrogen and one for liquid helium. These are at the forward end, as mounted on SOFIA, with the entrance window on the aft end toward the telescope. There are three layers of radiation shielding within EXES - a vapor cooled shield tied only to the cryogen fill tubes, one attached to the liquid nitrogen reservoir, and the third attached to the liquid helium reservoir. All optics except for the entrance window/lens are attached to the liquid helium level. Baffling tubes connected to the liquid nitrogen level reduce thermal emission impinging on the internal optics. Within the liquid helium level, the optics are all tied to a rigid optics box constructed out of aluminum, and the detector headerboard is isolated with G10 fiberglass and actively maintained at a uniform temperature.

8.1.2 Optics

The optics consist of an entrance window/lens, fore-optics, three wheels housing the slits, deckers and filters, an echelon chamber, and a cross-dispersion chamber. The entrance window/lens (2 inches diameter) forms an image of the SOFIA telescope secondary at the liquid helium cold stop within the fore-optics. The fore-optics, including the entrance window, changes the incoming f/19 beam to f/10. After coming to a focus, the beam expands through a pupil (at the cold stop) to an ellipsoidal mirror. The light is redirected off two flat mirrors to a focus at the slit plane.

As the beam comes to a focus, it passes through the slit/filter cassette. This consists of three wheels on a common axle containing (i) filters to isolate grating orders, (ii) deckers to determine the length of the slit, and (iii) slits of different widths. The filter wheel has 12 slots, and these will be loaded with specific filters for each cool-down cycle based on the planned observations. Broader filters for use in the low-resolution configuration are included in 4 of the decker wheel slots. The decker wheel has a total of 11 features, which include continuously variable length slits, fixed length slits, pinholes, and an open position. The continuously variable slit length is provided by a cutout on the decker wheel that gets larger as a function of angle. The smallest size is about $4\rlap{.}''5$ and the largest about $45''$. The slit length depends on the wavelength and the instrument configuration. With that caveat, slit lengths can range from $1''$ to $180''$ on SOFIA. The slit wheel contains six slits. On SOFIA, EXES will typically use four of them (Table 8). There is also a wide $9.4''$ slit intended for flux calibration.

Table 8: EXES observing configurations, modes, slits and spectral resolutions

Configuration	Available Modes	Available Slit Widths[a] arcseconds	Resolving Power[b]
High_Medium	nod_on_slit[c], nod_off_slit, map	1.4	112,000
		1.9	86,000
		2.4	67,000
		3.2	50,000
High_Low	nod_off_slit, map	1.4	112,000
		1.9	86,000
		2.4	67,000
		3.2	50,000
Medium	nod_on_slit, nod_off_slit, map	1.4, 1.9, 2.4, 3.2	5,000-20,000[d]
Low	nod_on_slit, nod_off_slit, map	1.4, 1.9, 2.4, 3.2	1,000-3,000[d]

[a] 1.4″ slit unavailable >12 μm, 1.9″ slit unavailable >16 μm, 2.4″ slit unavailable >21 μm
[b] Observers must check the most recent resolving powers as a function of slit width and wavelength at http://irastro.physics.ucdavis.edu/exes/etc/
[c] On-slit nodding not possible at all wavelengths. Observers must check this at http://irastro.physics.ucdavis.edu/exes/etc/
[d] Resolving power is a strong function of wavelength and slit width

After passing through the slit wheel, the beam hits a flip mirror mechanism, which is used to choose between instrument resolution configurations (Table 8) by either directing the beam into the echelon chamber (high-resolution) or into the cross-dispersion chamber (medium- and low-resolution). In the high-resolution configuration, the beam enters the echelon chamber and expands to an off-axis hyperboloid mirror that serves as both collimator and camera mirror for the echelon grating. The dispersed light, focused by the hyperboloid, bounces off a flat into the cross-dispersion chamber.

The cross-dispersion chamber is conceptually identical to the echelon chamber. The light expands from the input to an off-axis paraboloid that again serves as both collimator and camera mirror. The collimated beam is sent to the cross-dispersion grating which disperses the light in the plane of the grating. The camera mirror sends the light to our detector. When operating in single-order, long-slit spectral configurations — our medium and low resolution science configurations — the light never enters the high-resolution echelon chamber.

There is a wheel in front of the detector, which provides a lens for imaging the pupil through the instrument, and a dark slide for isolating the detector. The wheel would also be available for including transmissive optics to adjust the plate scale on the detector, if desired.

8.1.3 Detector

The detector is a Raytheon Vision Systems Si:As array with 1024×1024 pixels. The detector material is bonded to a SB 375 multiplexer. The array is mounted in a separate enclosure to reduce scattered light. The headerboard is thermally isolated from the rest of the optics box to permit active temperature control of the array. The photon fluxes in the low-resolution configuration will

be significantly above the level intended for the array, and it is expected that only a subsection of the array will be clocked out in this configuration for a faster read-out (as well as in any imaging configuration). It is expected that a quarter to half the array will be utilized in these configurations, so the effective slit length is about 60″.

8.1.4   Performance and Sensitivities

At the time of writing, EXES in-flight commissioning is ongoing. Many of the performance specifications quoted here are expectations, based on laboratory tests, and test runs on ground based telescopes. The angular resolution of EXES will match that achieved by the telescope. For the latest sensitivities, observers are recommended to consult the online Exposure Time Calculator (ETC) at http://irastro.physics.ucdavis.edu/exes/etc/. The ETC also provides the slit length as a function of wavelength and instrument configuration (and therefore whether on-slit nodding is possible or not), as well as the wavelength coverage in a single setting and echelon orders that can be targeted.

The wavelength coverage ranges from 4.5–28.3 μm. There are three resolution regimes — high, medium and low — with the exact resolving power depending on wavelength, grating angle and slit width. Generally, the resolution will be higher at shorter wavelengths in each regime. The high-resolution configurations will use the echelon grating and will achieve R = 50,000–100,000. If the cross disperser echelle angle is 35-65°, the configuration is called High_Medium and if 10-25° it is called High_Low. For these high-resolution configurations, there is non-continuous spectral coverage in high-resolution configuration for $\lambda > 19\,\mu$m, but the central wavelength can be tuned so that lines of interest do not fall in the gaps. The Medium configuration will use high angles on the echelle grating to achieve R = 5,000–20,000, and the Low configuration will use low angles to achieve R = 1000–3000.

The High_Medium configuration slits are 4″.5–45″ long, and the High_Low slits are 1-12″ long. The shorter slits in High_Low allow for more orders to be packed onto the array, thus increasing the instantaneous wavelength coverage, while maintaining the high spectral resolution (see Fig. 28 for an example). In the Medium and Low configurations the slit lengths vary from 25″ to 180″ depending on the number of rows to be read out.

The sensitivity of the instrument is shown in Figures 23 through 26 for the High_Medium, Medium, and Low configurations for both point sources and extended sources. The Noise Equivalent Flux Density for S/N of 10 in a **clock-time**[29] of 900 seconds is plotted as a function of wavelength. These values have been calculated for a point source assuming image quality between 2″ and 4″ (FWHM) and the narrowest of the available 1″.4 to 3″.2 slits, both of which vary with wavelength, and take into account estimated instrument efficiency. They assume an altitude of 41,000 feet, 40° elevation, and 7 μm precipitable water vapor.

---

[29]Note that the other instruments in this Handbook report sensitivities based on the **total time on-source**, not the **clock-time**. The latter includes the total time on-source + applicable overheads, excluding target acquisition and instrument set-up time.
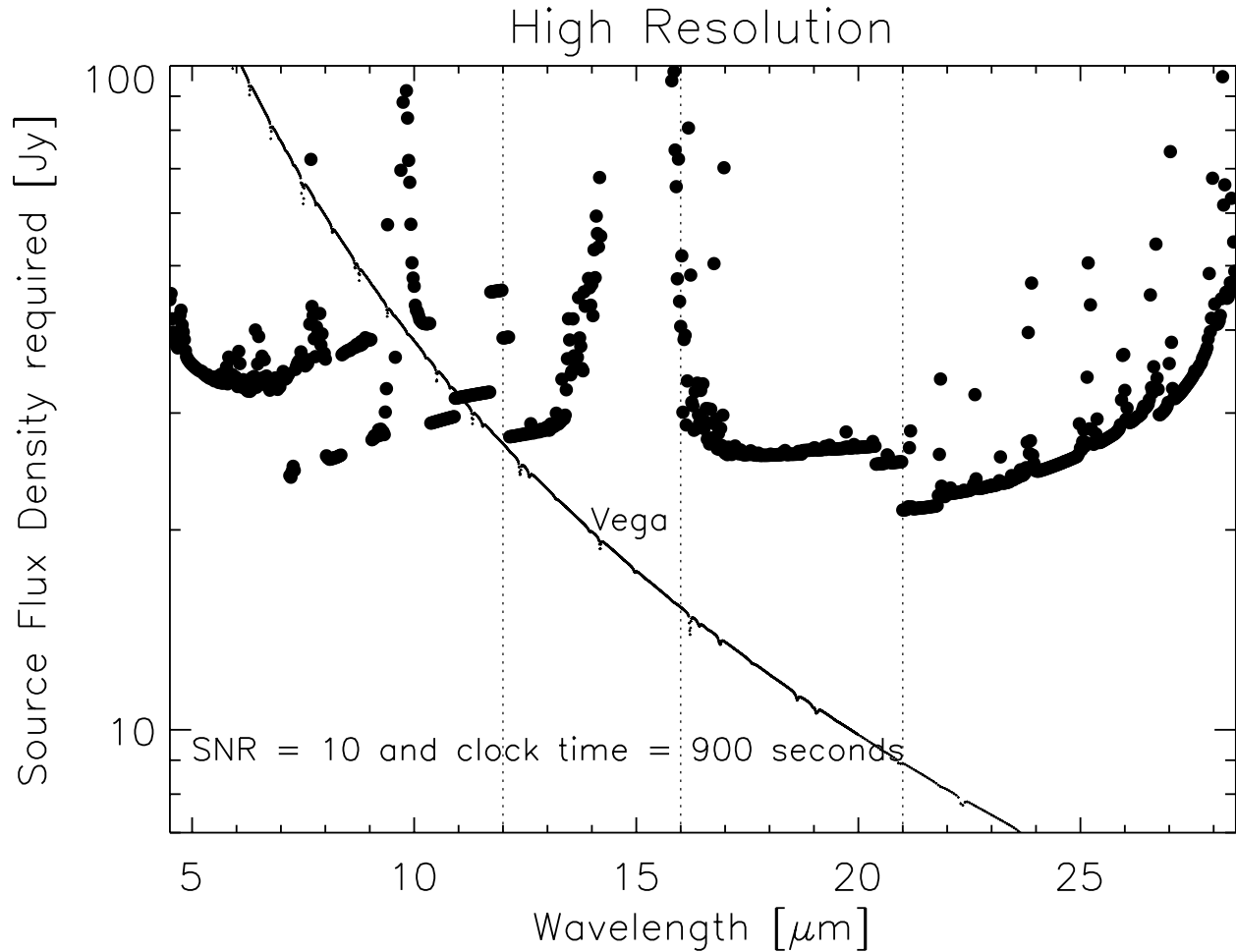
Figure 23: The minimum detectable *point source* flux as a function of wavelength for the EXES High‗Medium configuration, assuming the conditions mentioned at the end of §8.1.4. It takes into account that on-slit nodding is not possible at all wavelengths. The vertical dotted lines show the boundaries between the slit widths used (1″4, 1″9, 2″4, 3″2). For precise numbers at individual wavelengths and for the High‗Low configuration please use the online ETC.

8.2 Planning EXES Observations for Cycle 3

During Cycle 3, EXES will be offered in shared-risk mode. The in-flight performance of the instrument will be known only after the commissioning flights, planned during Cycle 2, are carried out. The technical feasibility of accepted programs may need to be re-evaluated after that. Another connotation of shared-risk observations is that the data quality may not reach the levels requested by the proposer.

The proposer needs to supply the central wavelength, the spectroscopic configuration, the slit width, and the observing mode for each observation (Table 8). These parameters define the default instrument set-up. Each central wavelength specified should count as a separate observation. In addition, the proposer should estimate the clock time necessary to reach the desired S/N. The
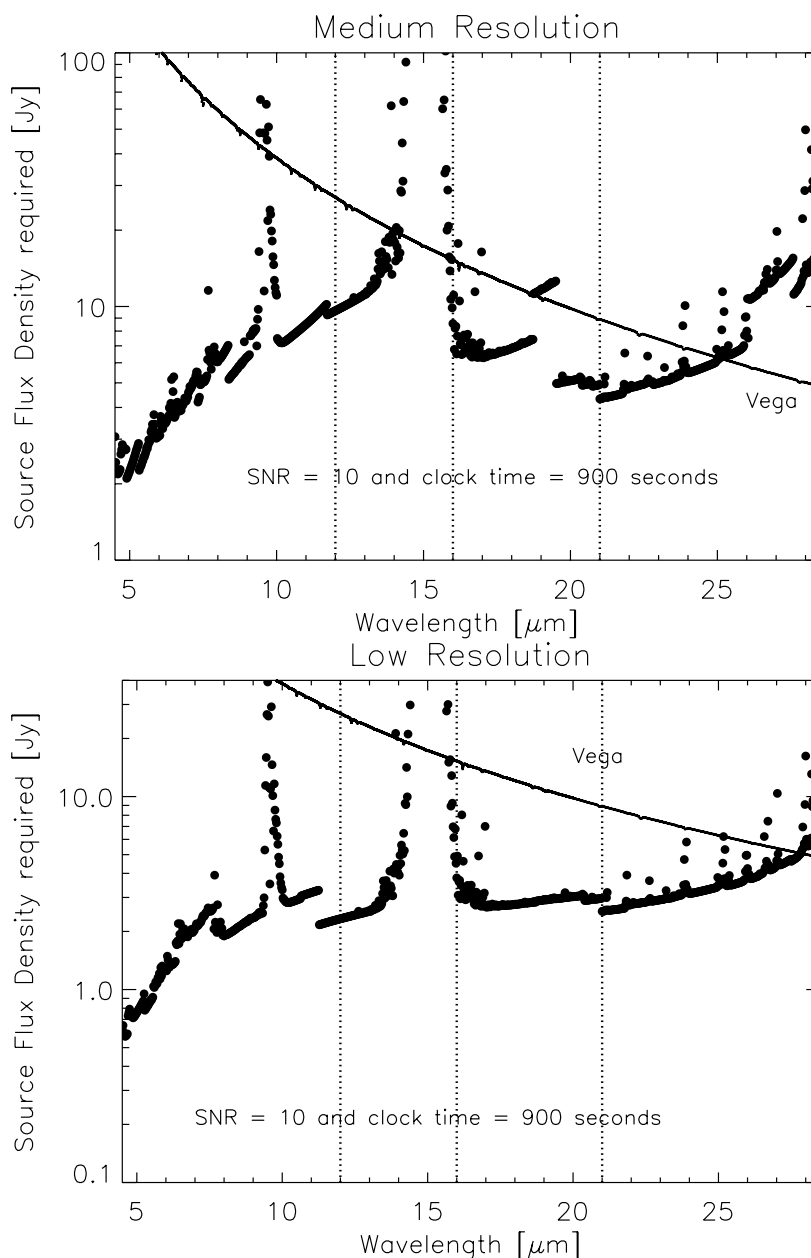
Figure 24: The minimum detectable *point source* flux as a function of wavelength for the Medium (top) and Low (bottom) configurations, assuming the conditions mentioned at the end of §8.1.4. The vertical dotted lines show the boundaries between the slit widths used ($1\rlap{.}''4$, $1\rlap{.}''9$, $2\rlap{.}''4$, $3\rlap{.}''2$).

calculation may be based on Figures 23 and 24 for point sources and on Figures 25 and 26 for extended sources, noting that the minimum detectable flux $\propto (S/N)/\sqrt{(t_{exp})}$. However, it is recommended that the online ETC at http://irastro.physics.ucdavis.edu/exes/etc/ is checked as well for the latest updates.

EXES operates in a wavelength region, parts of which are accessible from ground based tele-
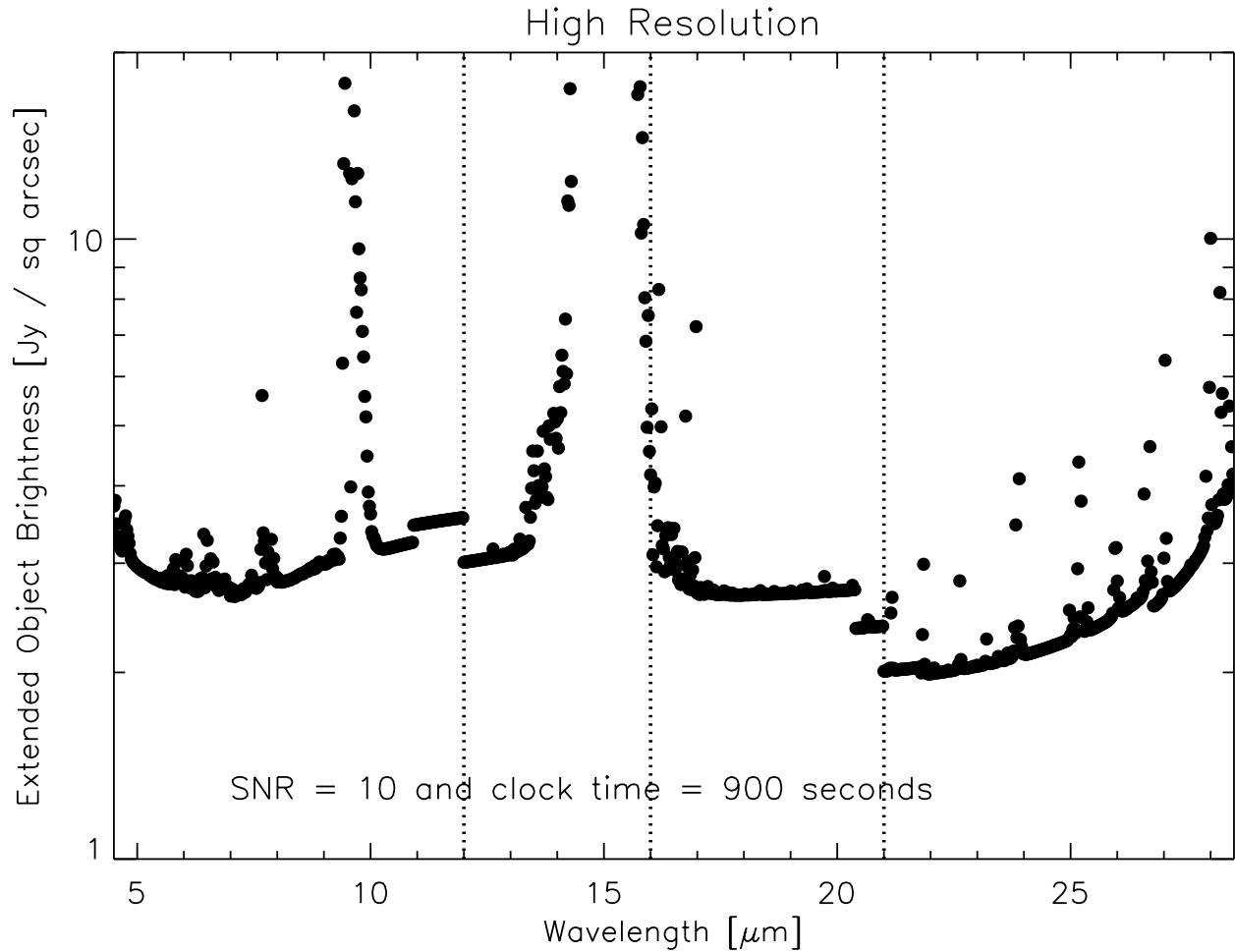
Figure 25: The minimum detectable *extended source* flux as a function of wavelength for the High_Medium and High_Low configurations (using off-slit nodding).

scopes. Proposers should carefully check the atmospheric transmission (using ATRAN at https://atran.sofia.usra.ed for example) and make sure that the observations require, or would greatly benefit from, using SOFIA. The proposer should take into account the Doppler shift of the target(s) due to their motion relative to the Local Standard of Rest, and to the Earth. If proposers find that the atmospheric transmission at the wavelength of interest is lower than the local median (calculated over a range $\pm 0.0125 \, \mu m$), then more time will be required to reach the desired S/N. Higher transmission would imply shorter required times. In general the, S/N scales as $transmission/\sqrt{((1 - transmission) + 0.3)}$. Note that the online ETC includes the impact of the atmosphere at precise wavelength of interest and so may differ from the Figures. The ETC provides the **clock-time** required to achieve the desired S/N per resolution element on a continuum object at the specific wavelength of interest and then indicates what the expected S/N should be for the entire setting.

   Proposers should specify the slit width, which sets the resolving power for each configuration (Table 8). Note that the narrowest slit $(1.4'')$ is only effective below 12 μm (above this wavelength no gain in resolving power is achieved, while flux is lost with respect to the wider slits). Similarly,
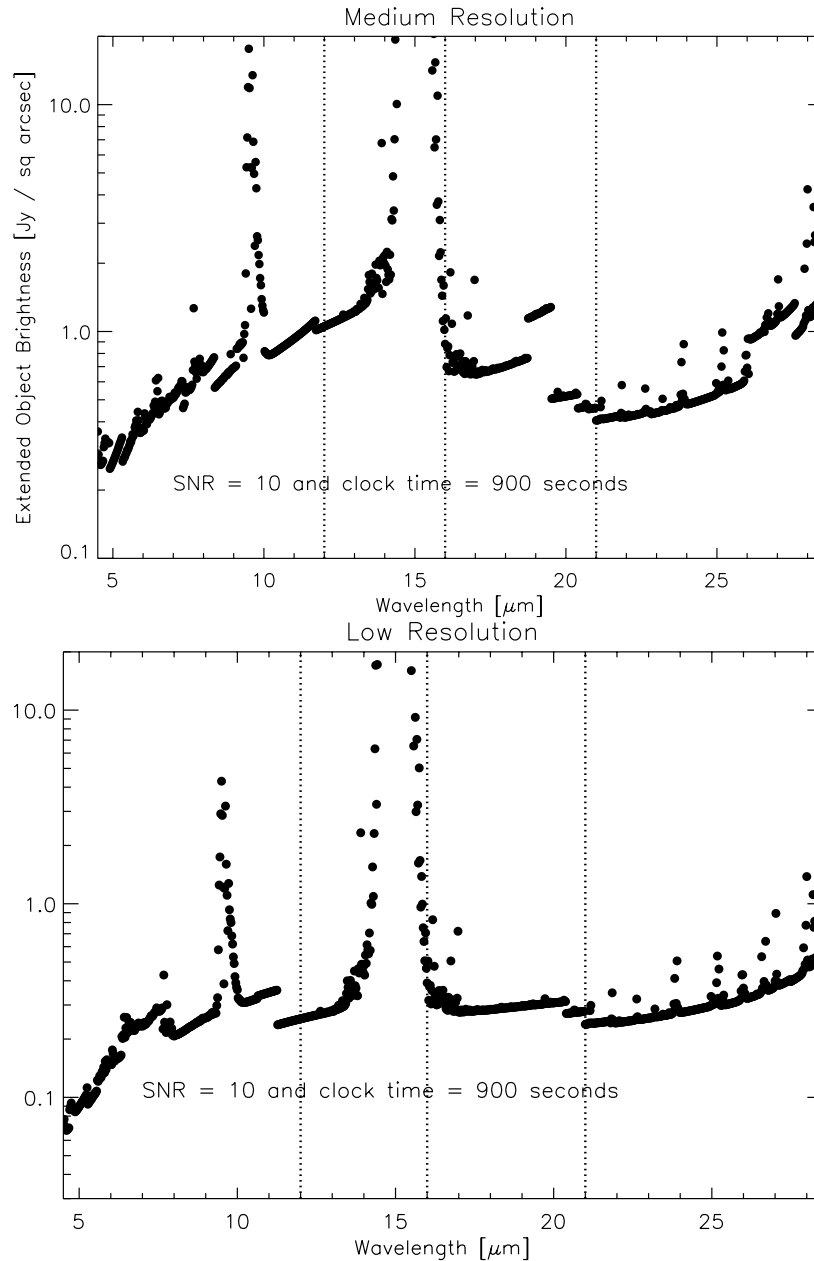
Figure 26: The minimum detectable *extended source* flux as a function of wavelength for Medium (top) and Low (bottom) configurations, assuming the conditions mentioned at the end of §8.1.4. The vertical dotted lines show the boundaries between the slit widths used ($1''\!.4$, $1''\!.9$, $2''\!.4$, $3''\!.2$).

the $1.9''$ slit can only be used below 16 μm, and the $2.4''$ slit below 21 μm.

In configurations using the medium resolution grating (Medium and High_Medium), the single setting spectral coverage ranges between 0.03 μm at the shortest wavelengths, and 0.3 μm at longer wavelengths (Fig. 27). For the low resolution grating (the Low and High_Low configurations) this is 0.2-0.8 μm. Note that while High_Low and High_Medium have the same spectral resolution, the
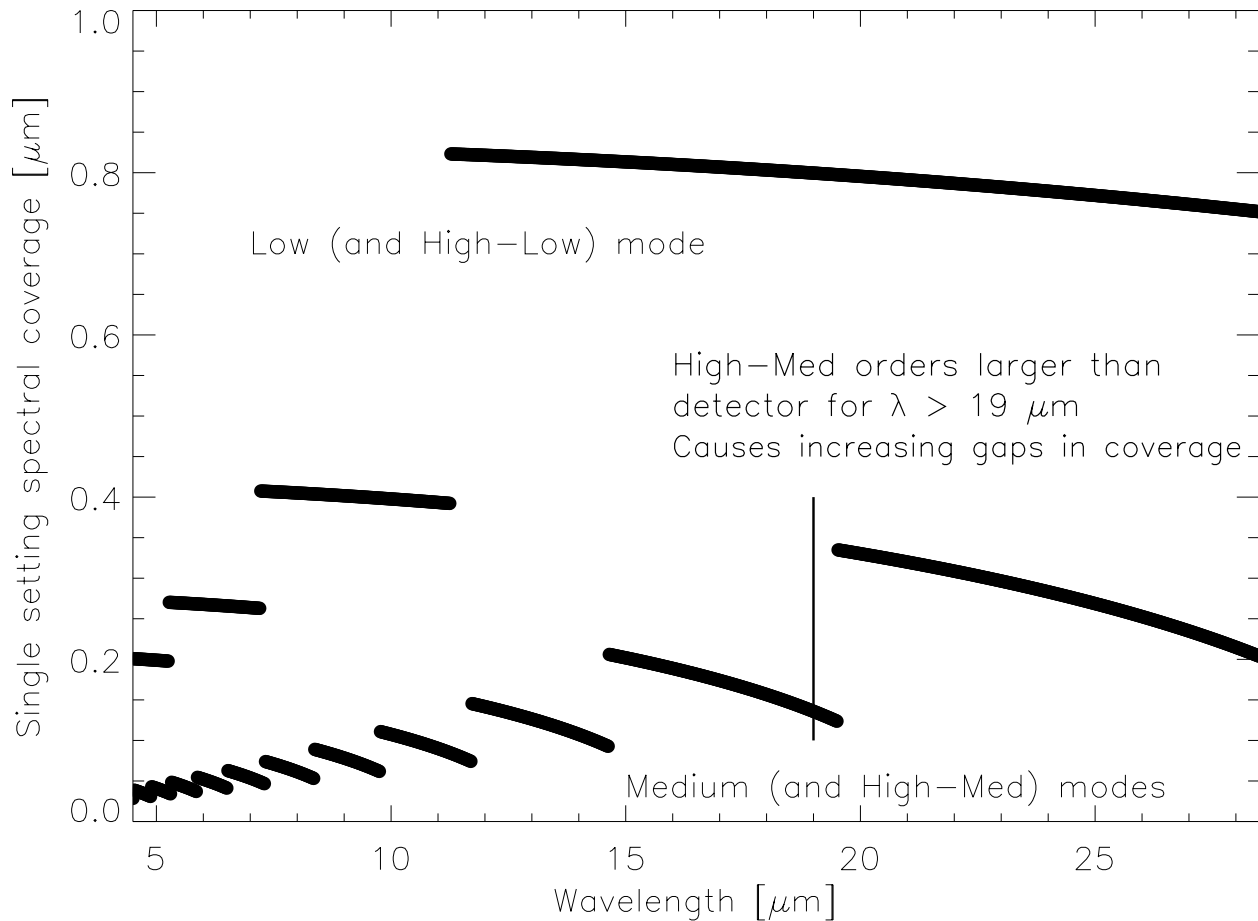
Figure 27: The single setting spectral coverage as a function of wavelength. Note that these values are the same for the High_Medium and Medium configurations, and for the High_Low and Low configurations.

larger wavelength coverage of High_Low comes at the expense of a smaller slit length, which is illustrated in Figure 28.

Proposers should choose a single line of interest for each observation. Fine tuning of the bandpass to observe lines at the extreme edges of a single setting should be done in consultation with the EXES team to see if existing data indicates such tuning is possible.

The slit orientation on the sky depends upon the time when the target is observed, and therefore the position angle cannot be specified.

EXES will not use the secondary for chopping in any of its observations. There will be two scientific modes - Nod and Map mode.

Nod mode: In this mode, the telescope is moved to a new position in order to remove the sky background. For point sources observed with a sufficiently long slit, the telescope is moved such that the object remains on the slit. For sources larger than about a quarter of the slit length, the telescope is moved such that the object is not on the slit. The time between telescope motions will

HIGH_MED Configuration   **HIGH_LOW Configuration**

13.730 μm
728.33 cm^{-1}

14.10 μm
709.22 cm^{-1}

13.629 μm
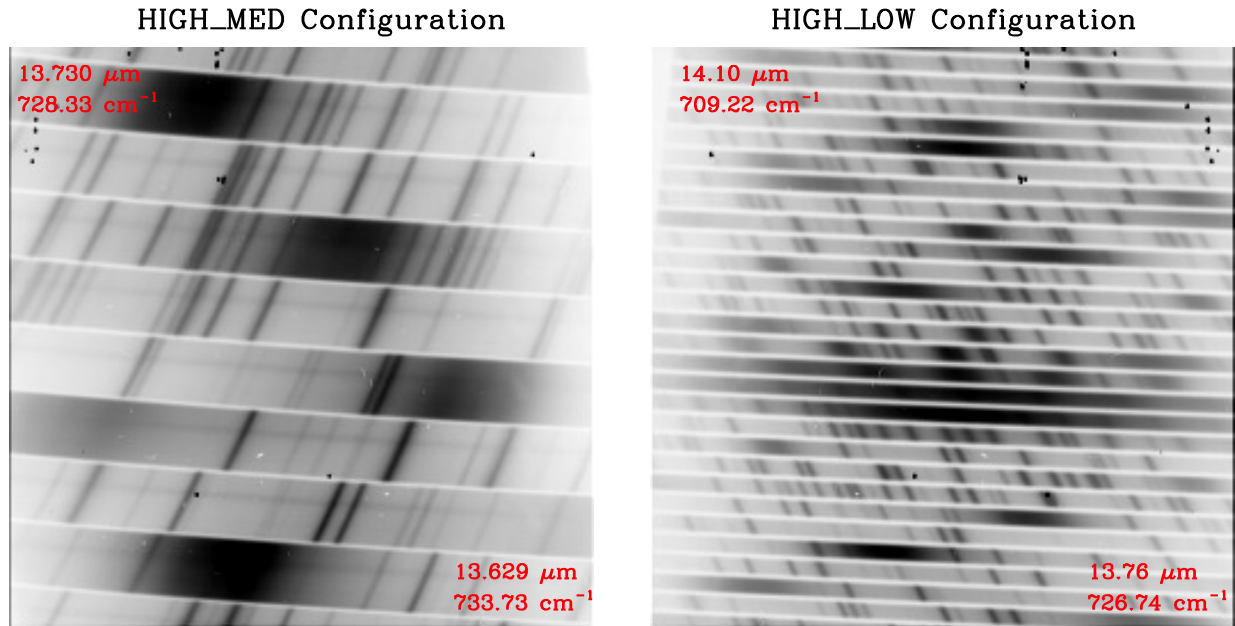733.73 cm^{-1}

13.76 μm
726.74 cm^{-1}

Figure 28: Comparison of raw 2D spectra of EXES in the High_Med (left) and High_Low (right) configurations obtained during commissioning flights. The spectra are not nod-subtracted, highlighting the sky emission lines (dark). This comparison shows that, while the High_Med and High_Low configurations have the same spectral resolution, High_Low has a much larger spectral coverage at the expensive of a shorter slit to be able to pack more orders on the array. In contrast, the Low and Medium configurations (not shown) have the same spectral coverage as High_Low and High_Medium, respectively, but a lower spectral resolution without cross dispersion. The approximate start and end wavelengths are indicated in red.

depend on the sky variation, the telescope settling time, and the integration time. The goal is to maximize the signal–to–noise per clock time. For observations of point sources, the detectable flux plot (Figs. 23, 24) includes assumptions regarding whether nodding off the slit is required due to short slit lengths. Therefore, proposals for point sources do not need to specify nod parameters. For nodded observations of extended objects, proposers should contact the EXES team to check if nodding on the slit is possible. If not, the observing time required should be doubled. Unless specific nod parameters are requested for such observations, the instrument team will define the nod amplitude, direction and frequency. The sensitivities for extended source observations shown in Figures 25 and 26 assume that the source is nodded off-slit and take into account the variation in spatial resolution with wavelength. The atmospheric and overhead factors for nodding are included. If the source is small relative to the slit length, then it may be possible to nod along the slit. In this case, the source brightness given in the figures is for a SNR of 10 in 450 seconds.

Map mode: In this mode, the telescope is moved sequentially such that a series of positions along a straight line on the sky (a "stripe") are observed to create a map. The sky background is taken from the first positions and, depending on the size of the map, from the last positions. In general, we anticipate the telescope motions to be half the slit width to create a well–sampled map.

Proposers should specify the number of steps in a map and the step size. Map steps are generally assumed to be perpendicular to the slit. The first three positions for taking data in a map must be blank sky. These could be the first three positions of the map or at a separate sky offset position specified by the user. It is recommended that additional blank sky positions are observed at the end of the map on the other side of the object. For all maps, the instrument software returns to the sky offset position for three final sky observations at the end of the observation.

Proposers should specify the required clock time based on the flux limit desired, using the values in Figures 25 and 26, including any assumptions regarding binning of map positions to yield the final required SNR. The SNR for a single map position can be estimated by assuming that the required time is similar to that for nodding an extended object on slit, i.e. 10σ in 450 seconds for a given source brightness. If any spatial binning is required – at least a 2-step sum is recommended – then the SNR will improve by the square root of the number of steps in the sum. The online ETC allows the user to specify the number of steps and bins according to the predicted image quality in producing a clock-time estimate.

8.2.1 Wavelength Calibration

Wavelength calibration with EXES will be performed by applying the grating equation to atmospheric lines observed in the source spectra. As long as there is a single telluric feature in the bandpass with depth of at least 5%, the wavelength calibration is expected to be accurate to $\simeq 0.5$ km s^{-1}. More concrete values for the calibration accuracy will be available once commissioning is completed.

If atmospheric models show no telluric features within the EXES instantaneous band pass for a given observation then obtaining a good wavelength solution will require a few additional steps. Note that the absence of telluric features from SOFIA suggests the observation may be better done from the ground. First, the order sorting filter (OSF) is rotated so that a different order from the echelle is observed that includes a suitable telluric line. The grating equation can then be applied, providing wavelength calibration accuracy down to ~ 1 km s^{-1}. The process of rotating the OSF, observing blank sky, and rotating the OSF back to the original orientation should take less than 5 minutes of additional time. A demonstration of this procedure can be found in Harper et al. (2009, ApJ, 701, 1464).

8.2.2 Flux Calibration and Atmospheric Line Correction

For every EXES science observation, the EXES temperature-controlled black body source and a nearby blank sky field will be observed. From these, a calibration spectrum will be constructed that, after division over the science observations, will correct for response variations, provide flux calibration, and correct for telluric absorption lines. The flux calibration is expected to be better than 20%, but the true accuracy is currently uncertain. Experiments focused on line profile information and those that can normalize the continuum level, or use past observations for setting the continuum, are likely to be lower risk. Telluric corrections are expected to be accurate in wavelength regions where the atmospheric transmission is >0.50. Projects requesting additional telluric calibration, in particular those observing lines near strong telluric features, will need to identify a

suitable target and include the observation time required to reach the desired signal-to-noise level in their proposal.

8.2.3 Overheads

The treatment of overheads for EXES differs from that of most other SOFIA instruments. Instead of on-source times, users are required to specify "wall clock" times in SPT and SSPOT, which is the on-source time plus all overheads except those related to acquisition and instrument set-up. The overheads include time on "empty" sky in the off-slit nodding and mapping modes, as well as read-out and other telescope and instrument inefficiencies. The ETC[30] gives both the on-source and clock times, but only the latter should be used. The figures in this manual only give clock times. SPT and SSPOT will add an additional 20 minutes for acquisition and instrument set-up.

8.3 EXES as a Principal Investigator Instrument

EXES is a Principal Investigator (PI) class instrument. The proposer is not required to contact the Instrument PI, Dr. Matt Richter, before preparing or submitting the proposal. However, it is recommended that they do so, in order to get the most up to date information about instrument capabilities. The data collection and reduction will be done by the instrument team, and it is expected that data analysis and preparation of the results for publication will be done by the General Investigator(s) in collaboration with the Instrument Team.

---

[30]http://irastro.physics.ucdavis.edu/exes/etc/

9 Instruments VI: FIFI-LS

9.1 Instrument Overview

The Far Infrared Field-Imaging Line Spectrometer (FIFI-LS) is an integral field, far infrared spectrometer. The instrument includes two independent grating spectrometers sharing one common field-of-view (FOV). Each spectrometer has a detector consisting of 400 pixels of Germanium Gallium-doped photoconductors. The short wavelength spectrometer (blue channel) operates at wavelengths between 50μm and $125\,\mu$m, while the long wavelength spectrometer (red channel) covers the range from $105\,\mu$m up to $200\,\mu$m. One of two dichroics has to be selected for an observation affecting the wavelength range of both channels in the overlap region.

The projection onto the sky of the 5×5-pixel FOVs of both channels is concentric ($10''$ offset), but the angular size of the FOVs differs. The red channel has a pixel size of $12'' \times 12''$ yielding a square $1'$ FOV , and the blue channel has a pixel size of $6'' \times 6''$, which yields a square $30''$ FOV.

The resolving power of both channels varies between 500 and 2000 dependent on the observed wavelength. The higher values are reached towards the long wavelength ends of each spectrometer.

The detectors are cooled down to about $1.7\,$K with superfluid helium. The spectrometers and all mirrors are cooled down to $4\,$K with liquid helium. The exception is the entrance optics featuring a K-mirror (see Sect. 9.1.3) and an internal calibration source. These optical components are cooled to about $80\,$K with liquid nitrogen.

9.1.1 Integral Field Concept

The integral field unit (IFU) allows FIFI-LS to obtain spectra at each point in its FOV in contrast to a spectrometer with a slit which only provides spectra along the slit. Each channel in FIFI-LS has an IFU, which consists of 15 specialized mirrors to "slice" the two dimensional 5x5 pixel FOV into five slices (of five pixels length each) which are then reorganized along a (one dimensional) line (25x1 pixel). This line forms the entrance slit of the actual spectrometer. The diffraction grating disperses the incoming light in the spectral dimension. Finally the dispersed light reaches the 16x25 pixel detector array. The result is a "data cube" with 5x5 spatial pixels (spaxels) and 16 pixels in the spectral "dimension". Figure 29 shows the concept.

9.1.2 Selection of the Dichroic

The two channels have an overlap in their wavelength range. That is necessary because a dichroic splits the light between the two channels allowing the common FOV for both channels. The drawback is that a dichroic has a transition region where neither the transmission nor the reflection is good. Thus, FIFI-LS has two dichroics with transitions at different wavelengths. The "$105\,\mu$m-dichroic" cuts off the blue channel at about $100\,\mu$m and opens the red at about $110\,\mu$m. The "$130\,\mu$m-dichroic" cuts off the blue channel at $125\,\mu$m and opens the red at $130\,\mu$m. One should look at Fig. 30 to choose the best dichroic and line combinations. The user needs to pair up wavelengths so that each pair can be observed efficiently with one of dichroics."

9.1.3 Beam Rotator

The SOFIA telescope is essentially an Alt-Az-mounted telescope. Thus, the sky rotates while tracking an object. However, the telescope can rotate around all three axes. The amount it can
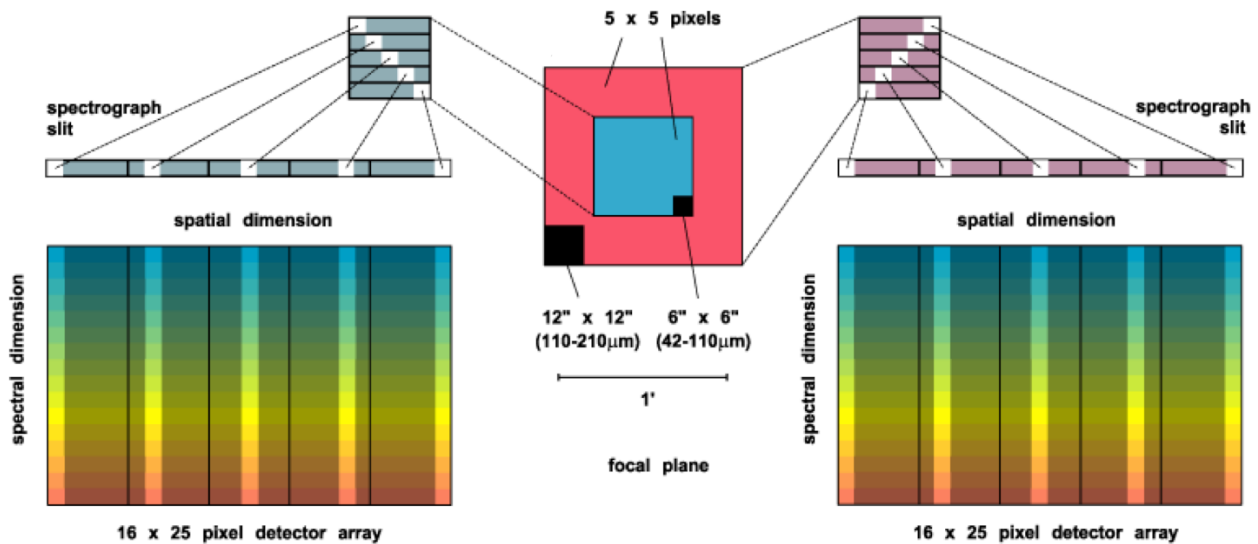
Figure 29: Illustration of the field imaging concept in FIFI-LS. The optics slice the rows of the 5x5 pixel field of view into a 25x1 pixel pseudo slit.

rotate in cross-elevation and line-of-sight is limited though. Thus, the normally continuous sky rotation is frozen-in for some time while the telescope is inertially stabilized. When the telescope reaches its limit in line-of-sight rotation, it needs to "re-wind" resulting in a rotated FOV of the telescope.

FIFI-LS has a beam rotator (K-mirror) that rotates the instrument's FOV, counteracting the sky rotation experienced by the SOFIA telescope. When a "re-wind" happens, the FIFI-LS beam rotator will automatically rotate the FOV of the instrument, so that the position angle of the instrument's FOV on the sky is maintained. An additional benefit is that the beam rotator enables the observer to line up the FOV with e.g. the axes of a galaxy and keep the alignment. The desired position angle of the FOV can be specified in Phase II of the proposal process.

9.1.4   Comparison with the PACS-Spectrometer

The FIFI-LS design is very similar to the Herschel/PACS-spectrometer sharing much of the design. The detectors are basically the same and the optical design is very similar (same sized gratings in Littrow configuration, same IFU). The difference is that FIFI-LS features two grating spectrometers whereas the PACS-spectrometer had only one. The two gratings make it possible to observe two different wavelengths simultaneously and independent of each other (one in each channel). This design also allows different pixel sizes ($6''$ vs $12''$) in each spectrometer, which means a better match to the beam size. The spectral range of FIFI-LS also goes down to $50\,\mu$m whereas PACS did not routinely observe the [OIII] 52 μm line.
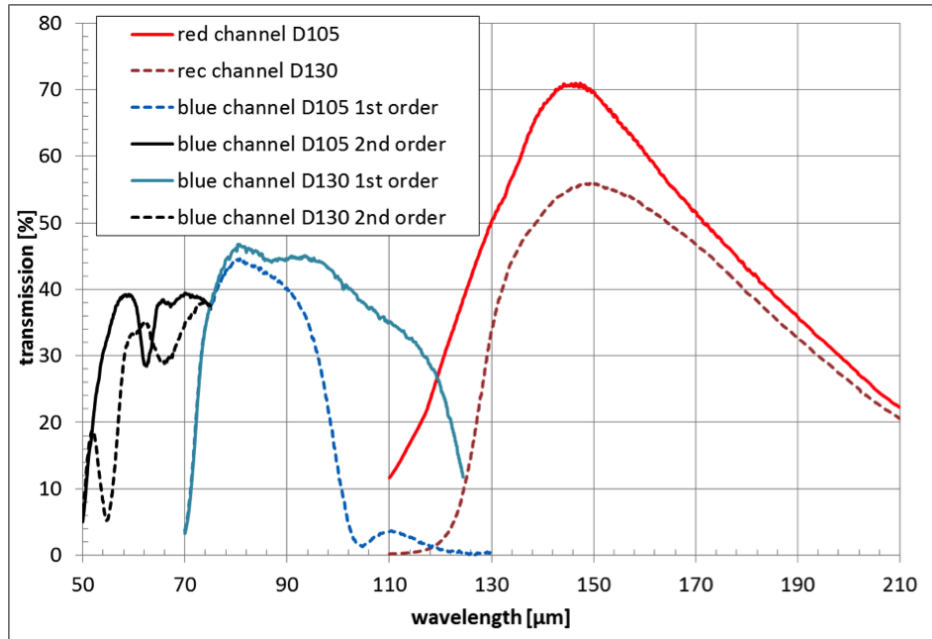
Figure 30: Throughput of optical system - Here the transmission of the overall optical system is shown for the six possible optical configurations using two dichroic beam splitters ($105\,\mu$m and $130\,\mu$m) and both grating orders (blue channel only).

9.2 Performance

The following sections cover the performance of FIFI-LS as estimated theoretically and as measured in the laboratory. The instrument had its commissioning flights just before the Cycle 3 Call for Proposals was released. Updates to the sensitivities and spectral resolution from on-sky measurements taken during these flights are pending.

9.2.1 Spectral Resolution

The blue spectrometer operates in 1$^{\text{st}}$ and 2$^{\text{nd}}$ order. An order-sorting filter blocks the unwanted order. The red spectrometer only operates in 1$^{\text{st}}$ order. The spectral resolution of FIFI-LS depends on the observed wavelength. It ranges from $R = \lambda/\Delta\lambda \approx 500$ to 2000. That corresponds to a velocity resolution of 150 to $600\,\text{km/s}$. The top panel of Fig. 31 shows the spectral resolution in velocity resolution and in R vs wavelength as measured in the lab (blue channel) and on the commissioning flights (red channel). The analysis of the measurements for the blue channel from the commissioning flight's is pending. Currently, the spectral resolution given for the blue channel is a conservative estimate.

FIFI-LS has 16 pixels in the spectral direction. The wavelength range covered by these 16 pixels also depends on the observing wavelength. The bottom panel of Fig. 31 shows the instantaneous spectral coverage or bandwidth (BW) in micron.
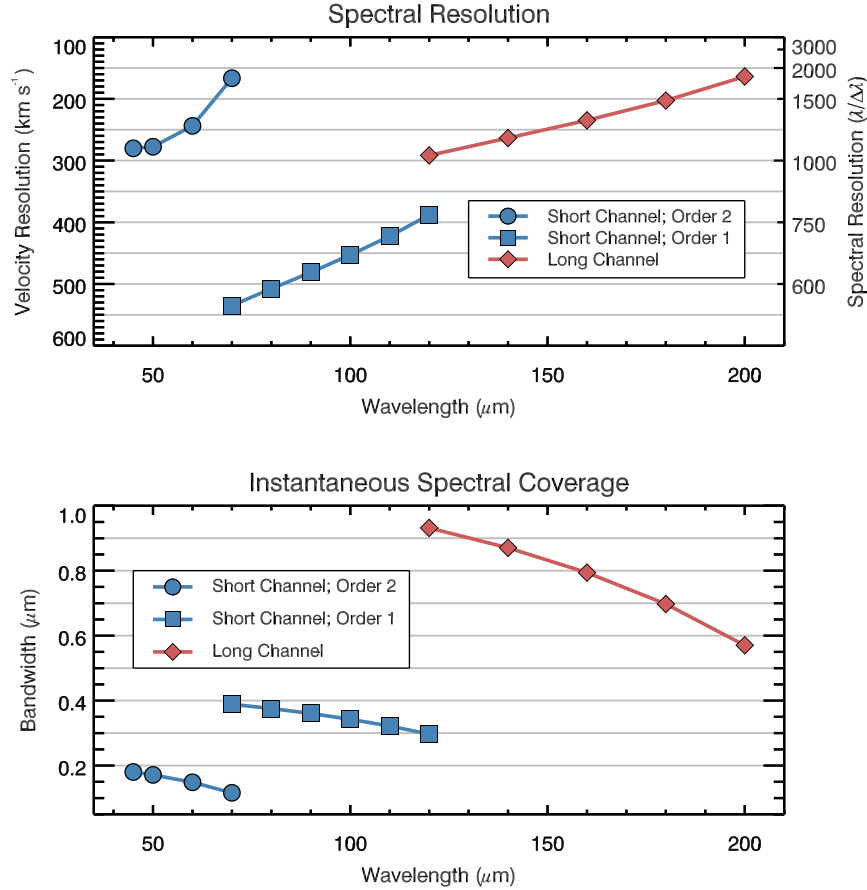
Figure 31: **Top:** The spectral resolution for both channels; **Bottom:** The instantaneous wavelength coverage of the 16 spectral pixels vs. wavelength.

9.2.2 Sensitivity

FIFI-LS will operate such that the detectors are always background-limited, infrared photode-tectors. Under this assumption, the overall performance of FIFI-LS as a function of wavelength has been estimated. Further assumptions about the emissivity of the telescope, optics, and baffling, the efficiency of the detectors had to be made. Figure 32 shows the resulting sensitivities for continuum and line fluxes as minimum detectable fluxes, i.e. detected with a signal to noise ratio (SNR) of 4 and an on-source integration time of 900 s or 15 min. To calculate the on-source integration time for a source flux F and a desired SNR use

$$t_{\mathrm{on}} = l \left(\frac{\mathrm{SNR}/4}{\alpha F/\mathrm{MDF}(\lambda)} \right)^2 900\,\mathrm{s}$$

where $\mathrm{MDF}(\lambda)$ is either the Minimum Detectable Continuum Flux (MDCF) in Jy per pixel or the Minimum Detectable Line Flux (MDLF) in W m^{-2} per pixel at the desired wavelength (see Fig. 32). Of course, F needs to be in the same units. The factor α is the transmission of the atmosphere for
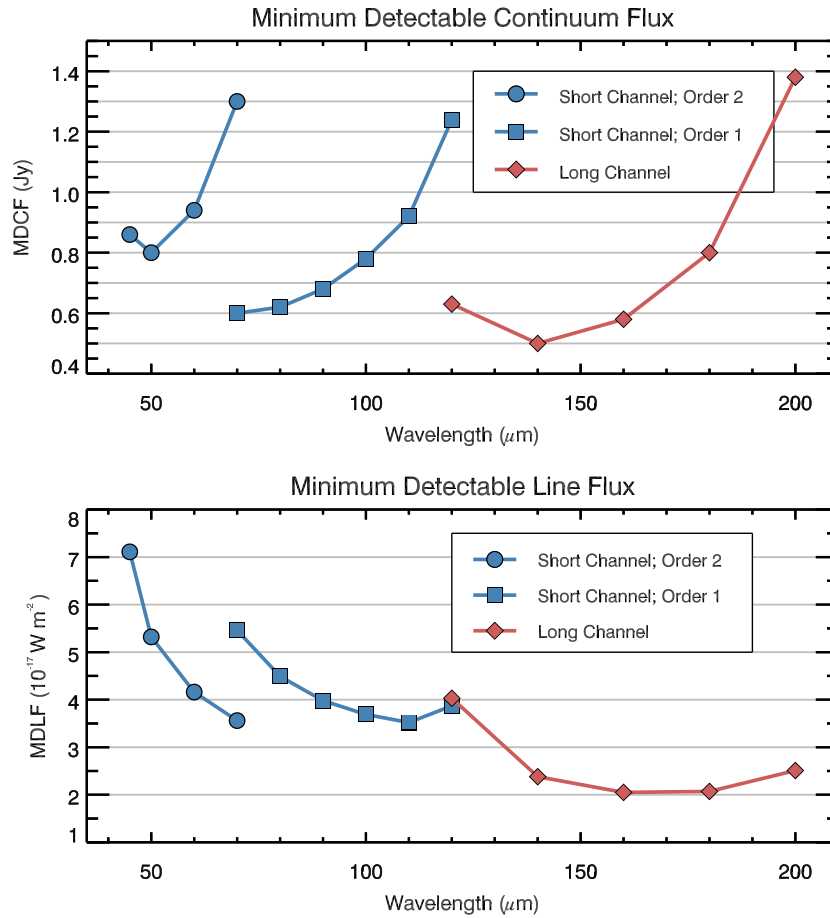
Figure 32: Continuum and emission line sensitivities for a monochromatic point source: The values are calculated for a SNR of 4 in $900\,\mathrm{s}$. The MDCF is in Jy per pixel and the MDLF is in Wm^{-2} per pixel. Both sensitivity values scale as $\mathrm{SNR}/\sqrt{t}$, where t is the on-source integration time.

the observing wavelength as calculated by, e.g., ATRAN[31] (see Sect. 3.6). The factor l equals 1 for unresolved lines. If the desired spectrum needs to be wider than the bandwidth, l is the ratio of the requested width of the spectrum and the bandwidth (Fig. 31).

The on-source integration time must be an integer multiple of t_nod, the on-source integration time per nod cycle (see 9.3.3), i.e. $t_\mathrm{on} = n \times t_\mathrm{nod}$ with n being the number of nod cycles. If the derived t_on is on the order of 5s, consider the Fast Asymmetric Chop mode ($t_\mathrm{nod} = 5s$ and $n = 1$). Otherwise one should derive n by rounding $t_\mathrm{on}/t_\mathrm{nod}$ to the nearest integer with $t_\mathrm{nod} = 30$s or 15s for the Symmetric and Asymmetric Chop Mode at their highest efficiency, respectively. After having adjusted t_on to be an integer multiple of t_nod, check if the SNR that will be achieved in the adjusted on-source integration time is still good.

To derive the total observing time, one has to take into account the overhead and the number of telescope pointings. The overhead depends on the observing mode (Sect. 9.3). The total observing

---

[31]http://atran.sofia.usra.edu/cgi-bin/atran/atran.cgi

time per pointing is calculated by multiplying t_{on} with a factor of 2.67 (Symmetric Chop), 5.33 (Asymmetric Chop), or 6 (Fast Asymmetric Chop). Multiply total observing time per pointing with the number of telescope pointings to derive the total observing time. More on mapping can be found in Sect. 9.3.5.

Be conservative with the time estimates! A first reduction of the commissioning data revealed that due to inconclusive data provided by the water vapor monitor the sensitivity of the instrument currently is still limited by atmospheric calibration rather than by detector performance, which was used to estimate the sensitivities. That should change in Cycle 3.

9.3 Observing Modes

The high sky background in the far infrared requires careful subtraction. That is achieved by chopping with SOFIA's secondary mirror and by nodding the telescope. The secondary will chop at 2Hz to efficiently remove the sky emission. To remove residual background not canceled by chopping, the telescope is nodded (moved to an off-position) typically every 30s.

The following sections describe the possible observing modes. Additional details of how all the parameters for each mode is to be entered into SSPOT during Phase II of the proposal process can be found on the Cycle 3, Phase II web page[32].
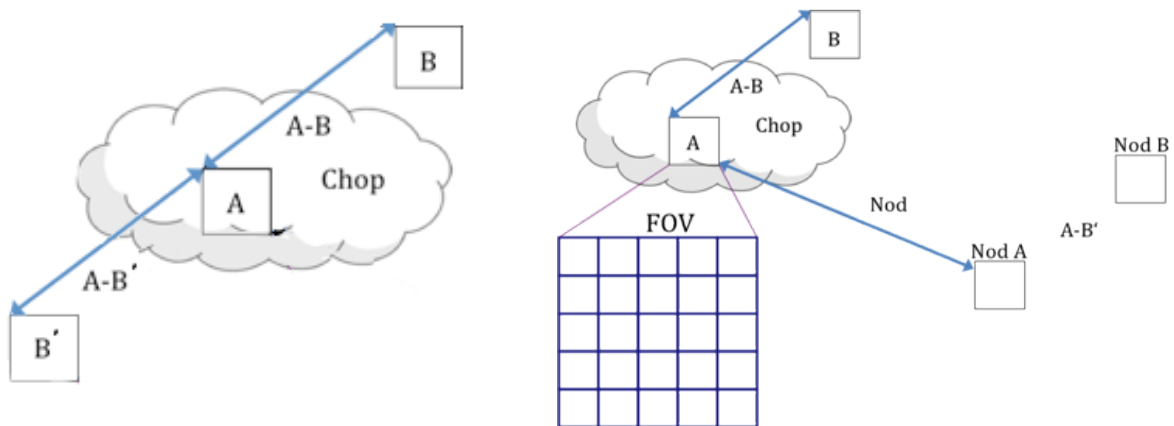
Figure 33: The geometry of chopping and nodding in the Symmetric Chop mode (left) and the Asymmetric mode (right).

9.3.1 Observing Mode: Symmetric Chop

If possible this observing mode should be used, because it is twice as efficient as the Asymmetric Chop Mode. This mode combines chopping symmetrically to the telescope's optical axis with a matched telescope nod to remove the residual telescope background. This mode is also known as nod-match-chop (NMC) mode (cf. FORCAST Sect. 5.3.1) or beam switching (BSW, cf. GREAT Sect. 6.1.1).

---

[32]http://www.sofia.usra.edu/Science/proposals/cycle3/phase2_fifils.html

When observing using a symmetric chop, large chop amplitudes degrade the image quality due to the introduction of coma. This effect causes asymmetric smearing of the PSF in the direction of the chop. However, the effect is small (effect on SNR less than 10%) in the red channel for all chop throws and in the blue channel for total chop throws less then $5'$ and wavelengths longer than $63\,\mu$m. For wavelengths shorter than $63\,\mu$m, we recommend total chop throws of less than $4'$. Generally, it is recommended to use a chop as small as possible, but keep the FOV in the off-positions outside of any detectable emission.

The position angle of the chop can be specified relative to equatorial coordinates or telescope coordinates (e.g. horizontal). Keep in mind that the telescope nod matched to the chop creates two off-positions symmetric to the on-position.

The total observing time in this mode is about 2.7 times the on-source integration time, since the source is only observed during 50% of the observation and additional time is required for telescope moves. The relative overhead increases for on-source integration times of less than 30s per nod cycle, because the telescope moves per nod cycle take up 20s regardless of the observing time.

9.3.2   Observing Mode: Asymmetric Chop and Fast Asymmetric Chop

If the target's size or environment does not allow to use the Symmetric Chop Mode, one has to use the Asymmetric Chop Mode allowing larger chop throws at shorter wavelengths and is not creating symmetric off-positions around the source. The asymmetric chop keeps the on-beam on the optical axis. This results in an image unaffected by coma. Consequently, the off-beam is off-center by twice the amount compared to the symmetric chop with the same chop throw resulting in twice as much coma. But that is of no consequence as the off-beam should only see empty sky. The telescope is nodded to an off-position where the same chopped observation is executed to provide the residual background subtraction. Figure 33 illustrates this geometry. Note that this mode is similar to FORCAST's asymmetric chop-offset-nod (C2NC2) mode (see 5.3.1).

The total observing time in this mode is about 5.3 times the on-source integration time, since the source is observed during 25% of the observation plus additional time for telescope moves. The relative overhead increases rapidly for on-source integration times of less than 15s per nod cycle, because the telescope moves per nod cycle take up 20s, regardless of the observing time. The efficiency of a map can be improved for an on-source exposure time of 5s, because then two map positions can be observed per nod-cycle. The total observing time for the so called Fast Asymmetric Chop Mode is 6 times longer than the total on-source observing time.

For mapping very bright sources, like bright planets, one can choose not to observe the reference position, because the signal is much stronger than the residual background after subtracting the chopped signal. This variation of the Asymmetric Chop Mode with higher efficiency but lower sensitivity is available only after consulting with the support scientist and is currently not supported by SSPOT.

9.3.3   Summary of Observing Efficiencies

Following is the summary of how to achieve the highest observing efficiencies for the different modes. The efficiency depends on the on-source exposure time per nod cycle t_{nod}.

Symmetric Chop Mode

Use $t_{\mathrm{nod}} = 30$s. The nod cycle will take 80s, thus the observing efficiency is 37.5%.

Asymmetric Chop Mode

Use $t_{\rm nod} = 15$s. The nod cycle will take 80s, thus the observing efficiency is 18.75%.

Fast Asymmetric Chop Mode

Use $t_{\rm nod} = 5$s. The nod cycle will take 60s, thus the observing efficiency is 16.67%, because two map positions are observed per nod cycle.

The total observing time is the duration of the nod cycle times the number of nod cycles and times the number of map positions.

To illustrate the loss of efficiency when a shorter $t_{\rm nod}$ is used, note that the efficiency of the Symmetric and the Asymmetric Chop Modes drop to 16.67% and 12.5% for $t_{\rm nod} = 5$s, respectively. However, the Asymmetric Chop Mode will do two map positions per nod cycle for $t_{\rm nod} \leq 5$s becoming the Fast Asymmetric Chop Mode automatically. The Fast Asymmetric mode is preferred for $t_{\rm nod} = 5$s, though this mode and the Symmetric Chop mode have the same efficiency in this case, because the grating scan has double the time to complete in the asymmetric modes compared to the Symmetric Chop Mode with the same $t_{\rm nod}$.

SSPOT will calculate slightly different observing times, because it includes a 1 min set-up time for each observation in the overhead and it uses rounded off overhead factors. Future development work is directed at improving the overheads by exploring how much longer the nod cycle can be and by devising more efficient observing modes.

9.3.4 Spectral Dithering

Spectral and spatial dithering (see mapping) is recommended for self flat-fielding and increased redundancy. Spectral dithering is always implemented via a grating scan. The grating is moved in small steps, so that the spectrum moves over different pixels in the spectral dimension of the detector array.

The default pattern to cover the bandwidth (BW, Sect. 9.2.1) is to move the grating 12 steps, each corresponding to half a spectral pixel width. This pattern results in a spectrum about 30% wider than the BW. The central 70% of the BW are observed during the whole observing time reaching the full SNR, while the remaining 15% on each side of the BW should reach on average 86% of the SNR. The SNR reached on the extra 30% should still be 46% on average based on the observing time for each part of the spectrum.

For wider spectral coverage, the step size and number of steps of the grating scan will be adjusted to achieve the desired spectral coverage. The grating scan may be interleaved with the telescope nods, if the grating scan takes longer than $t_{\rm nod}$ or $2t_{\rm nod}$ for the Symmetric or Asymmetric Chop Mode, respectively.

9.3.5 Mapping

Mapping is supported by both observing modes. It can be done on a rectangular grid with a user-defined spacing and extent. It is also possible to supply a list of mapping positions to achieve a map with a custom shape optimized to the source geometry. For both map types, a spacing of half a red array or $30''$ might be a good choice, providing half pixel steps to achieve super-resolution with a good overlap for the red array and full coverage (but no overlap) for the blue array. Similarly, a spacing of $15''$ yields super-resolution with a good overlap for the blue array and a very strong

overlap for the red array. These details need to be specified only in Phase II of the proposal process (see the FIFI-LS Cycle 3, Phase II web page[33]). In Phase I, the effective map area needs to be entered in SPT and the proposal should explain the suggested mapping strategy. The on-source integration time to be entered in SPT has to be the on-source integration time per raster point multiplied by the number of raster map points.

If the source geometry allows the off-beam to be positioned symmetrically on both sides of the source, then one should use the much more efficient Symmetric Chop Mode for mapping. If that is not possible the Asymmetric Chop Mode has to be used. Figure 34 illustrates mapping with an asymmetric chop. The off-beam (positions B1 to B3) covers an area while chopping that is the same size as the map itself. If this is undesirable, the map needs to be broken up into sub-maps with varying chop parameters to be specified in Phase II. The availability of guide stars might be another reason to break up a large map into sub-maps. In this case the sub-maps will be identified between Phase II and the actual observation by the support scientist in close collaboration with the guest investigator and the telescope operator.
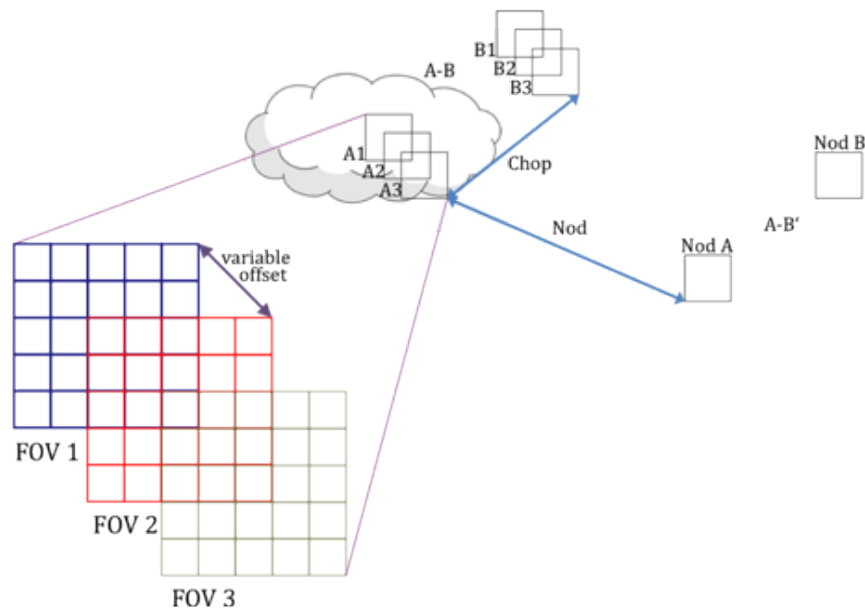

Figure 34: The geometry of chopping and nodding while mapping using the asymmetric chop mode.

When estimating the on-source integration time (Sect. 9.2.2), take into account the differing overlap of the red and blue FOV at the desired raster map spacing. The SNR entered into the calculation of t_{on} is the SNR for a single raster map point. The final SNR for a point in the map should reach $\sqrt{n} \times \text{SNR}$ with n being the number of raster points from which a point is covered by the respective FOV. For example in Fig. 34, the area of the pixel in the middle is covered by 3 FOVs while 16 pixels are covered by 2 FOVs and the outer parts of the map are covered by 1 FOV.

For small sources where mapping is not necessary, spatial redundancy can be achieved by a raster map with pixel-sized spacing. This is recommended unless the observing efficiency is impacted. The spacing between the raster points should be large enough to bring the flux to the next spatial pixel

---

[33]http://www.sofia.usra.edu/Science/proposals/cycle3/phase2_fifils.html

(spaxel) and should therefore be not smaller than 1 blue spaxel ($6''$). To achieve the same for the red array, a step size of at least one red spaxel ($12''$) is needed (alternatively, two $6''$ steps).

10   The Data Cycle System

SOFIA proposals and observation data are managed by the SOFIA Data Cycle System (DCS)[34]. The DCS is designed primarily to support Science and Mission Operations activities associated with Guest Investigator (GI) programs for the observatory. From a GI point of view, observatory data flow is cyclic in nature (see Figure 35). The GI first develops and submits a proposal to the SOFIA Science Mission Operations (SMO). Once approved, the proposal becomes an observing plan that the GI uses to create and update astronomical observation requests (AORs) that are used in both flight planning and on-aircraft execution. After execution of the observations in-flight, the resulting data are archived and, for Facility Science Instruments (FSIs), automatically processed (pipelined) to produce the final data products, which are then served back to the original GI via a simple user-interface – thus completing the cycle begun by the original proposal and perhaps driving new proposals. The data products are made available to the astronomical community for archival research purposes after an appropriate proprietary period.
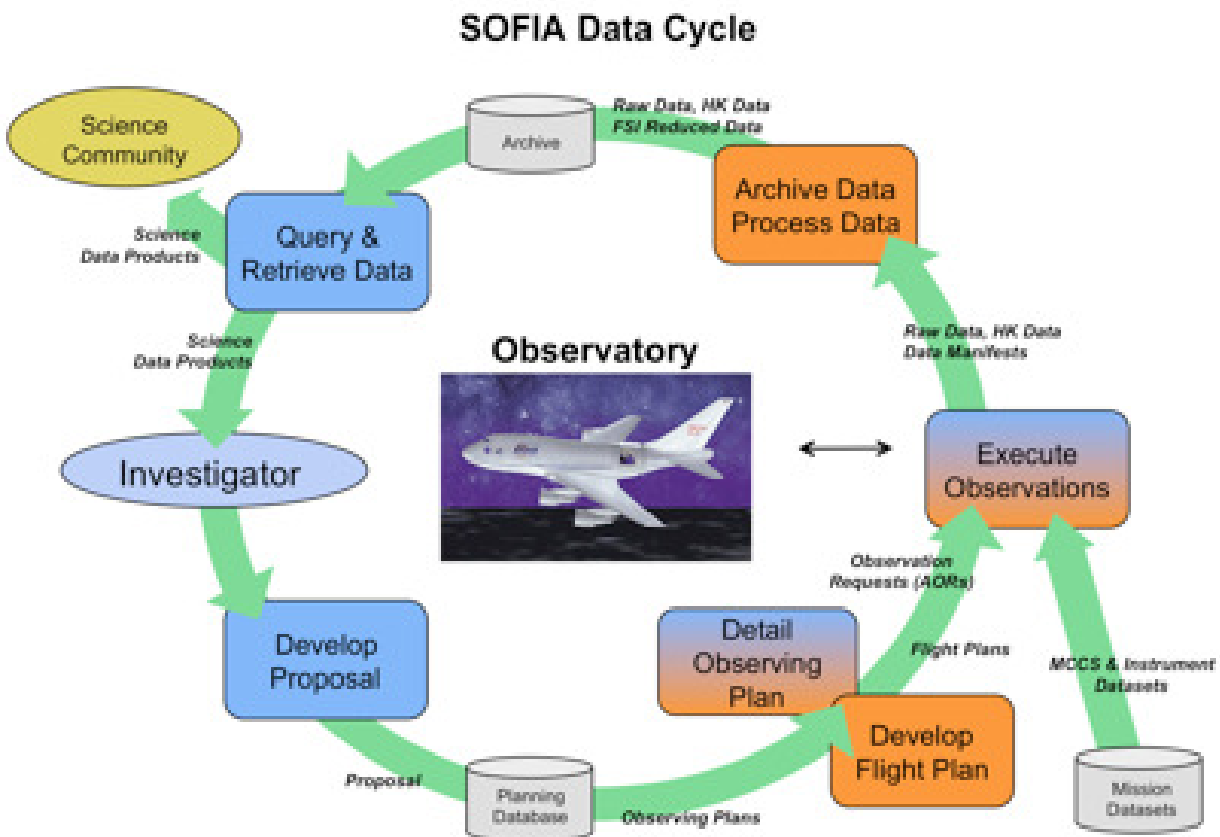

Figure 35: Cartoon of the SOFIA Data Cycle

---

[34]https://dcs.sofia.usra.edu

The goal of the SOFIA DCS is to maximize the scientific productivity and efficiency of the observatory by providing a suite of easy-to-use tools and infrastructure that are integrated with each other as well as other applications (e.g. Flight Management Infrastructure) at each step in the data cycle.

The DCS Archive is the permanent repository for all raw scientific and housekeeping data accumulated during SOFIA flights and any pipeline products produced thereafter (for example, pipeline reduced data for FSIs). Access to the SOFIA Data Archive is via the DCS web pages. GIs are able to retrieve their data from the archive during the proprietary period using an assigned DCS login username and password. The proprietary period for Cycle 3 will be 1-year from the date of ingestion into the DCS Archive. Once the proprietary period expires, the data becomes public and can be accessed by anyone in the general community.

In order to make use of most of the features of the DCS website, users must register by clicking on the "Register with DCS"[35] link on the DCS home page. After the registration form has been submitted, the user will be notified by e-mail when the account has been created. (Users should verify that mail from "sofia.usra.edu" is not blocked by any spam filters.) After logging in, a registered user can change his/her profile and password at any time using the View Profile link displayed next to the login name at the top of the DCS pages.

The DCS includes a suite of software tools to archive data and to assist GIs in preparing and submitting proposals:

- **SOFIA Proposal Tool (SPT):** SOFIA proposals are created and modified using the SPT, a stand-alone Java application available for a wide variety of platforms. The "Download SPT page"[36] includes links to download the Java application and installation instructions for all supported platforms. Complete help files are included with the application distribution and can be accessed via the Help menu options with the SPT.

- **Time Estimators:** In order to assist in the creation of SOFIA observing proposals, the DCS web site provides an online SOFIA Instrument Time Estimator (SITE)[37] that calculates the total observation time required or signal-to-noise achieved for FLITECAM and FORCAST imaging modes. The DCS also maintains the on-line FLITECAM Grism Exposure Time Calculator[38] and the on-line FORCAST Grism Exposure Time Calculator[39].

  Exposure time calculators for GREAT and EXES are also available, and links may be found on the SITE page.

- **Atmospheric Transmission Estimator (ATRAN):** To allow proposers to estimate the effects of atmospheric transmission on potential observations and exposure times with SOFIA instruments, the DCS provides access to a web-based version[40] of the ATRAN program written by Steve Lord. For a specified observing altitude and wavelength range, the web page will run ATRAN and generate an output file and plot of the atmospheric transmission as a function of wavelength. Both the output file and plot can be downloaded to the user's

---

[35]https://dcs.sofia.usra.edu/userSupport/registration.jsp

[36]https://dcs.sofia.usra.edu/proposalDevelopment/installSPT/index.jsp

[37]https://dcs.sofia.usra.edu/proposalDevelopment/SITE/index.jsp

[38]http://flitecam.sofia.usra.edu/cgi-bin/flitecam/flitecam_calc2.cgi

[39]http://forcast.sofia.usra.edu/cgi-bin/forcast/forcast_calc2.cgi

[40]http://atran.sofia.usra.edu/cgi-bin/atran/atran.cgi

desktop. A brief description of the input parameters and how to run ATRAN is given at the top of the web page.

- **Visibility Tool (VT):** The Target Visibility Tool provides the capability to estimate what date, time, and aircraft heading are required to observe an astronomical target. The tool is a Java applet that is accessible on the Visibility Tool page[41]. Details of which operating systems and browsers are compatible with VT are provided on the Visibility Tool page. A stand-alone version of VT is available for download.

  To find the visibility of a given target, the user enters its co-ordinates (J2000 RA and DEC), the estimated latitude and longitude of the observation (which defaults to the SOFIA take-off location of Palmdale, CA), the start date and time, and the duration of interest. The application plots the target elevation for the period of interest. A target is visible to SOFIA if the elevation is in the range $20°$ to $60°$.

  The nominal period of observations for Cycle 3 is 1 March, 2015 to 31 January, 2016. GIs should use VT to ensure that the proposed targets are in the allowed elevation range for visibility. For flights that take off from and return to Palmdale, the southernmost observable declination is -36°. However, there will be up to two Southern Hemisphere Deployments during Cycle 3.

  Instructions on how to use VT and help on specific topics are available as part of the tool, using either the "Help" pull-down menu or the "?" button, both at the top, left of the applet window.

In addition, the DCS provides users with a variety of search options for proposals, data, and observing plans.

- **Proposal Search:** All proposals submitted via SPT are stored in the DCS observation planning database and can be accessed from the DCS web pages. Users can retrieve summary data for available proposals by using the Proposal Search page[42] and entering the relevant search criteria for the proposal(s) of interest. Summary information will be displayed for each proposal (appropriate to the permissions of the user).

- **Archive Search:** Summary information is available for all public data in the DCS archive. From the Science Archive Search page[43], MCCS Archive Search page[44], or the Ancillary Files Search page[45], users can specify search criteria to identify data of interest. Summary info for resulting matches is shown in a table with appropriate links based upon user permissions. Data that are still proprietary are available only to the GIs on the associated observing plan. Hence, *users must log in using a DCS username to view any proprietary data.* Proprietary data can only be seen by the program GIs and SMO staff members. From the Summary Information table for science data, users can click through to a list of all data products associated with a particular observation (e.g., raw or pipelined data), or identify data to be downloaded.

---

[41]https://dcs.sofia.usra.edu/observationPlanning/visibilityTool.jsp

[42]https://dcs.sofia.usra.edu/proposalAccess/propSummary.jsp

[43]https://dcs.sofia.usra.edu/dataRetrieval/SearchScienceArchiveInfo.jsp

[44]https://dcs.sofia.usra.edu/dataRetrieval/SearchMCSArkInfo.jsp

[45]https://dcs.sofia.usra.edu/dataRetrieval/SearchAncillaryFileInfo.jsp

- **Observing Plans Search:** Once a proposal is approved, it becomes an observing plan, which can be accessed and modified as needed to support science and mission requirements by the proposal GI and selected SMO staff members. Observing plans can be accessed from the planning database using the Search Observing Plans[46] link on the DCS web page. Summary information will be displayed for each observing plan along with links to the Observing Plan Details page. The Observing Plan Details page provides all the information available for a plan and corresponding links to the editor functions to make changes (for users with appropriate permissions).

- **Data Retrieval:** Data can be retrieved by identifying desired data in the summary table and then clicking the "Retrieve Data" button. In order to retrieve any data, the user must be logged in. Only GIs with appropriate permissions and SMO staff are able to retrieve data that is still within the proprietary period. Once designated for retrieval, the files are staged to a public FTP server and a direct link is e-mailed to the user. All science data products are available in their original format (e.g., FITS). The same retrieval process is used for the MCCS and Ancillary data files.

10.1   Data Rights and Availability

All scientific data from SOFIA observations will be distributed via the SOFIA Data Cycle System's Science Archive[47]. All data will be archived as Level 1 data (raw). Where appropriate, Level 2 (corrected for instrumental and atmospheric effects) and Level 3 (flux calibrated) will also be archived. These data will be accessible to the general community after a proprietary period of twelve months, starting at the ingestion of the calibrated data into the archive.

In order to query the archive and retrieve data, it is necessary to register with the DCS. This can be done by following the appropriate link ("Register With DCS") on the main DCS page[48]. Registration is not required for using the proposal preparation and submission tools.

---

[46]https://dcs.sofia.usra.edu/observationPlanning/observingPlanSearch.jsp
[47]https://dcs.sofia.usra.edu/dataRetrieval/SearchScienceArchiveInfo.jsp
[48]http://dcs.sofia.usra.edu/

11 Proposing for Cycle 3

The SOFIA proposals are to be submitted using the SOFIA Proposal Tool (SPT)[49], which is based on the Astronomer's Proposal Tool developed for HST by AURA/STScI.

Both US and German proposers must use the SPT to submit their proposals. Deadlines for proposal submission are available in the "SOFIA Cycle 3 Call for Proposals" (CfP). The CfP also provides details about SOFIA proposal requirements with information about who may propose, the selection process, and grants for GIs.

11.1 SOFIA Proposal Tool (SPT)

The SOFIA Proposal Tool (SPT) provides the user with a simple form-based interface for preparing a proposal and for electronic submission to the SOFIA Science Mission Operations center. The SPT is available for download from the DCS SPT page. After downloading the appropriate package and following the installation instructions, the user starts a new proposal by launching the SPT application. The proposer then fills out the necessary form fields including proposer information, abstract, instrument(s), and target lists. The Science and Technical Justification must be prepared in a separate text editor (e.g. MS Word, LaTeX, etc.) and saved as a PDF file. Using the SPT, the proposer then identifies this PDF file on a local disk for attachment to the proposal summary information and submits the proposal in its entirety directly to the SOFIA Science Mission Operations center. A unique identifier is then returned for later reference. Proposals that have been submitted to the SMO can be resubmitted using SPT at any time up to the proposal deadline (note that old versions are not retained).

On starting SPT, general help may be found from the "Help" pull-down menu. Instructions on filling out the fields in the form may be accessed by clicking on the "?" button at the top-right corner of the SPT window, and then on the field of interest. In the following we describe some of these, including all those for which there are restrictions during Cycle 3.

- **Proposal Information Page**

  - *Status of Observations in Last Two Years* – Suitable text such as "not applicable" should be entered in this dialog box. It cannot be left empty.
  - *Blackout Dates* – Blackout dates are not permitted during Cycle 3, and the default values of "None Selected" should not be changed.
  - *Observation Modes* – Users must specify which type of Observing Mode they are requesting.
    * *Queue Observation* – Most GIs will be proposing for Queue Observations.
    * *Target of Opportunity* – This box should only be checked for Target of Opportunity programs as defined in the CfP.
    * *Long Term Observation* – This type of program is not available during Cycle 3, so this box should not be checked.
    * *Survey Program* – This box should only be checked for Survey Programs as defined in the CfP.

---

[49]http://dcs.sofia.usra.edu/proposalDevelopment/installSPT/index.jsp

- **Instruments**

  - *Water Vapor Overburden* – The proposer should choose the Water Vapor Overburden (using the pull-down menu) necessary to accomplish the scientific objectives proposed. This selection should be justified in the Technical Description section of the proposal.
  - *Total Observing Time (seconds)* – This field cannot be edited, but will be updated to reflect the total time on the sky required for an observation calculated from the user entered integration times, the overhead values, and the total number of observations (see below).

- **Observations**

  - *Source Type* – The source types allowed are "Solar System" and "Sidereal". The latter is to be used for all non-solar system targets.

    For observations of Solar System objects, the user should supply the Target Name as usual and then select the NAIF-ID from the pull-down list. All Solar System object observations are treated as "Time Critical," so the user must supply a date range over which the observation can be completed. If the GI's object is not on the list, she or he can simply write in the NAIF-ID (if known). If a NAIF-ID has not been assigned to the object, then the user must specify the coordinates for their desired observation date.
  - *Coordinates (J2000)* – For **solar system targets only**, the "Coordinates" fields (RA and DEC) should be left blank. When submitting the proposal, an error dialog box will be generated. Include the following explanation, "Solar System Targets" in the box, and proceed with the submission. The blank fields will be handled by the software.
  - *Instrument* – Instruments available are FLITECAM, FORCAST, GREAT, HIPO, EXES, and FIFI-LS. Multiple instruments may be combined in a single proposal, except for FLITECAM/HIPO (FLIPO) and HIPO, each of which must be in separate proposals.
  - *Integration Time* – For all instruments **except EXES**, the Integration Time for each observation is the total on-source time required to achieve the required S/N for the science goals of the proposal. For EXES, only, the Integration Time is the **clock time**. Details are available in the individual instrument chapters.

    SPT provides default overheads for each proposed observation based on the instrument configuration and mode selected. The total overhead for each observation is defined as:

    $$Overhead = A * (IntTime) + B$$

    where

    A = overhead factor, related to overall observing efficiency (e = 1 / (1 + A))

    B = Setup constant, applied to all observations of any length.

    The total duration (wall clock time) of any observation is then:

    $$Duration = IntTime + Overhead$$

    Once the user selects the appropriate configuration/mode based on his/her science needs (see instrument chapters for descriptions of configurations and modes), SPT will display

the nominal overhead for the observation (A and B values), and then apply the nominal overhead to the Integration Time supplied in the following line of the form. The user may also **override** the default overhead by providing a value in the Alternate Overhead text box—this is not recommended unless the GI has consulted with an instrument scientist at the SSC via the SOFIA Help-Desk.

– *Order of Observation* – This entry is intended to be used if the order in which a series of targets or a series of instrument set-ups within a single target observation matters. For the average proposal, the order of observations is not critical. Instead, they can simply specify the priority of their target relative to the other targets in their proposal, if necessary. For example, say one wishes to observe Target 1 before Target 2 and both targets are to be observed with Filter 1 and Filter 2. Then the individual observations produced in the SPT should list the Order of Observation as "1" for Target 1, Filters 1 & 2, and list the Order of Observation as "2" for Target 2, Filters 1 & 2. The GI should be certain to justify the Order of Observations in the text of the proposal.

11.1.1 Proposal Text

Proposal Sections The uploaded PDF file must contain the following sections in the order indicated for each proposed observing program. The page length limits are indicated.

- *Scientific Context* (up to 0.5 pages) – Briefly summarize the proposed investigation with the following elements:

  Context – What is the context and significance of this proposal to the broader field of astronomy?

  Aims – How will the observations address the specific scientific questions in this proposal?

  Methods – What are the key measurement techniques utilized in this investigation?

  Anticipated results – What are the expected data sets that will be produced in this investigation?

- *Scientific Justification* (up to 3 pages) – Describe the scientific objectives of the proposed investigation, clearly stating the goals and their significance to astronomy, and why SOFIA data are essential to the investigation. The results and status of previous, related, SOFIA observations should be summarized. The page limit includes all text, figures and tables. An additional page for references only is allowed.

- *Feasibility* (up to 2 pages) – This section forms the basis for assessment of the technical feasibility of the proposed observations. The requested exposure time for each observation must be justified. The section should include the expected target fluxes and the signal-to-noise ratio required for each observation. The source (or method) for the flux estimates, and their accuracies should be mentioned. Where applicable the spectral resolution required must be explicitly stated. Any other information about the proposed observations that would help the reviewer relate the technical needs to the scientific goals should be included in this section. Observing overheads and other indirect time estimates should follow the instructions

given in the Observers Handbook. This section should also contain the justification for special calibration procedures, if they have been requested.

- *Principal Investigator and Co-Investigator Biographical and Publication Data* (one page for the PI with one additional page for CoIs) – A short biographical sketch for the PI should be provided and include a list of the most recent refereed publications relevant to the scientific proposal. Short biographical data, including their roles in the proposed project, should be provided for the CoIs

11.1.2   Proposal Submittal

Once the forms in SPT have been filled out and the proposal text attached, the proposal is ready for submission to the SMO. Before submission, the proposer should verify that all required form fields have been filled in by pressing the "Errors and Warnings" button on the SPT tool bar (there is also an "errors and warnings" indicator at the bottom right of the SPT tool that shows status at all times). The resulting "Diagnostic Report" will indicate if there are any fields missing. Once all fields have been filled in, the diagnostic report should be empty and a green check mark will appear in "errors and warnings" indicator at the lower right hand corner of the SPT window. The proposer should save the proposal to the local desktop at this point.

To submit the proposal to the SMO, users must go to the "Submit" page, enter any "Submission Comments" in the text box provided, and then press the "Submit Phase 1" button. If there are no errors and warnings, a pop-up window will appear indicating that the proposal has been assigned a unique identifier (Proposal ID) and has been successfully received by the SOFIA Science Mission Operations center. In the Submission Window, the submission log should now show the Proposal ID and the date and time of submission. In addition, a confirmation email will be sent to the proposer using the address provided in the proposal. If any required fields are missing, the proposal will not be submitted and a pop-up window will appear indicating that there are errors in the proposal. The proposer should go back and run the Errors and Warnings check again, making necessary corrections before attempting to submit again.

Proposals can be resubmitted to the SOFIA Science Mission Operations at any time before the proposal due date. Note that a resubmitted proposal replaces all previously submitted versions (i.e. there is no version management, the SMO keeps only the latest proposal submission). To change and resubmit a proposal, the proposer should start SPT, select "Open" or "Open Recent" from the "File" menu, and choose the local copy of the proposal to be updated. The Proposal ID should be shown in both the "Node Tree" at the left hand side of the SPT window, and in the Window Title itself. Once changes are made, the proposer should check the proposal for errors and warnings as described above and then go to the "Submit" page. After entering any comments, the proposer would then press the "Resubmit Phase 1" button. A pop-up window will appear indicating that the proposal has been received and the submission log should now show the date and time of the re-submission. Once again, a confirmation email will be sent to the proposer using the address provided in the proposal.

11.2   Phase II

Once the Cycle 3 proposals have been reviewed and the selections made, the GIs will be notified of the outcome. Those GIs with programs that were awarded time must then begin the Phase II process. During this stage, each proposal will be assigned a member of the SMO staff who will act as the Support Scientist. The GIs will then design their observations, formatted as an Astronomical Observing Request (AOR) using the SOFIA Spot (SSpot) observation planning tool.

Once the AORs have been submitted through SSpot, they will be validated by the Support Scientists. After being verified, the programs will be scheduled by the Flight Planning staff. Many details of the observations, e.g., the rate of field rotation, which determines the frequency of LOS rewinds, are unknown until flight planning is complete. Consequently, in many cases, additional input from the GIs will be needed after flight planning has been completed. At this time, the order of observations will need to be respecified.

11.2.1   SOFIA Spot (SSpot)

SOFIA Spot (SSpot) must be used for preparing and submitting all Phase II observing proposals, except those using HIPO. The SSpot tool is built on the same architecture as Spitzer Spot and Herschel HSpot. Those who have experience using Spot or HSpot should find the use of SSpot straightforward.

The GIs will use SSpot to specify the values of the parameters relevant to their proposed observations with each SOFIA instrument and visualize the proposed observations on an image of the target field. The set of parameters for any given observing mode and instrument configuration comprise an Astronomical Observing Template (AOT); the completed template with the specified values is known as an Astronomical Observation Request (AOR).

Full details on using SSpot can be found in the SOFIA Spot Users Guide[50].

GIs can find instrument specific instructions for generating AORs using SSpot linked on the Cycle 2 - Phase II[51] page.

Questions about SSpot and the Phase II process should be directed to the SOFIA Help-Desk.

---

[50]http://www.sofia.usra.edu/Science/proposals/cycle1/SSpot_User_Guide.pdf
[51]http://www.sofia.usra.edu/Science/proposals/cycle2/phase2.html